A SYNTHETIC, ELECTROCHEMICAL AND KINETIC STUDY OF POLYSILOXANE-BOUND RHODIUM CARBONYL COMPLEXES

A dissertation submitted in accordance with the requirements for the degree

Magister Scientiae

in the

Faculty of Natural and Agricultural Science

Department of Chemistry

at the

University of the Free State

by

Rahab Mametsi Sebitlo

Supervisor

Prof. J.C. Swarts

Co-Supervisor

Dr. E. Erasmus

2012

Acknowledgements

Highly above all, I honour God the Father, the Son and Holy Spirit for the gift of life, the privilege and ability to study. For it is not by might nor by power but by The Spirit of the Lord.

My utmost respect and acknowledgement goes to my super-visor, Prof J.C. Swarts. You were not just my boss but you became a father figure from which I drew strength when it got tough. I could not have chosen a better supervisor. I truly Thank you! Not forgetting my co-supervisor Dr E. Erasmus, I humbly thank you for your time and academic advice throughout my project. I was academically led by a special two of a kind. You pulled me through the roughest times of the project and I am unable to express myself for my gratitude. A special thank you goes to Prof. Dr. Hartmut Frank (affiliated Professor of Physical Chemistry at the UFS) for helpful suggestions and guidance during the initial stages of the project.

To my parents, Moipone and Moalusi, I am grateful for your parental guidance, discipline and unwavering support. You taught me that independence is a great responsibility. To my wonderful sister Madikgoele, you are my anchor and pool of strength. Thank you to my extended family for your love and support. To a special friend of mine, Mpeyake Maseme, thank you for always telling me "I can", I believed it and now I got it…

To my spiritual homes, Apostolic Faith Mission of SA (Parys) and Global Reconciliation Church (Bloemfontein), sometimes my mind was able but it required further spiritual empowerment to bring me this far.

I would like to thank the Physical Chemistry group for the good times we shared; it really did help take the pressure away. To my friends, thank you for the genuine encouragement.

I could not have achieved anything without the financial assistance from National Research Fund. Thank you.

Mametsi Rahab Sebitlo

Contents

List of Structures

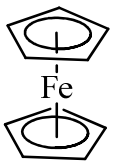

1

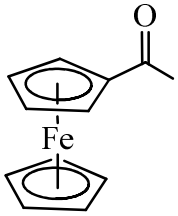

2

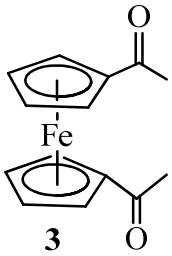

3

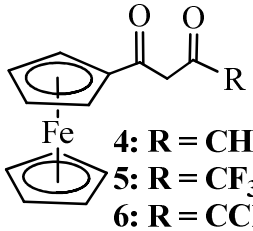

4: R = CH_3
5: R = CF_3
6: R = CCl_3
7: R = Ph
8: R = Fc

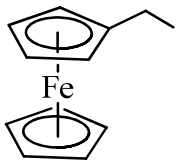

9

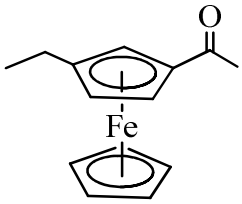

10

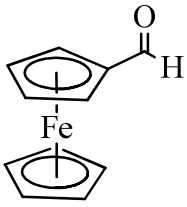

11

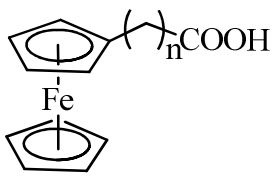

12

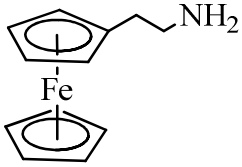

13

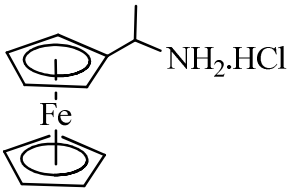

14

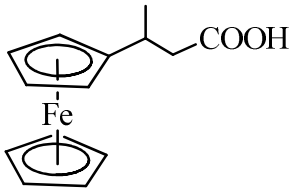

15

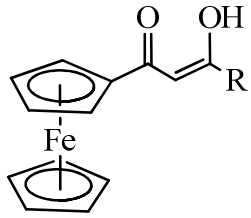

16

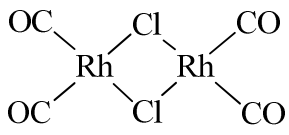

17

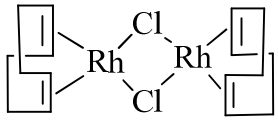

18

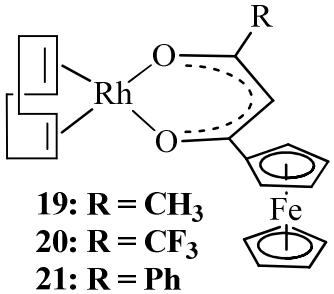

19: R = CH_3
20: R = CF_3
21: R = Ph
22: R = Fc

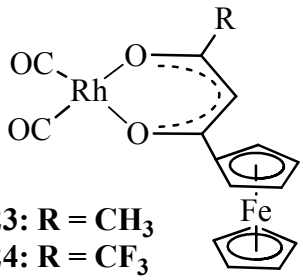

23: R = CH_3
24: R = CF_3
25: R = Ph
26: R = Fc

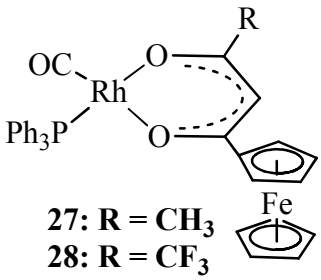

27: R = CH_3
28: R = CF_3
29: R = Ph
30: R = Fc

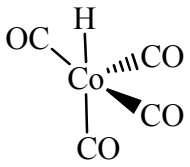

31

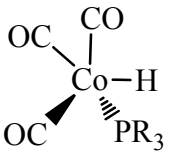

32

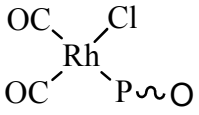

33: P∿O = $PPh_2CH_2OCH_3$

34: P∿O = $PPh_2(CH_2)_2OC_2H_5$

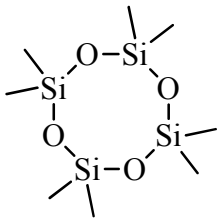

35

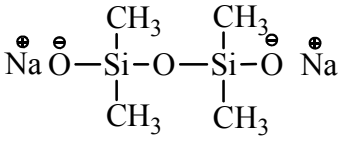

36

37

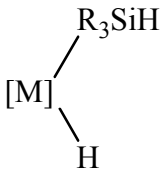

38

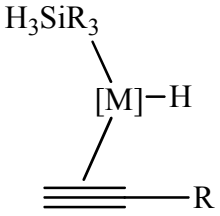

39

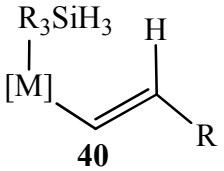

40

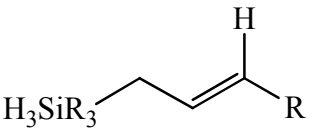

41

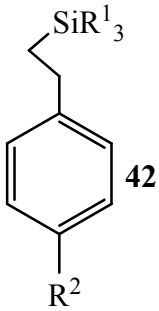

42

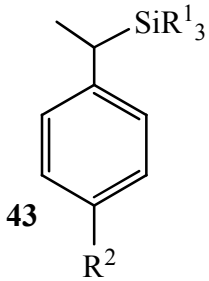

43

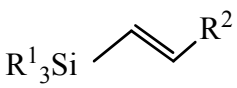

44

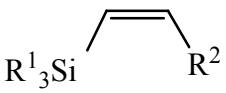

45

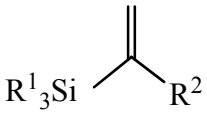

46

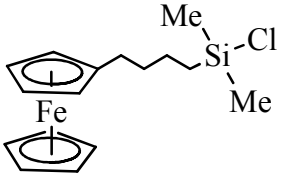

47

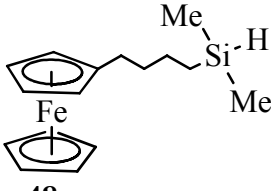

48

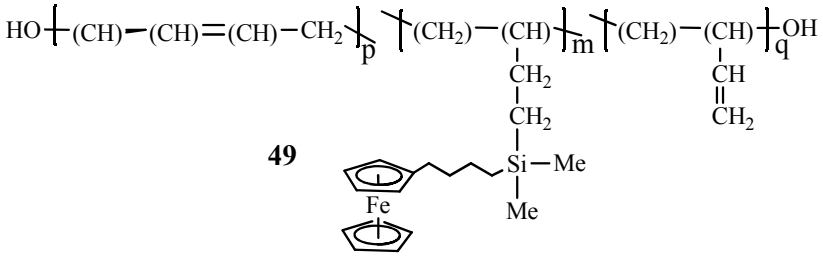

49

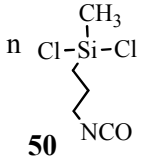

50

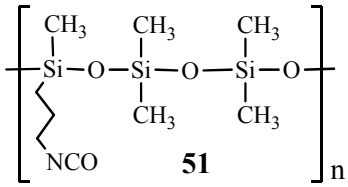

51

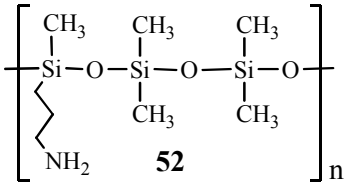

52

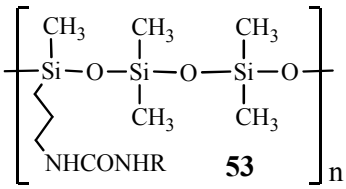

53

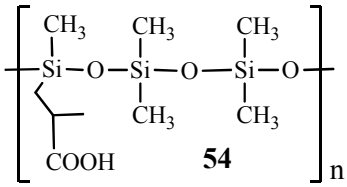

54

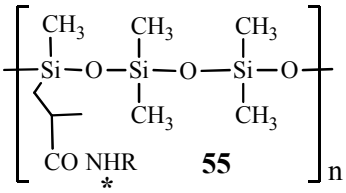

55

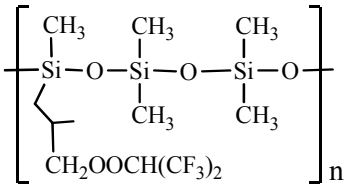

56

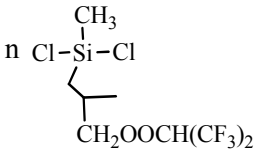

57

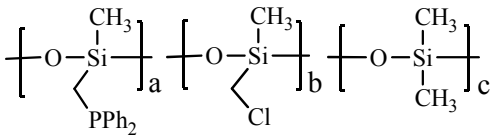

58

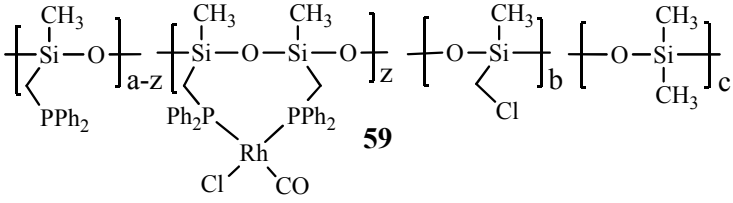

59

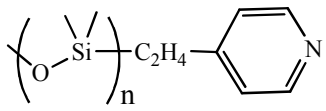

60

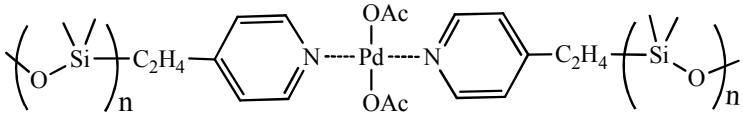

61

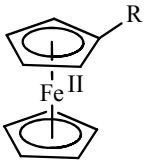

62

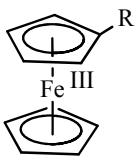

63

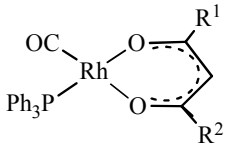

R^1, R^2 = 64: C_6H_5, C_6H_5; 65: C_6H_5, CH_3;
66: C_6H_5, CF_3; 67: CH_3, CF_3 ;
68: CF_3, CF_3

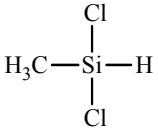

69

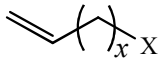

70: *x* = 1, X = Cl
71: *x* = 2, X = Br
72: x = 3, X= Br

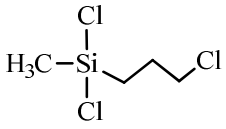

73

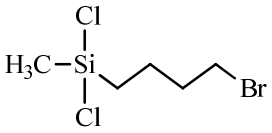

74 a

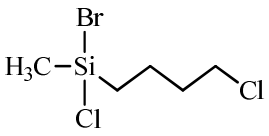

74 b

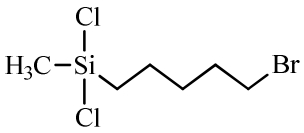

75 a

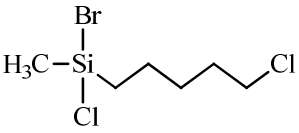

75 b

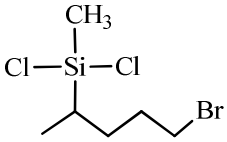

75 c

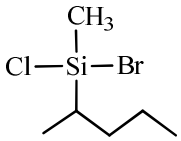

75 d

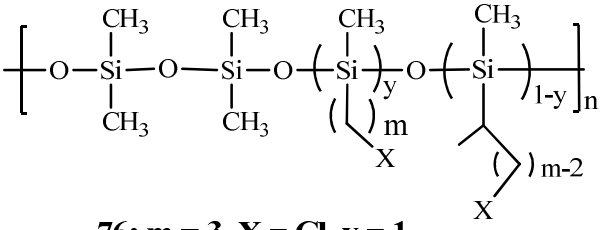

76: m = 3, X = Cl, y = 1
77: m = 4, X = Br,Cl, y = 1
78: m = 5, X = Br,Cl, y = 0.81

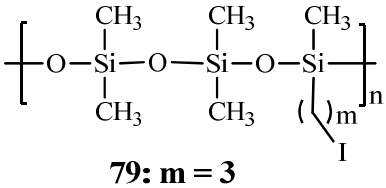

79: m = 3
80: m = 4

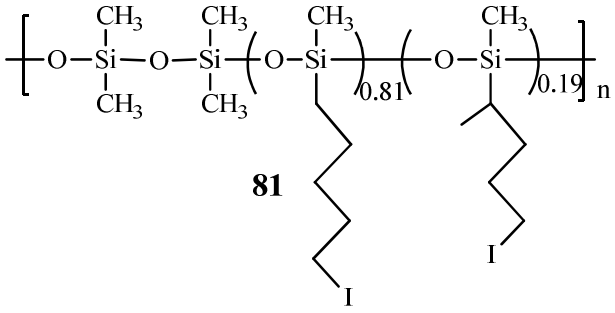

81

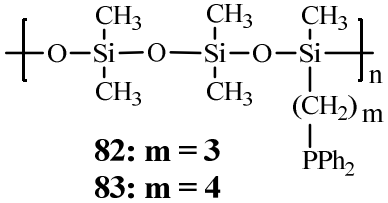

82: m = 3
83: m = 4

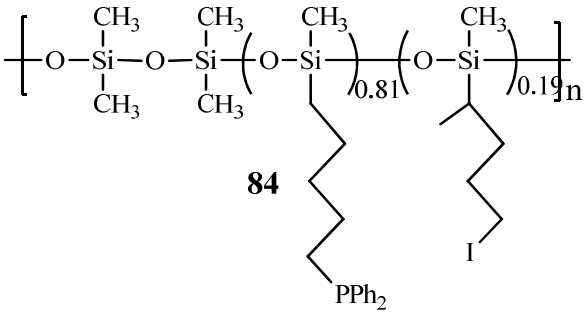

84

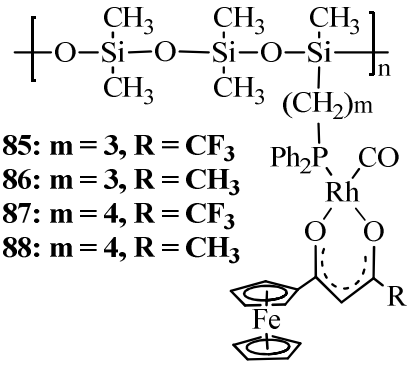

85: m = 3, R = CF_3
86: m = 3, R = CH_3
87: m = 4, R = CF_3
88: m = 4, R = CH_3

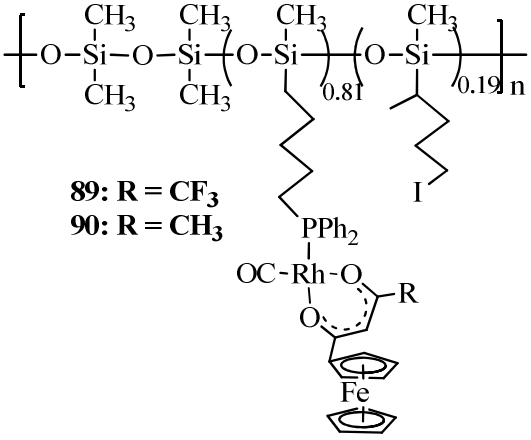

89: R = CF_3
90: R = CH_3

List of Abbreviations

A	absorbance
pKa	acid dissociation constant
CH_3CN	acetonitrile
k_B	Boltzmann's constant
CO	carbon monoxide or carbonyl
M	central metal atom
CV	cyclic voltammetry
cod	1,8-cyclooctadiene
δ	chemical shift
CH_2Cl_2	dichloromethane
DMF	dimethylformamide
Fc^*	decamethylferrocene
Δ	delta
PPh_2	diphenylphosphine
Et	ethanol
eq	equivalents
ΔS^*	entropy of activation
ΔH^*	enthalpy of activation
E°'	formal reduction potential
Fc	ferrocene
FTIR	Fourier Transformer Infra-red
χ_R	group electronegativity (Gordy scale)
R	gas constant
X	halogen
LDA	lithium diisopropylamide
LSV	linear sweep voltammetry
$LiPPh_2$	lithium diphenyl phosphine
ε	molar extinction coefficient
MeOH	methanol
Me	methyl
MeI	methyl odide

k_{obs}	observed rate constant
l	path length
E_p	peak oxidation potential
E_{pa}	peak oxidation potential
E_{pc}	peak reduction potential
^{1}H NMR	Proton Nuclear Magnetic Resonance
^{31}P NMR	Phosphorus Nuclear Magnetic Resonance
h	Planck's constant
Ph	Phenyl
H_3PO_4	phosphoric acid
ppm	parts per million
$RhCl_3$	rhodium trichloride
k	rate constant
υ	stretching frequency/ scan rate
SWV	square wave voltammetry
ΔE_p	separation of anodic and cathodic peak
$TBA[B(C_6F_5)_4]$	tetrabutylammonium(tetrakispentafluorophenyl)borate
THF	tetrahydrofuran
$[N^nBu_4][PF_6]$	tetrabutylammonium hexafluorophosphate
T	temperature
t	time
PPh_3	triphenylphosphine
UV/vis	ultra violet/visible
η	viscosity
λ	wavelength
XPS	X-ray Photoelectron Spectroscopy

1 Introduction and Aim of Study

1.1 Rhodium complexes in catalytic reactions

Kinetic studies play an essential role in developing improved efficient industrial catalytic processes. The Monsanto process is an important process used for the production of acetic acid, an important industrial chemical. In this process, methanol condenses with carbon monoxide. The reaction takes place in the presence of a catalytic specie, $[Rh(CO)_2I_2]^-$. Originally, cobalt tetracarbonyl iodide, $[Co(CO)_4]I$ was used as catalyst at high CO pressures and temperature (670 atm and 250 ˚C).[1] Later discoveries showed the rhodium dicarbonyl diiodo catalyst to have higher selectivity at milder conditions (30-60 atm and 150-200 ˚C).[2] **Scheme 1. 1** is a schematic representation of the catalytic cycle.[3]

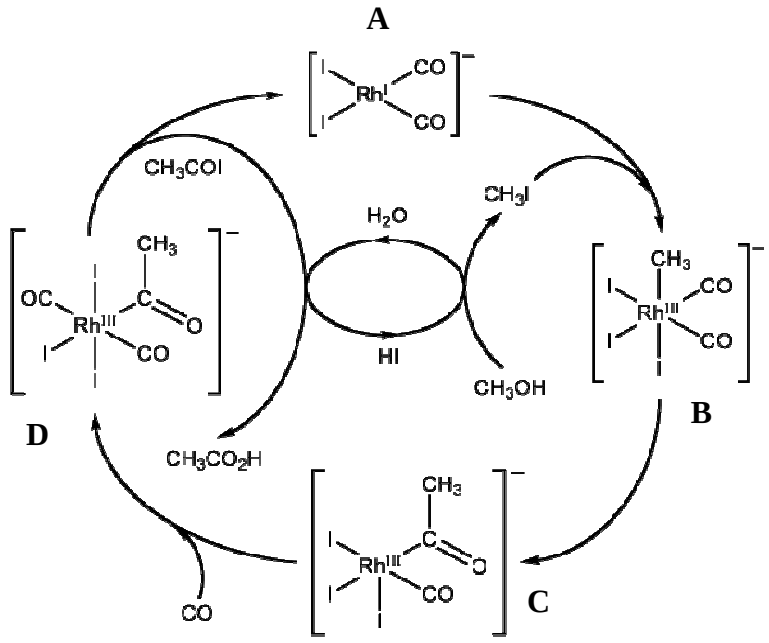

Scheme 1. 1. The Monsanto catalytic cycle to yield acetic acid from methanol. Diagram from J.H. Jones, *Platinum Metals Rev.*, 2000, 44, 94.

There are fundamental steps in the catalytic cycle shown in **Scheme 1. 1**.[4] The catalytic cycle begins with a rapid methanol to methyl iodide conversion, followed by the rate determining oxidative

[1] S. Bhaduri and D. Mukesh, *Homogeneous catalysis: Mechanism and industrial application*, John Wiley and Sons, New York, 2000, 1st edition, p. 56 - 68.

[2] S. Matar, M.J. Mirbach and H.A. Tayin, *Catalysis in Petrochemical Processes*, Kluwer Academic Publishers, 1989, p. 136.

[3] J.H. Jones, *Platinum Metals Rev.*, 2000, **44**, 94.

[4] F.A Cotton, G. Wilkinson and P.G. Gaus, *Basic Inorganic Chemistry*, John Wiley and Sons, New York, 1976, 3rd edition, p. 722.

addition of methyl iodide to the d^8 square planar Rh(I) complex **A** to form a six coordinate rhodium(III)-alkyl complex **B**. A rhodium(III)-acyl complex **C** is then formed after insertion of carbon monoxide between the rhodium-alkyl bond subsequently a new CO is introduced into the metal coordination sphere. Finally **D** reacts to reductively eliminate acetyl iodide and regenerates the original square planar Rh(I) complex. The liberated acetyl iodide then reacts with water to form acetic acid.

Although this process has been very successfully employed over the years it has disadvantages. Complete catalyst recovery after a completed production cycle is economically essential but in practice cannot be achieved. Furthemore, the need to eliminate production of byproducts during the cycle, the instability of rhodium and the high water levels required for the conversion ensures continued research into better new catalysts for this important industrial reaction.

1.2 Polymeric metal complexes

Polysiloxanes are stable inorganic silicon polymers, that are resistant to high temperatures, UV light and oxidation. These organosilicon polymers are used as high performance protective coatings in heat exchanges, ovens, boilers, furnaces and aircraft components.[5,6] Polysiloxanes have been synthesized[7,8,9] but very little has been done regarding the study of derivatives which are functionalized in such a way that they can be coordinated to inorganic species. Rhodium(I) complexes coordinated to poly(methylsiloxanes) containing diphenylphosphine groups were shown to give complexes with catalytic activity towards hydroformylation.[9] Vinyl-functionalized polysiloxanes were prepared and used as supports for polymer-immobilized platinum catalyst for terminal alkene hydrosilylation reactions.[10] Rhodium catalysts coordinated to the same polymeric siloxane carrier were also studied.[10] Other polymer metal complexes like those with azo benzene derivatives were anchored to poly(N-isopropyl-acrylamide) and used as monitors for efficient separation of polymers in biphasic reactions.[11]

---

[5] A. Rahimi and P. Shokrolahi, *Int. J. Inorg. Mat.*, 2001, **3**, 843.

[6] R. G. Jones, *J. Am. Chem. Soc.*, 1997, **38**, 9086.

[7] Z. Li, J. Li, J. Qin, A. Qin and C. Ye, *Polymer*, 2005, **46**, 363.

[8] B. Boutevin, L. Abdellah and M.N. Dinia, *Eur. Polym. J.*, 1995, **31**, 1127.

[9] M.O. Farrell, *J. Organomet. Chem.*, 1979, **172**, 367.

[10] Z.M. Michalska, L. Rogalski, K. Rozga-Wijas, J. Chojnowski, W. Fortuniak and M. Scibiorek, *J. Mol. Cat. A. Chem.*, **208**, 2004, 187.

[11] D.E. Bergbreiter, P.L. Osbourn and C. Li, *Organic letters*, **4**, 2002, 737.

1.3 Aims of the study

With this background, the following goals are set for the study:

1. Synthesis and charaterisation of polysiloxane precursors, disodium siloxane salt, **36**, and silane monomers, **E**, with an active site (halide group) that can be chemically modified. The monomers are shown in **Figure 1. 1**.
2. Synthesis and characterization of high molecular mass polysiloxanes, **F**, by step reaction polymerisation of monomers **36** and **E** described in aim 1.

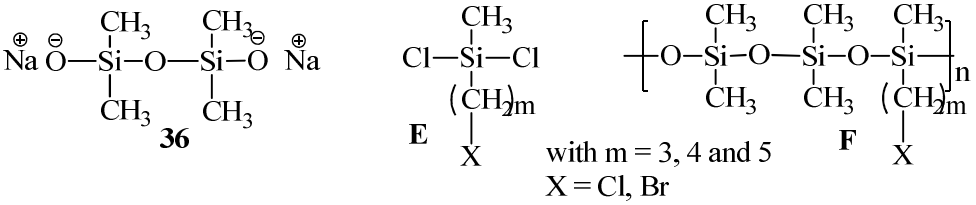

Figure 1. 1. Disodium salt, 36, and silane, E, mononers that may be utilized to form polymer type F.

3. Obtain an anchoring site for a rhodium metal centre by refunctionalization of the halide site into a phosphine group.
4. Anchoring of a rhodium active centre on the phosphine functionalized polysiloxane by reacting it with complexes of the type $[Rh(FcCOCHCOR)(CO)_2]$, where Fc = ferrocenyl, R = CH_3 and CF_3, to give derivatives of structure **G** shown in **Figure 1. 2**.

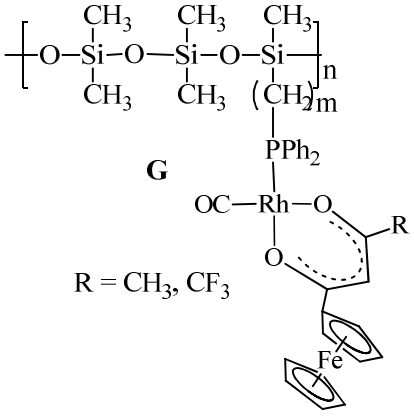

Figure 1. 2. Rhodium phosphine functionalized polysiloxane.

5. An electrochemical study utilizing cyclic voltammetry, square wave voltammetry and linear sweep voltammetry to investigate the electrochemical properties of the new rhodium-

containing polysiloxanes and comparing it to the monomeric rhodium- and ferrocene-containing compounds.

6. A preliminary kinetic study of the oxidative addition reaction of methyl iodide to the rhodium-containing polymers.

2 Literature survey

2.1 Introduction

With respect to goals (1-6) set for this study in Chapter 1, a relevant literature review is provided in this chapter. It covers the synthesis of β-diketones, functionalized polysiloxanes, phosphines and rhodium complexation. Electrochemical and kinetic aspects of rhodium complexes are also reviewed.

2.2 Ferrocene Chemistry

Ferrocene, **1**, is a metallocene, the chemistry of which is well documented with many good reviews.[12,13,14,15,16] Structurally, two cyclopentadienyl ligands sandwich the Fe^{II} metal centre between them. Both cyclopentadienyl ligands are aromatic and due to their good stability and ability to maintain the ligand-metal bond, a wide variety of organic transformations are possible on the cyclopentadienyl ligands, **Scheme 2. 1**.

[12] R.D.A Richard, *J. Organomet. Chem*., 2001, **3**, 47.
[13] M.A. Buretea and T.D. Tilley, *Organometallics*, 1997, **16**, 1507.
[14] E.W. Neuse and M.S. Loonat, *J. Organomet. Chem.*, 1985, **286**, 329.
[15] E.W. Neuse, B.S. Mojapelo and J. Ensling, *Transition Met. Chem.*, 1985, **10**, 135.
[16] E.W. Neuse and F.B.D. Khan, *Transition Met. Chem.*, 1986, **11**, 70.

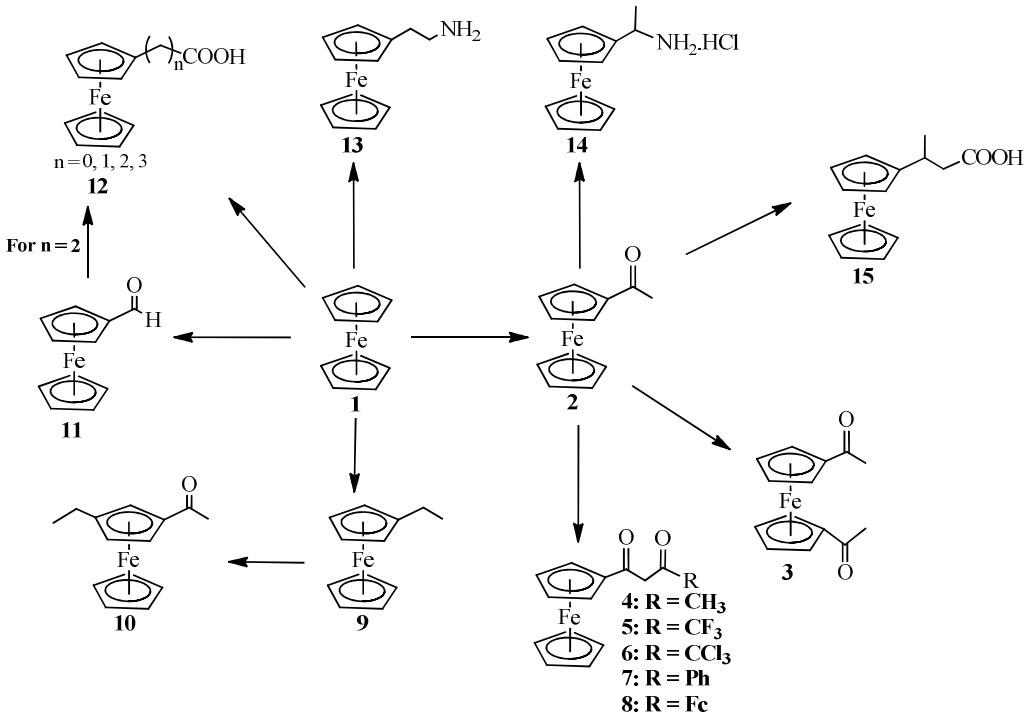

Scheme 2. 1. Conversion of ferrocene to ferrocene derivatives.

Ferrocene, **1**, can undergo Friedel-Crafts catalyzed acetylation. Acetylation can take place very readily on one ring to yield acetylferrocene, **2**, and less readily on both of the rings to give 1,1'-diacetylferrocene, **3**. With the use of acetic anhydride as an acetylating reagent, diacetylation is greatly limited. The catalyst used for acetylation can be any Lewis acid; most frequently used is $AlCl_3$, but the use of H_3PO_4 limits the amount of disubstituted product formed. Base-catalyzed Claisen condensation of **2** with an appropriate ester yields various β-diketones including **4-8**.[17] This particular transformation was exploited in this study. A discussion on β-diketones follows in paragraph 2.3.

Alkylated ferrocene compounds, for example ethylferrocene, **9**, can be synthesized by Friedel-Crafts[18] alkylation of the appropriate alkyl halide with the use of a strong Lewis acid as catalyst. The 1,2'-disubstitution product, **10**, can be obtained by acetylation of **9** on the same cyclopentadienyl ring due to the activation of the substituted cyclopentadienyl ring by the electron-donating alkyl group. Ferrocenecarboxaldehyde, **11**, may be prepared by treating ferrocene directly with N-

17 W.C. du Plessis, T.G. Vosloo and J.C. Swarts, *J. Chem. Soc. Dalton Trans.*, 1998, 2507.
18 M. Vogel, M. Rausch and H. Rosenberg, *J. Org. Chem.*, 1957, **22**, 1016.

methylformamide[19] and phosphorus oxychloride, or by reacting it in the presence of aluminium chloride with 1,1-dichloromethyl ethyl ether.[20]

Ferrocene can also undergo metalation with n-butylithium to give monolithiated and dilithiated ferrocene product mixtures. The monolithiated ferrocene compound can be converted further to yield ferrocenoic acid,[21] **12** (**n=0**), via a carbonation reaction. N,N-dimethylaminomethylferrocene methiodide can be cyanated with potassium cyanide to yield ferrocenylacetonitrile, hydrolysis of this nitrile functional group ultimately liberates ferrocenylacetic acid,[22] **12** (**n=1)**. 3-Ferrocenylpropanoicacid, **12** (**n=2**), and 3-ferrocenylbutanoic acid, **15**, can be respectively prepared by reacting ferrocenecarboxaldehyde[23] and acetylferrocene with malonic acid followed by hydrogenation of the obtained intermediates in each case. Clemmensen reduction of 3-ferrocenoylpropanoicacid also gives 4-ferrocenylbutanoic acid, **12 (n=3)** as product**.** Lithiated ferrocene compound have also been used for synthesizing aminoferrocene, **13**, by reaction with methoxyamine.[24] 1-Ferrocenyethylamine, **14**, can be synthesized from ferrocene in multiple steps from acetylferrocene utilizing cyano borohydride as the reducing agent.[25]

2.3 Synthesis of β-diketones

β-Diketones are very well known as ligands for most metals. [26,27,28] They have found applications in catalysis[29] and extraction of metals into organic solvents.[30] It has been shown that β-diketone complexes with rhodium(I) and rhodium complexes of ferrocene-containing β-diketones show appreciable antineoplastic activity.[31]

---

19 P.J. Graham, R.V. Lindsey, G.W. Parshall, M.L. Peterson and G.M. Whitman, *J. Am. Chem. Soc*., 1957, **79**, 3416.

20 P.L. Pauson and W.E. Watts, *J. Chem. Soc*., 1962, 3880.

21 R.A. Benkeser, D. Goggin and G. Schroll, *J. Am. Chem. Soc*., 1954, **76**, 4025.

22 C.U. Jr. Pittman, R.L. Voges and R. William, *Macromolecules*, 1971, **4**, 291.

23 G.D. Broadhead, J.M. Osgerby and P.L. Pauson, *J. Chem. Soc*., 1958, 650.

24 E.M. Acton and R.M. Silverstein, *J. Org. Chem*., 1959, **24**, 1487.

25 K. Heinze and M. Schlenker, *Eur. J. Inorg. Chem*., 2004, 2974.

26 F.A. Cotton, G. Wilkinson, C.A. Murillo and M. Bochmann, *Advanced Inorganic Chemistry*, 6th edition, John Wiley & Sons, New York, 1999, p. 479 – 480.

27 J.G. Leipoldt, S.S Basson, G.J. Vanzyl and G.J.J Steyn, *J. Organomet. Chem*.,1991, **418**, 241.

28 V. G. Gnanasoundari and K. Natarajan, *Transition Metal Chemistry*, 2005, **30**, 433.

29 W.R. Cullen, S.J. Rettig and E.B. Wickenheizer, *J. Organomet. Chem.*, 1989, **370**, 141.

30 R. Cierpiszewski, D. Rusińska-Roszak, J. Szymanowski, W. Mickler and E. Uhlemann, *J. Radioanal. Nuc. Chem.*, 1998, **71**, 228.

31 G. Sava, S. Zorzet, L. Perissin, G. Menstroni, G. Zassinovich and A. Bontempi, *Inorg. Chim. Acta*, 1987, **137**, 69.

β-Diketones are most often synthesised by Claisen condensation[32,33] in the presence of a base. The preparation involves the reaction of carbonyl-containing compounds, for example a ketone and an acetyl group (ester, acid chloride or acid anhydride) in a basic medium. The general reaction can be written as

$$\mathbf{RCOX + HCH_2COR' \xrightarrow{base} RCOCH_2COR' + HX}$$

(X = OCOR, Cl, OR)

The mechanism involves the removal of an acidic α-proton from the ketone by a base to form a carbanion, which is stabilized by a Li^+ cation. This is followed by the nucleophillic attack by the negatively charged α-carbon on the carbonyl carbon of the ester and the subsequent loss of an ethoxide ion to form a β-diketone. The strong basic ethoxide ion removes a methine proton from the newly-formed acidic β-diketone. After treatment with acid the free β-diketone is regenerated. Bases that have been used for the removal of the α-hydrogen include NaOH (weakest base and seldom used), alkyloxides (R-OM, M = alkalimetal), hydrides, alkalimetals, simple amides[34] (MNH_2, M = alkalimetals, these are the strongest bases) or a sterically hindered base such as lithiumdiisopropylamide (LDA). The mechanism using lithium diisopropylamide[29] (LDA) and R_2COOEt as base and ester respectively is shown in **Scheme 2. 2**.

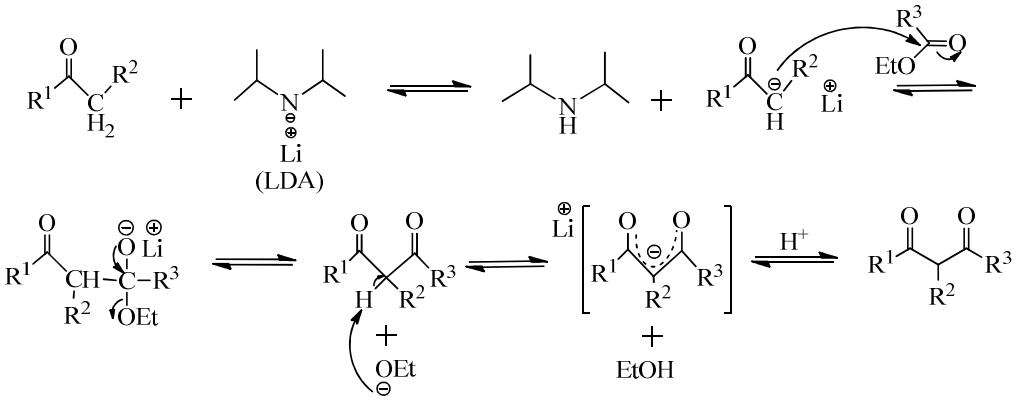

Scheme 2. 2. Mechanism for the formation of a β-diketone, R^2 = H in most cases.

A variety of factors can influence the synthesis of a β-diketone. The difficulty with which the α-hydrogen of the starting ketone is removed by the base is determined by the pK_a of the starting ketone. Generally, the more-electron donating the R^1 and R^2 groups are in the ketone, $R^1C(O)CH_2R^2$, the stronger the base required to remove the α-hydrogen. The nucleophillic attack by

---

32 C. R. Hauser, F. W. Swamer and J. T. Adams, *Organic Reactions*, John Wiley and Sons, New York, 1954, **8**, p. 59, 98.

33 A. I. Vogel, *Practical Organic Chemistry including Qualitative Organic Analysis*, 3rd edition., Longman, London, 1977, p. 864-865.

34 J.T. Adams and C. R. Hauser, *J. Am. Chem. Soc*., 1944, **66**, 1220.

the carbanion on the ester and formation of the salt (see **Scheme 2. 2**) is also influenced by steric properties of the R^2 and R^3 groups. Generally the rate of acylation of a ketone becomes slower with bigger R^2 and R^3 groups.[35]

2.4 Synthesis of ferrocene-containing β-diketones

When synthesising ferrocene-containing β-diketones, active strong bases such as alkali metal amides and alkoxides ensure the best yields during the Claisen condensation reaction between an appropriate ester and acetylferrocene[36] as shown in **Scheme 2. 3**. Since Hauser and colleagues synthesized the first ferrocene-containing β-diketone, $FcCOCH_2COPh$ with only 22 % yield[36] utilizing potassium amide as base, new synthetic paths have improved yields substantially.[37,38,39] The influence of a hindered base like lithium diisopropylamide (LDA) was shown by Cullen[29] to give a yield of 38% for ferrocenoylacetone[29]. Weinmayr[40] synthesized ferrocenoylacetone and ferrocenoyltrifluoroacetone in 29 and 80 % yields respectively utilizing sodium methoxide as base. These methods were extended by Du Plessis and co-workers[17] for further synthesis of other ferrocene-containing β-diketones where R = CH_3, CF_3, CCl_3, Fc, C_6H_5 as shown in **Scheme 2. 3**.

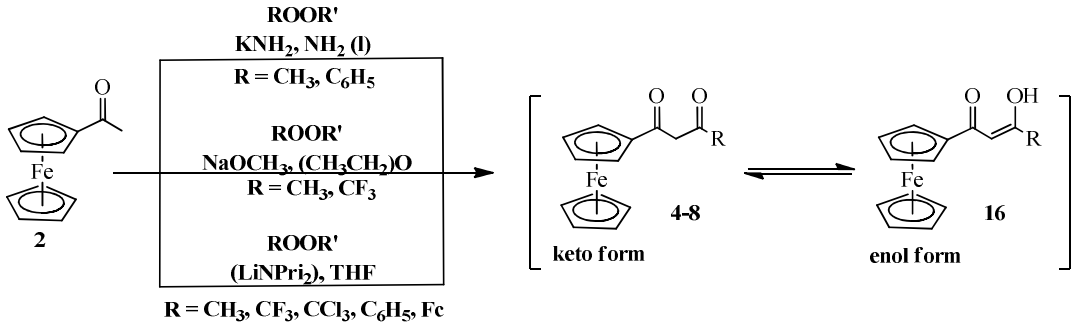

Scheme 2. 3. Synthesis of ferrocene-containing β-diketones 2-8 with Fc = ferrocenyl

2.5 Keto-enol tautomerism of β-diketones

Hydrogen bonding and proton transfer are two important aspects influencing the reactivity of compounds.[41, 42] β-Diketones exhibit both these features and they represent the prime example of keto-enol tautomerism. Keto-enol isomerization involves the transfer of a methine proton from the

[35] C.R. Hauser, F.W. Swamer and J.T. Adams, *Organic reactions*, John Wiley & Sons, 1954, **8**, p. 65.
[36] C.R. Hauser and C.E. Cain, *J. Org. Chem*., 1958, **23**, 1142.
[37] C.M. Zakaria, C.A. Morrisson, D. McAndrew, W. Bell and C. Glidewell, *J. Organomet. Chem*., 1995, **485**, 201.
[38] W.R. Cullen, S.J. Rettig and E.B. Wickenheiser, *J. Mol. Catal*., 1991, **66**, 251.
[39] C.E. Cain, T.A. Mashburn and C.R. Hauser, *J. Org. Chem*., 1961, **26**, 1030.
[40] V. Weinmayr, *Naturwissenschaften*, 1958, **45**, 311.
[41] M. Calvin and K.W. Wilson, *J. Am. Chem. Soc.*, 1945, **67**, 2003.
[42] R.H. Holm and F.A. Cotton, *J. Am. Chem. Soc.*, 1958, **80**, 5658.

keto-form to an oxygen atom to generate the more stable enol form. The dominant enol isomer is determined by electronic[43] and resonance factors.[44] Enol isomers of ferrocene-containing β-diketones in particular can be stabilized by various canonical forms involving the ferrocenyl groups as described elsewhere.[45] In the absence of an enol form, a β-diketone is unable to coordinate to metals. The keto-enol equilibrium position is influenced by several features such as electronic effects of the R-substituents (R-CO-CH_2-CO-R) as well as the nature of the solvent.[46,47,48]

It has been found that the most dominant form of ferrocene-containing β-diketones in solution is such that the C=O group is adjacent to the ferrocenyl group and that the enol C-OH group is adjacent to the R side group in Fc-CO-CH=C(OH)-R[17] (see **Scheme 2. 3**). This is due to the different electron-donating properties of the ferrocenyl and R-group. If the R-group is more electronegative than the ferrocenyl group, the character of the carbon atom adjacent to the ferrocenyl group becomes more negative than the carbon atom next to the R group. This makes the enol isomer **16** shown in **Scheme 2. 3** to be more dominant. Amongst others, techniques such as ^{1}H NMR spectroscopy,[46,47] kinetics,[49] infrared spectroscopy [50] and energy of enolization[51] have also been used to study keto-enol tautomerisation. Some physical properties such as group electronegativities χ_R, acid dissociation constant pK_a' and % enol in solution of various ferrocene-containing β-diketones compounds are shown in **Table 2.1.**[17]

Table 2.1. pK_a' values and % enol tautomer of various ferrocene-containing β-diketones ($FcCOCH_2COR$).

R	χ_R	pK_a'	% Enol in solution
CF_3	3.01	7.15 (0.02)	97
CH_3	2.34	10.01 (0.2)	78
C_6H_5	2.21	10.41 (0.02)	91
Fc	1.87	13.1 (0.1)	67

43 M.P. Noskova and N.N. Kazanova, *J. Struct. Chem*, 1969, 10, 610.
44 G.K. Schweitzer and E.W. Benson, *J. Chem. Eng. Data*, 1968, **13**, 452.
45 W.C. du Plessis, J.J.C. Erasmus, G.J. Lampretch, J. Conradie, T.S. Cameroon, M.A.S. Aquino and J.C. Swarts, *Can. J. Chem*, 1999, **77**, 378.
46 H.S. Jarret, M.S. Sadler and J.N. Shoolery, *J. Chem. Phys.*, 1953, **21**, 2092.
47 L.W. Reeves, *Can. J. Chem.*, 1957, **35**, 1351.
48 S. Moon and Y. Kwon, *Magn. Reson. Chem*., 2001, **39**, 89.
49 R.J. Irving and M. A. V. Ribeiro da Silva, *J. Chem. Soc. Dalton Trans*, 1998, 798
50 S. Bratoz, D. Hadzi and G. Rossmy, *Trans. Faraday Soc*., 1954, **52**, 464.
51 G. W. Wheland, *Advanced Organic Chemistry*, 3rd edition, John Wiley and Sons, New York, 1960.

Gordy scale group electronegativity values, χ_R,[52,53] have been reported for the R-groups. Group electronegativity expresses the combined tendency of a group of atoms to attract bonding electrons involved in a covalent bond as a function of the number of valence electrons, *n*, and the covalent radius, *r*. It is an important parameter which can be used to quantify the electron density around a metal centre. The group electronegativity, χ_R, has been shown to have a linear relationship with other parameters such as pK_a' [74] and ferrocenyl group formal reduction potential[45] (in V vs. Fc/Fc^+ in CH_3CN) for the β-diketone $FcCOCH_2COR$ (see **Figure 2. 1**) By coordinating either electron-donating or electron-withdrawing ligands to a metal like rhodium, the electron density on the metal centre can be manipulated as desired.[17,54]

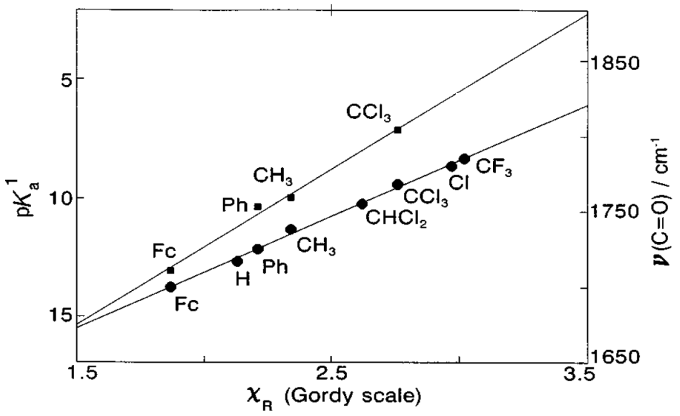

Figure 2. 1. Linear relationship between group electronegativities, χ_R and pK_a' values (upper graph) of the ferrocene-containing β-diketones of the type $FcCOCH_2COR$, as well as the carbonyl stretching frequencies ν(CO) (lower graph) of the methyl esters of the type $RCOOCH_3$. Ethyl ester was used for R = CF_3. R-groups are shown on each plot. Diagram duplicated from W.C. du Plessis, T.G. Vosloo and J.C. Swarts, *J. Chem. Soc. Dalton Trans.*, 1998, 2507.

2.6 Rhodium catalysis in oxidative addition

2.6.1 Introduction on rhodium

The platinum group metals iridium, palladium, platinum, ruthenium and rhodium are well known for their extraordinary properties, such as catalytic behaviour, resistance to corrosion, high melting points and high lustre. They are utilized in the electrical, chemical and petroleum industries.[55]

[52] P.R. Wells, *Progress in Physical Organic Chemistry*, John Wiley and Sons, New York, 1968, **6**, p. 111-145.
[53] R.E. Kagarise, *J. Am. Chem. Soc*., 1955, **77**, 1377.
[54] K.C. Kemp, E. Fourie, J. Conradie, J.C. Swarts, *Organometallics*, 2008, **27**, 353.
[55] L.B. Hunt and F.M. Lever, *Platinum Metals Rev.*, 1969, **13**, 126 – 136.

Rhodium is used as a catalyst in the Monsanto process[56,57] for its selectivity during the carbonylation of methanol into the acetic acid. It is also used in catalytic convertors for reduction of nitrogen oxide in vehicle emissions, which promotes a "green planet". Rhodium is a rare silvery white metal, known for its hard and brittle property. It is resistant to acids but reacts with oxygen to form rhodium(III) oxide, Rh_2O_3, at high temperatures. It can also form chloride complexes like $[Rh(Cl_6)]^{3-}$ when heated with chlorine or metal chlorides. Rhodium exists in several oxidation states 0, I, II and III being the most common. Typical rhodium(III) complexes are stable, low spin, octahedral and diamagnetic compounds. The rhodium(I) metal centre in complexes has been shown to undergo easy oxidation. In general the larger a transition metal and the lower its oxidation state, the more reactive the metal is towards oxidative addition. This oxidative addition tendency of transition metals is shown in **Figure 2. 2.**

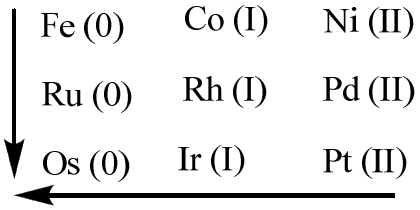

Figure 2. 2. Tendency of transition metals to undergo oxidative addition. It increases from top to bottom and right to left.

2.6.2 Synthesis of rhodium complexes

Two methods have been used for the synthesis of rhodium(I) dicarbonyl complexes containing β-diketonato ligands,[36,39,58] as shown in **Scheme 2. 4**. Chloro-bridged dimeric rhodium intermediates, $[Rh_2(Cl)_2(CO)_4]$, **17**, and $[Rh_2(Cl)_2(cod)_2]$, **18**, can be formed from rhodium trichloride, $RhCl_3.xH_2O$. In method 1, direct interaction between dimer **17** and a β-diketone gives the rhodium β-diketonato dicarbonyl complex [Rh(β-diketonato)(CO_2)], **23-26**, as product. Alternatively, dimer **18** is converted to [Rh(β-diketonato)(cod)], **19-22**, *via* synthetic method 2. In an equilibrium process, **19-22** undergo carbon monoxide exchange in solution to liberate pure rhodium(I) complex, **23-26**, at the point of carbon monoxide saturation. Reaction of **23-26** with an equivalent amount of PPh_3 gives phosphine rhodium complex, [Rh(β-diketonato)(CO)(PPh_3)], **27-30**, as product.

---

56 (a) P.M Maitlis, A. Haynes, G.J Sunley and M.J. Howard, *J. Chem. Soc. Dalton Trans*., 1996, 2187.
(b) A. Haynes, P.M. Maitlis, G.E. Morris, G.J. Sunley, H. Adams, P.W. Badger, C.M. Bowers, D.B. Cook, P.I.P. Elliot, T. Ghaffer, H. Green, T.R. Griffin, M. Payne, J.M. Pearson, M.J. Taylor, P.W. Vickers and R.J. Watt, *J. Am. Chem. Soc*., 2007, **126**, 2847.

57 S. Matar, M.J. Mirbach and H.A. Tayim, *Catalysis in Petrochemical Processes*, Kluwer Academic Publishers, Dordrecht, The Netherlands, 1989, p. 136.

58 J. Conradie, G.J. Lamprecht, S. Otto and J.C. Swarts, *Inorg. Chim. Acta.*, 2002, **328**, 191.

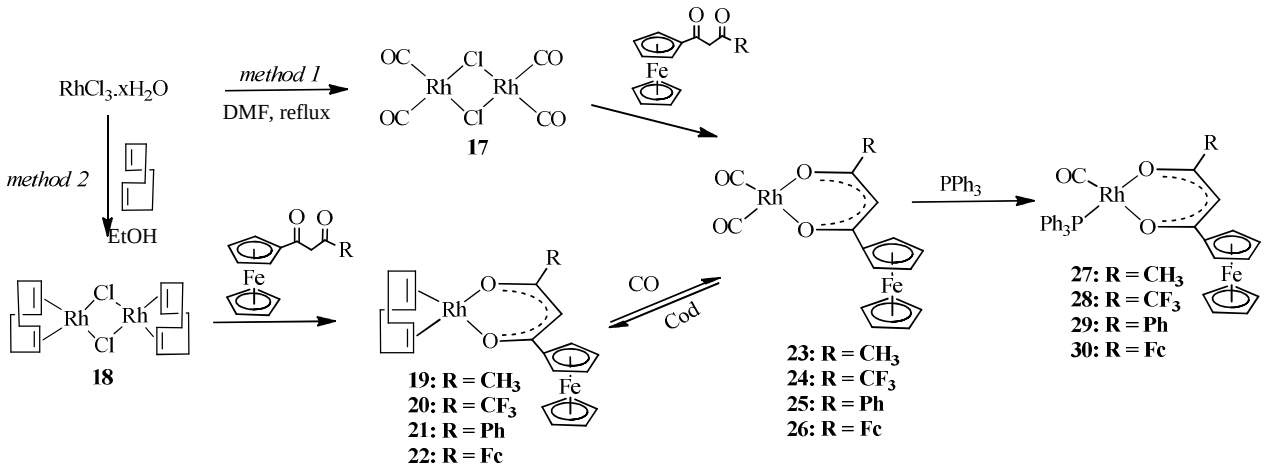

Scheme 2. 4. Synthesis of rhodium(I) complexes, [Rh(β-diketonato)(CO_2)], 23-26, and [Rh(β-diketonato)(CO)(PPh_3)], 27-30, using method 1 and 2, with R = CH_3, CF_3, C_6H_5 and Fc, Fc = ferrocenyl.

2.6.3 Rhodium in catalysis

Rhodium has been widely used in homogeneous catalysts for a large range of industrial processes. Amongst these a few classics exist like olefin and acetylene hydrogenation by means of a Wilkinson's catalyst,[59] [$RhCl(PPh_3)_3$], olefin and alkene hydroformylation utilizing [$Rh(CH_3COCHCOCH_3)(CO)_2$][60] and [$RhH(CO)(PPh_3)_2$][61] catalysts respectively and the production of acetic acid by methanol carbonylation in the presence of a [$Rh(CO)_2(I)_2$] catalyst[56] (the Monsanto process). These processes have induced research into developing more efficient catalytic systems with high activity and regioselectivity. It is known that [$Rh(CO)_2(I)_2$] accelerates the oxidative step in the catalytic cycle of methanol carbonylation.[56] By changing the ligand coordinated to the catalytic metal centre, the metal centre itself and the solvent medium, the rate of oxidative addition may be altered.

2.6.4 Influence of a phosphine ligand on catalysis

Recent research has shown that ligands that are electron-donating increase the rate of oxidative addition reactions. Phosphine ligands in particular have generated great interest with the synthesis of different classes of organophosphines to improve the nucleophilic character of a metal centre.

59 C.A. Tolman, P.Z. Meakin, D.L. Lindner and J.P. Jesson, *J. Amer. Chem. Soc*., 1974, **96**, 2762.
60 M.G. Pedrós, A.M. Masdea-Bultó, J. Bayardon and D. Sinou, *Catal. Lett*., 2006, **107**, 205.
61 J. D. Antwoord, *Coord. Chem. Rev*., 1988, **83**, 93.

Phosphines have the general formula PR_3 where R = aryl, alkyl, halide.[62,63] In general, strong σ–donor ligands such as phosphines are known to facilitate oxidative addition whereas π-acceptors such as alkenes, CO or CN^- suppress oxidative addition rates.

Bond formation of phosphine ligands (PR_3) with a metal is achieved by σ–donation of the lone pair on the phosphine to an empty metal orbital or by π–backdonation from the metal p or d orbital to an empty phosphine ligand antibonding orbital as shown in **Figure 2. 3**. A few phosphine ligand examples that have been studied with the objective of improving the oxidative addition step in catalytic cycles will be discussed.

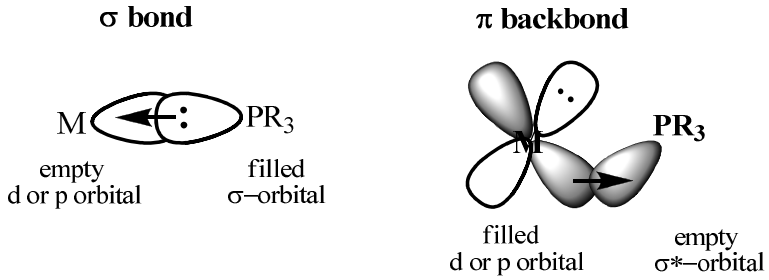

Figure 2. 3. Bond formation between a metal (M) and a phosphine ligand (PR_3).

Following the discovery of the original hydroformylation catalyst $HCo(CO)_4$, **31**, it was demonstrated that by replacing one of the CO ligands with an electron-donating alkylated phosphine ligand in this cobalt-catalyzed process, as shown by **32** in **Scheme 2. 5**, caused dramatic changes in the regioselectivity and the reaction rate.[64] Low partial pressures of CO were required to stabilize the catalyst by preventing precipitation of Co metal at high temperatures. Subsequently, hydrogenation of aldehydes to alcohols by the phosphine-containing catalyst was also shown to be an effective reaction. However better hydroformylation ability of the phosphine-containing catalyst also resulted in increased formation of alkane side products instead of aldehydes. Hydroformylation reactions are catalyzed by rhodium-based phosphine-containing catalysts. Water-soluble phosphine ligands have the additional advantage of easier catalyst separation from the formed product.[65]

62 C.A. Tolman, *Chem. Rev*., 1977, **77**, 313.
63 C.A. Tolman, *J. Am. Chem. Soc*., 1970, **92**, 2953.
64 L.H. Slaugh and R.D. Mullineaux, *J. Organomet. Chem*., 1968, **13**, 469.
65 F. Joo, Z. Toth and M.T. Beck, *Inorg. Chim. Acta*., 1977, **25**, L61.

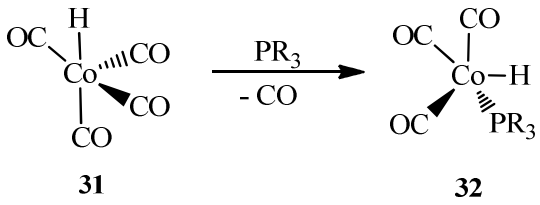

31 **32**

Scheme 2. 5. Conversion of $HCo(CO)_4$ to $HCo(CO)_3(PR_3)$

Ether-phosphine ligands of the form, $Ph_2P(CH_2)_nOR$ where n=1, R = CH_3, **33**, and n = 2, R = C_2H_5, **34**, have been reported[66]. They are synthesized by complexing ether-phosphine ligands with $[Rh(CO)_2Cl]_2$. The reactivity of these rhodium complexes was tested by reacting them with CH_3I and I_2. They were shown to first undergo oxidative addition of CH_3I and I_2 followed by CO insertion to yield rhodium (III) acyl species, $[Rh(CO)(COCH_3)(Cl)(I)(P\cap O)$ and $[Rh(CO)(Cl)(I_2)(P\cap O)$, respectively where $(P\cap O)$ represents an ether-phosphine ligand. The catalytic activity in methanol carbonylation to acetic acid was also studied. Conversions of 37% and 100% for **33** and **34** were achieved respectively. Many more examples of ether-phosphine multidentate ligands are known.[67,68]

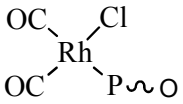

33: $P\sim O = PPh_2CH_2OCH_3$

34: $P\sim O = PPh_2(CH_2)_2OC_2H_5$

Figure 2. 4. Dicarbonyl rhodium(I) complexes containing ether-phosphine ligands.

The influence of phosphine bulkiness in rhodium(I) complexes , $[Rh(cupf)(CO)(PX_3)]$ with cupf = cupferron, PX_3 = PCy_3, PPh_3, P(o-Tol)$_3$, $PPh_2C_6F_5$, P(*p*-ClC_6H_4)$_3$ and P(*p*-MeO C_6H_4)$_3$ were also studied by Basson[69] and co-workers. The reactivity of these complexes was studied by varying the phosphine ligand PX_3 and solvent during oxidative addition of CH_3I in acetone. The reaction rates for both PX_3 = (PCy_3) and P(*o*-Tol)$_3$ were smaller than those of more bulky ligand, P(*p*-MeO C_6H_4)$_3$. $PPh_2C_6F_5$ gave the smallest rate compared to all six ligands. The oxidative addition followed pseudo-first order kinetics in CH_3I concentration and the rate constants can be written as

66 D. Pankaj, S. Manab, K. Nandini, K. Dilip and K.D. Dipak, *Appl. Organometal. Chem*., 2002, **16**, 302.
67 N.W. Alcock, J.M. Brown and J.C. Jeffrey, *J. Chem. Soc., Chem. Commun*, 1974, 829.
68 E. Lindner and E. Glaser, *J. Organomet. Chem*., 1990, **391**, C37.
69 S.S. Basson, J.G. Leipoldt, A. Roodt and J.A. Venter, *Inorg. Chim. Acta*., 1987, **128**, 31.

$$k_{obs} = k_2 + k_1 [CH_3I]$$

where k_1 and k_2 represent the rate of formation of the 5-coordinate intermediate and the solvent-stabilized intermediate respectively.[69] A study on [Rh(acac)(CO)(PX_3)] complexes also showed that smaller phosphines react slower.[70,73] The electron-donating acetylacetone (acac) ligand also accelerated the rate of oxidative addition compared to the cupferron ligand. A discussion on the influence of β-diketonato ligands towards oxidative addition follows in paragraph 2.6.5.

2.6.5 Influence by the β-diketonato ligand on oxidative addition

A large variety of rhodium(I) complexes of type [Rh(β-diketonato)(CO)(PPh_3) have been further studied by Basson[71,72,73] for the oxidative addition of methyl iodide. In these complexes, the electronegativity on the β-diketonato bidentate ligand was varied by introducing different side-groups on the ligand. The kinetics of the β-diketonato side groups CH_3 and CH_3, CF_3 and CH_3, CF_3 and $CH(CH_3)_2$ and lastly CF_3 and CF_3 were studied.[71]

Swarts[74] studied oxidative addition of methyl iodide to ferrocene-containing β-diketonato carbonyl phosphine rhodium(I) complexes of the type [Rh(FcCOCHCOR)(CO)(PPh_3)] where Fc = ferrocenyl and R = CF_3, CH_3, Ph and Fc, **Figure 2. 5**. It was found that a ferrocenyl group on a β-diketonato ligand enhances the acyl formation rate of new Rh^{III}-acyl specie as well as the following CO insertion and deinsertion rate significantly.[75] FTIR, UV/vis and NMR spectroscopic techniques were used to measure the kinetics.

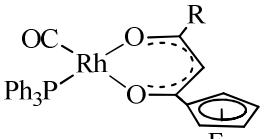

27: R = CH_3
28: R = CF_3
29: R = Ph
30: R = Fc

Figure 2. 5. Ferrocene-containing β-diketonato carbonyl phosphine rhodium(I) complexes.

---

70 J.G. Leipoldt, S.S. Basson and L.J. Botha, *Inorg. Chim. Acta.*, 1990, **168**, 215.
71 S.S. Basson, J.G. Leipoldt and J.T. Nel, *Inorg. Chim. Acta.*, 1984, **84**, 167.
72 G.J.J. Steyn, A. Roodt and J.G. Leipoldt, *Inorg. Chem.*, 1992, **31**, 3477.
73 .S. Basson, J.G. Leipoldt, J.G., A. Roodt, J.A. Venter and T.J. van der Walt, *Inorg. Chim. Acta.*, 1986, **119**, 35.
74 J. Conradie and J.C. Swarts, *Organometallics*, 2009, **28**, 1018.

The study showed the mechanism of oxidative addition consists of three sets of reactions each involving two isomers that are distinctly different. The mechanism begins with an oxidative addition of methyl iodide to yield Rh(III)-alkyl, shown by the disappearance of an IR carbonyl stretching frequency of the Rh(I) specie (at about 1980-2000 cm^{-1}) and the appearance of the Rh(III)-alkyl carbonyl stretching frequency (at about 2050-2100 cm^{-1}). This is followed by different isomerizations involving CO insertion between the Rh-CH_3 bond to yield a Rh(III)-alcyl specie which is identified by an IR carbonyl stretching frequency in the region 1700-1750 cm^{-1}. The oxidative addition reaction was shown to follow first order kinetics with respect to methyl iodide concentration. The rhodium complex where R = Fc was shown to undergo oxidative addition at the fastest rate. Very slow rates were observed for R = CF_3.

These rates were found to be proportional to the electron density of the rhodium(I) centre with a linear relationship between ln k_1 and pK_a, where k_1 is the first-order rate constant for the first reaction set (see **Scheme 2. 6**). Supplementary to the discussion in paragraph 2.5, it was confirmed that the rate of oxidative addition of these complexes with different R-substituents is proportional to the group electronegativity, χ_R, of both the ferrocenyl group and R-group. A general mechanism for the methyl iodide oxidative addition to these Rh(I) complexes is shown **Scheme 2. 6**.[74] Complex **28** (**Figure 2. 5**) is used as an example.

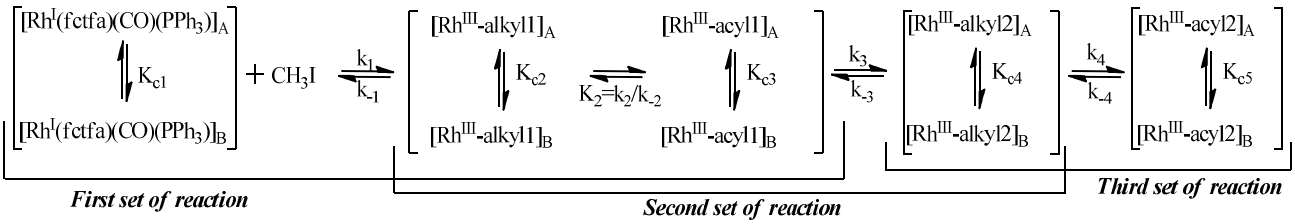

Scheme 2. 6. General mechanism for the methyl iodide oxidative addition on [Rh(FcCOCHCOCF$_3$)(CO)(PPh$_3$)] type complexes, where fctfa = (FcCOCHCOCF$_3$)$^-$.

2.7 Macromolecular compounds: Silicon derivatives

2.7.1 Introduction to polymers

Polymers are large molecular weight materials that consist of repeating structural units (monomers) bound together to form large macromolecules. Short oligomer chains can also be formed, especially

[75] J. Conradie, G.J. Lamprecht, A. Roodt and J.C. Swarts, *Polyhedron*, 2007, **26**, 5075.

in condensation reactions.[76] Copolymerization reactions can result in various types of distribution patterns namely random, alternating, block and graft polymerization. **Figure 2. 6** demonstrates these distributions where A and B represents two different monomers.

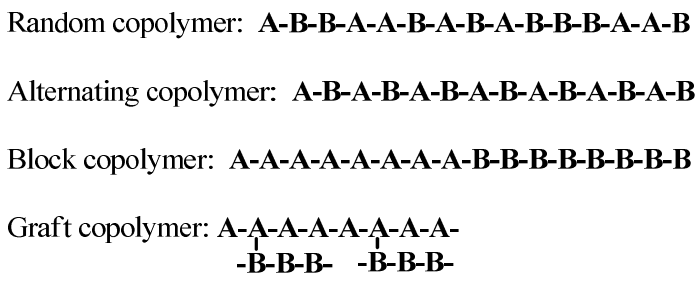

Figure 2. 6. Types of monomer distributions that may arise during a copolymerization process.

Although major breakthroughs in catalysis have been made since the discovery of the Monsanto catalyst, $[Co(CO)_4]I$, efforts in preserving excellent catalytic stability, obtaining complete conversions of the substrate, 100% selectivity of the desired product and easy complete catalyst recovery, remains an objective of many researches. This study intends to establish whether incorporating catalytic specie to a macromolecular support system influences catalytic activity. Polymeric supports that have been investigated for this purpose in the past include organic and inorganic supports such as cross-linked polymers like polysiloxane,[77,78,79,80] polystyrene,[81] and phosphazene[82] or inorganic surfaces like silica.[83] For the purpose of this study, silicon-containing polymers were synthesized with grafted side chains having a random distribution. Polysiloxanes consist of R_2SiO repeating units where R can be a hydrocarbon group or a hydrogen atom as shown in **Figure 2. 7**. The large Si-O bond lengths and angle, 1.63 Å and 130° respectively give polysiloxanes more flexibility compared to C-C polymers having C-C bond length 1.54 Å and angle 112°. This enables better movement (rotation) and easier conformation changes around the silicon-oxygen bond.

---

76 Odian G, *Principles of Polymerization*, 4th edition, John Wiley & Sons, New Jersey, 2004, p. 1-9.

77 M.O. Farrel and C.H. van Dyke, *J. Organomet. Chem*., 1979, **172**, 367.

78 H. Frank, I. Abe and G. Fabian, *J. High. Resol. Chromatogr.*, 1992, **15**, 444.

79 H. Frank, I. Abe and T. Nishiyama, *J. High. Resol. Chromatogr*., 1994, **17**, 9.

80 M. Herbet, F. Montilla and A. Galindo, *Polyhedron*, 2010, **29**, 3287; *Dalton. Trans*., 2010, **39**, 900; *Organometallics*, 2009, **28**, 2855; *Inorg. Chem. Commun*., 2007, **10**, 735.

81 W.T. Ford, J. Lee and M. Tomoi, *Macromolecules*, 1982, **15**, 1246.

82 G.A. Carriedo, F.J.G. Alonso, P.A. González, C.D. Valenzuela and N.Y. Sáez, *Polyhedron*, 2002, **21**, 2579.

83 M.K. Dongare, V.V. Bhagwat, C.V. Ramana and M.K. Gurjar, *Tetrahedron Letters*, 2004, **45**, 4759.

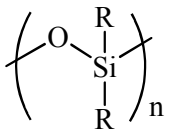

Figure 2. 7. A dialkylated siloxane repeating unit in polysiloxanes.

Due to the strength of the silicon-oxygen bond, polysiloxanes tend to be chemically inert except when exposed to very low pH conditions. They possess extreme resistance to high temperatures (up to 250 ˚C), which makes them a good carrier choice for extreme environments such as those in catalysis.

2.7.2 Polysiloxane polymer backbone

High molecular weight and oligomeric polysiloxanes can be typically synthesized from cyclic organosilicon compounds by acid or base catalyzed ring-opening polymerization reactions.[84] To open these cyclic compounds two methods namely, anionic[85] and cationic[86] polymerization can be utilized although the anionic polymerization reaction has been shown to be more important in designing polymeric structures. Typical cyclic siloxanes such as hexamethylcyclotrisiloxane and octamethylcyclotetrasiloxane, **35**, can be polymerized by cleavage of the Si-O bond by means of a base to form anionic oligosiloxanolates, **36**, bearing ionic terminal groups.[87] The ease of this bond cleavage is affected by the stability of the cyclic siloxane. For example, hexamethylcyclotrisiloxane has a large degree of ring strain and therefore lower activation energies are needed to achieve ring opening. Conversely more stable cyclic siloxanes with more than three siloxane units like **35**, ring opening requires more stringent reaction conditions. Hence weaker basic ring opening initiators are used for hexamethylcyclotrisiloxane than for **35**. The ring-opening mechanism of **35** utilizing NaOH as example is shown in **Scheme 2. 7**. Initiation begins with a nucleophilic attack by the ⁻OH ionic specie on the electropositive silicon atom within the ring followed by loss of water to form a reactive linear disiloxanolate specie. The disiloxanolate specie undergoes further attack by the ⁻OH ionic specie and dehydration to yield a more stable disodium salt **36**. The crystal structure of **35** has been reported to contain crystal hydrates.[88]

---

84 J.E. McGrath, *ACS Symposium Series*, 1985, **286**, 1.
85 I. Manners, *Adv. Organomet. Chem*., 1995, **37**, 131.
86 A. Kowalski, A. Duba and S. Penczek, *Macromolecules*, 2000, **33**, 7359.
87 D.T. Hurd, R.C. Osthoff and M.L. Corrin, *J. Am. Chem. Soc*., 1954, **76**, 249.
88 Y.T. Struchkov, V. M. Kopylov, A. M. Muzafarov, P. L. Prikhod and A. A. Zhdanov, *Structure*, 1982, **23**, 63.

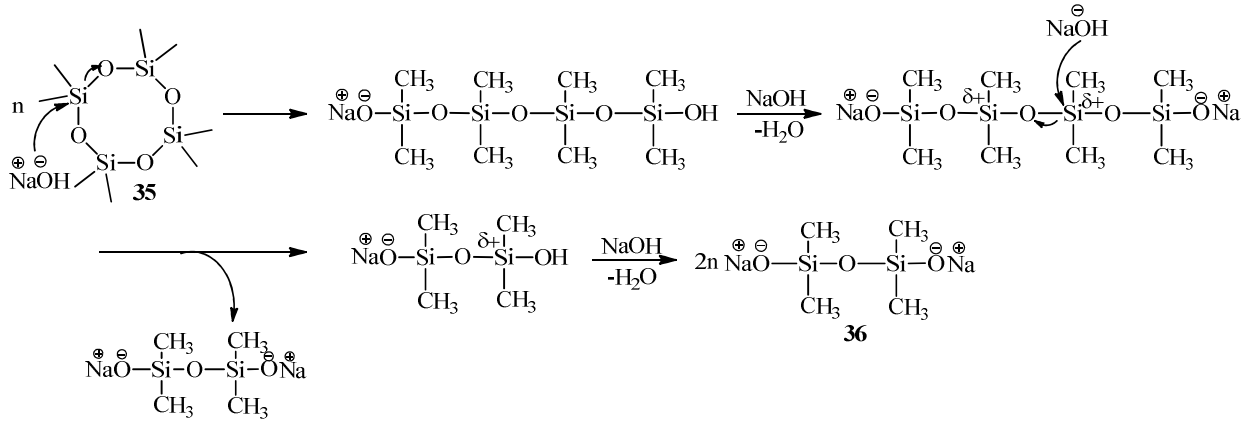

Scheme 2. 7. Base catalyzed ring-opening mechanism to form an oligosiloxanolates, 36.

The salt, **36**, can be used as a monomer in polymerization reactions. It can be copolymerized with reactive siloxane monomers bearing sites to which a functional group can be introduced. These functional groups may provide possible binding sites for introducing side chains that will make the polymer useful in certain applications such as catalysis. Side chain examples introduced include haloalkyl,[77] aryl, cyanoalkyl,[78] amines,[89] epoxy-[90] and poly ethers.[91] **Figure 2. 8** summarizes some functional groups that could be introduced as a side chain onto polysiloxanes.

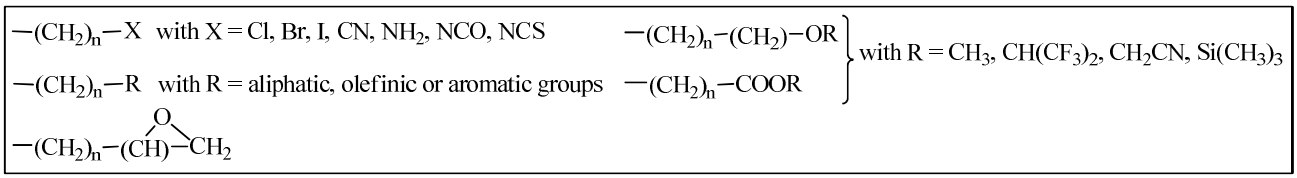

Figure 2. 8. Examples of functional groups that can be introduced to polysiloxanes.[78,79]

2.7.3 The hydrosilylation reaction

Active silane monomers can be synthesized by a catalyzed hydrosilylation reaction. Hydrosilylation is a reaction where a silicon hydride is added to an alkene or alkyne to form a Si-C organosilicon as shown in **Scheme 2. 8**. The reaction takes place in the presence of a platinum catalyst; mostly chloroplatinic acid, H_2PtCl_6. Several other transitional metal complexes like rhodium,[92] palladium[93] and cobalt complexes or salts are seldom used as hydrosilylation catalysts.[94]

---

89 J.F. Bermejo, P. Ortega, L. Chonco, R. Eritja, R. Samaniego and M. Mullner, *J. Eur. Chem.*, 2007, **13**, 483.
90 J.V. Crivello and J.L. Lee, *J. Polym. Sci Parts A: Polym. Chem.*, 1990, **28**, 479.
91 B. Marciniec, H. Maciejewski, K. Szubert and M. Kurdykowska, *Monatshefte für Chemie.*, 2006, **137**, 605.
92 E. de Wolf, E.A. Speets, Berth-Jan Deelman and G. van Koten, *Organometallics*, 2001, **20**, 3686.
93 Y. Uozumi and T. Hayashi, *J. Am. Chem. Soc.*, 1991, **113**, 9887.
94 L.D. Field and A.J. Ward, *J. Organomet. Chem.*, 2003, **681**, 91.

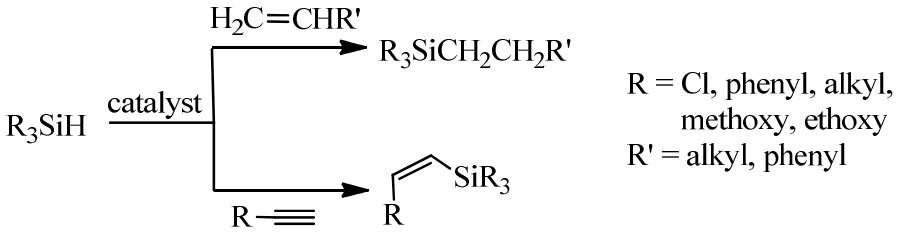

Scheme 2. 8. Hydrosilylation of unsaturated carbon compounds.

The mechanism these catalysts follow is still not clear but several studies have illuminated this reaction.[95,96] Chalk and Harrod[96] proposed the first of the two acceptable hydrosilylation mechanisms involving alkenes and platinum as catalyst (see **Scheme 2. 9**). After the silane, R'_3SiH, is added oxidatively to the catalyst, the coordination of the alkyne follows to give rise to **39**. Migration of the hydride between the alkyne-metal bond gives the metal silyl vinyl **40** which finally undergoes reductive elimination to yield R'_3Si-CH=CH-R, **41**.

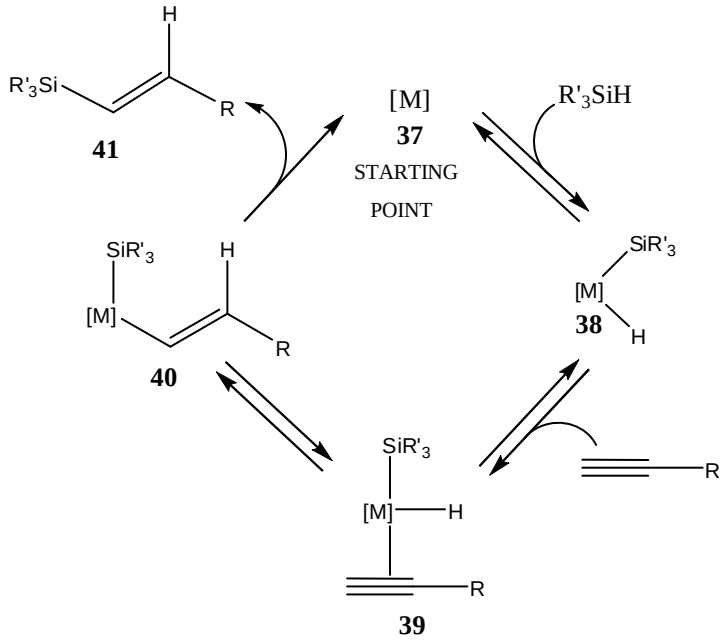

Scheme 2. 9. Chalk-Harrod mechanism for hydrosilylation of alkynes utilizing platinum transition metal complexes, here donated as [M].[96]

2.7.4 Selected examples of hydrosilylation

95 L.N. Lewis, *J. Am. Chem. Soc*., 1990, **112**, 5998; L.N. Lewis and N. Lewis, *J. Am. Chem. Soc*., 1986, **108**, 7228.
96 A.J. Chalk and J.F. Harrod, *J. Am. Chem. Soc*, 1956, **87**, 16.

Early reports of hydrosilylation started with the synthesis of methyl-(γ-chloropropyl)dichlorosilane from methyldichlorosilane.[97] The silane could only be synthesized at low yields of 5-40% at high temperatures (230-300 ˚C). Wagner[98] and co-workers described explicit use of platinized silica, platinum black and platinized asbestos as catalysts for the reaction between olefins and trichlorosilane. It was observed later that platinum deposited on charcoal showed unusual activity with trichlorosilane and olefins such as allyl chloride, acetylenes, butadienes, vinylidenes and acetylenes at low temperatures of 130 ˚C although much higher temperatures were still required in some examples.[99] Speier[100] compared the activity of platinum black, chloroplatinic acid, ruthenium chloride and iridium as catalysts. Solutions of chloroplatinic acid, $H_2PtCl_6.nH_2O$ in isopropanol showed the highest yields of 93-100 % for 1-pentene, 2-pentene and cyclohexene in the shortest times compared to other catalysts. It is proven to be one of the few extremely active catalysts in preparing organosilicon products with different functionalities. Other platinum catalyts like the Karstedt catalyst[101] are known to have added advantages although very expensive compared to chloroplatinic acid. Since then many organic substrates containing unsaturated carbon-carbon bonds have been catalytically hydrosilylized in various ways.

Hydrosilylation is a selective reaction that generally gives > 90% of β-addition products (see **Scheme 2. 10**, silane **42**). However, there are several factors that affect the type of addition that takes place. Firstly, not all combinations of silanes and alkenes give the same selectiveness. In the additions of silane compounds of type R_3SiH to styrenes, for example, both the β product, **42**, and α product, **43**, can be obtained in 60:40 mixtures respectively while other olefins give very high selectivities for β-addition.[100]

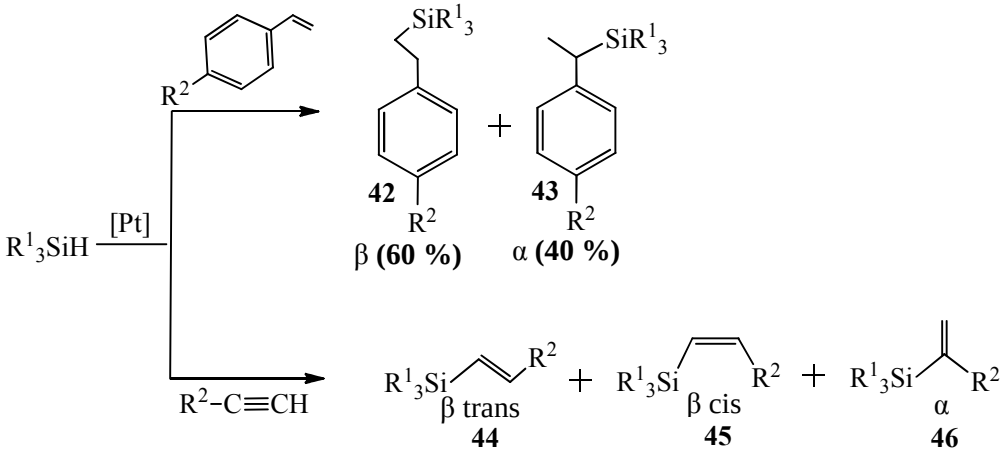

97 L.H. Sommer, F.P. Mackay and O.W. Steward, *J. Am. Chem. Soc.*, 1957, ***79***, 2764.

98 G.H. Wagner and C.O. Strother and O. Corneille, U.S. Patent 2632013, 1953.

99 G.H. Wagner, U.S. Patent 2637738, 1953.

100 J.L. Speier, J.A. Webster and G.H. Barnes, *J. Am. Chem. Soc*., 1956, **79**, 974; J.C. Saam and J.L. Speier, *J. Am. Chem. Soc*., 1958, **80**, 4104.

Scheme 2. 10. Hydrosilylation of styrene and an alkyne by silane $R^1{}_3SiH$ with different addition modes β or α.

For alkynes, β-trans addition products, **44**, are generally accepted to be dominant when platinum metal is used as catalyst but α products, **46**, and β-cis products, **45**, have been observed which makes the addition more complex.[102] Secondly, the position of the double bond also affects the ease with which hydrosilylation occur. For example, terminal double bonds are easier hydrosilylized than other alkenes. Lastly, the electronic nature of R^1 and R^2 groups play a role in determining the rate of hydrosilylation. When R^1 (the silane substituent) and R^2 (alkene substituent) are electron withdrawing and electron- donating respectively, the rate of hydrosilylation is enhanced. The effect is less pronounced if alkenes are replaced with alkynes.[102]

Silanes can also be synthesized *via* reduction reactions of chlorosilanes with $LiAlH_4$. This chemical transformation was observed during the synthesis of butacene, **49** (see **Scheme 2. 11**).[103] In the synthetic path compound **47** was treated with lithium aluminium hydride to give (4-ferrocenylbutyl)dimethylsilane, **48**, before it was hydrosilylized with hydroxyl terminated polybutadiene to give butacene.

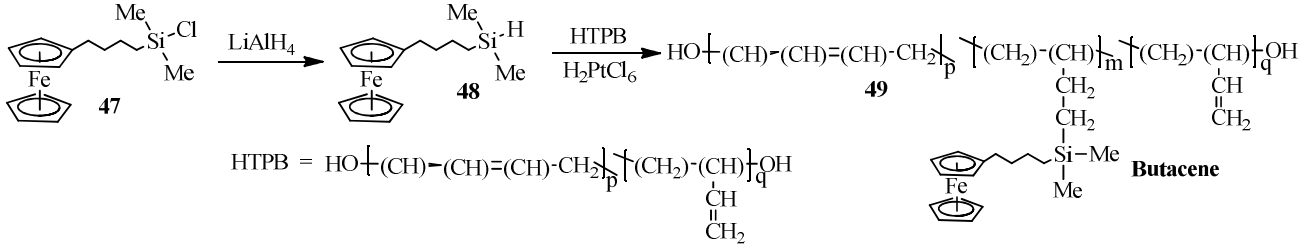

Scheme 2. 11. Reduction of silane 47, to give (4-ferrocenylbutyl)dimethylsilane, 48, during the course of the synthesis of butacene, 49.

2.7.5 Applications of polysiloxanes

Frank[77] developed a synthetic strategy for flexible reactive polysiloxanes containing functional groups. Amino-functionalized and chiral-functionalized polysiloxanes were synthesized for use as chromatographic stationary phase selectors for compound separation. The isocyanatopropyl-fucnctionalized polysiloxane, **51**, and hexafluoroisopropyl ester-functionalized polysiloxane, **56**,

101 M.F. Lappert and F.P.A. Scott, *J. Organomet. Chem*, 1995, **492**, C11.

102 J.L. Speier, *Adv. Organomet. Chem*., 1979, **17**, 407.

103 P.J. Swarts, M. Immelman,G.J. Lamprecht, S.E. Greyling and J.C. Swarts, *S. Afr. J. Chem*, 1997, **4**, 50.

were obtained by block condensation reactions between an oligosiloxanolate salt, **36**, and either the reactive dihaloisocyanato silane, **50**, or the fluoroalkyl ester, **57**, respectively as shown in **Scheme 2. 12**. Further re-functionalization of these compounds was done. Polymer **51** may be converted to an amino-polysiloxane, **52**, by treatment with acid, or it can be reacted with an amine to give a poly-urea, **53**. The fluorinated polymer, **56**, was treated with excess NaOH to give the carboxylic acid-functionalized polymer, **54**. Further treatment of polymer **54** with chiral *t*-butylamide in the presence of a coupling agent, N,N'-carbonyldiimidazol (CDI), gave **55**. Direct nucleophillic substitution of **56** also yields the chiral-functionalized polysiloxane, **55**. Polysiloxane **55** was successfully tested for separation of amino acid enantiomers.

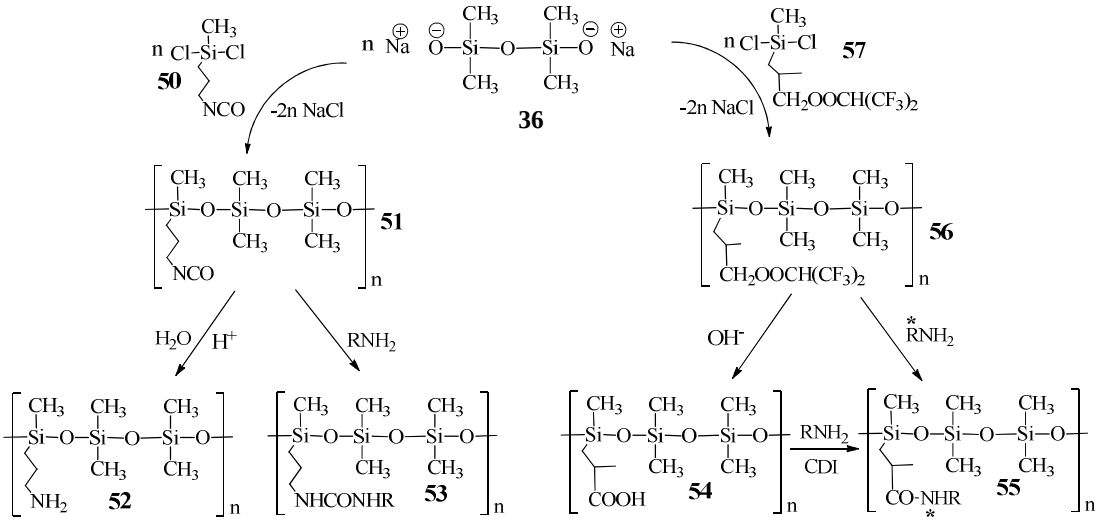

Scheme 2. 12. Synthetic pathways for side chain-functionalized polysiloxanes, 51-56.

Finally silicone polymers containing transition-metal complexes have also been reported. Farrel and van Dyke[77] synthesized a series of soluble carbon-functional phosphinated poly(methylsiloxanes), **58**, as support materials by varying the Me_2SiO spacer (c) units as shown in **Scheme 2. 13.**

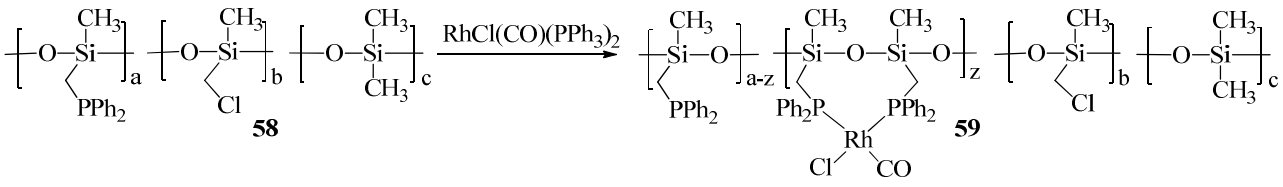

Scheme 2. 13. Carbon-functional phosphinated poly(methylsiloxanes) attached to a chlorocarbonylrhodium(I) complex.

These phosphinated polysiloxanes, **58**, were treated with a metal complex of type $RhCl(CO)(PPh_3)_2$ to give a polymer-attached chlorocarbonylrhodium(I) complex, **59**, with both PPh_3 groups substituted with the polymer-bound phosphino group. The catalytic activity of these complexes was

evaluated during hydroformylation reaction of hex-1-ene to give normal and branched aldehyde mixtures.

Recently, polysiloxanes-bound metal complexes were synthesized to facilitate easier catalysis in non-polar media.[79] The polysiloxanes are well soluble in almost all organic solvents including the very non-polar medium supercritical carbon dioxide ($scCO_2$). Reacting pyridine ligand of a functionalized-polydimethylsiloxane, **60**, with palladium (II) acetate gave polymer **61** as product. When catalytic activity of the complex was investigated during alcohol oxidation reactions of 2-octanol, a yield of 35% was obtained. Nevertheless, great catalyst stability was observed compared to the monomeric analogous catalyst, $Pd(OAc)_2$. Other metals like copper, rhenium and molybdenum were incorporated in a similar manner,[104] including incorporation of Grubbs[105] and Jacobsen[106] catalysts.

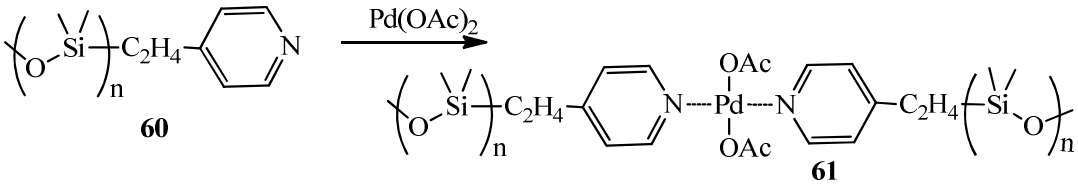

Scheme 2. 14. Synthesis of polydimethylsiloxane-functionalized palladium complexes.

2.8 Electrochemistry

2.8.1 An introduction to electrochemistry

The electron transfer properties of a chemical compound in solution can be studied by electrochemical techniques such as cyclic voltammetry. In cyclic voltammetry, the potential (E) applied to an unstirred chemical solution is varied while the resulting current (*i*) flowing between the auxiliary (normally a thin Pt wire) and working electrode is measured over a certain period of time (*t*). Different voltagrams (see **Table 2. 2**) can be produced depending on how the potential was modulated. Cyclic, square-wave and linear-sweep voltammetry are widely used.

---

104 M. Herbet, F. Montilla and A. Galindo, *Inorg. Chem. Commun*., 2007, **10**, 735; *Organometallics*, 2009, **28**, 2855; *Dalton. Trans.*, 2010, **39**, 900.

105 M.T. Mwangi, M.B. Runge and N.B. Bowden, *J. Am. Chem. Soc*., 2006, **128**, 14434; *J. Organomet. Chem*., 2006, **691**, 5278.

106 J.R. Jnr Pliego and M.A. Schiavon, *J. Phys. Chem. C*, 2008, **112**, 14830.

Table 2. 2. Common voltammetric experiments that can be peformed.

Type of Voltammetry	Potential waveform	Typical Voltammetry
Cyclic Voltammetry	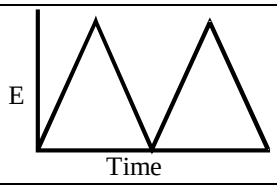	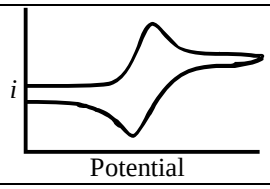
Square-wave Voltammetry	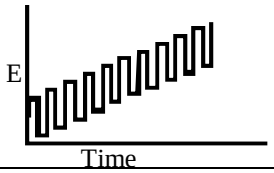	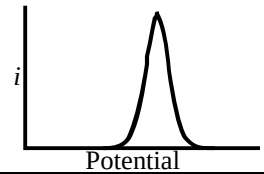
Linear-sweep Voltammetry	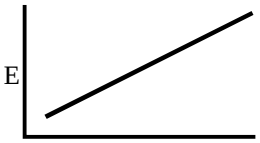	

Linear-sweep voltammetry can be performed by scanning the potential linearly but slowly. It is a useful technique for practically determining the relative number of electrons transferred during oxidation of reduction process. Cyclic voltammetry is the most used technique where the applied potential is varied in cycles in the forward direction (or positive direction) and then reversed to the negative direction and *vice versa* at the switching potential[107]. A simple response that can be obtained is shown in **Figure 2. 9.**

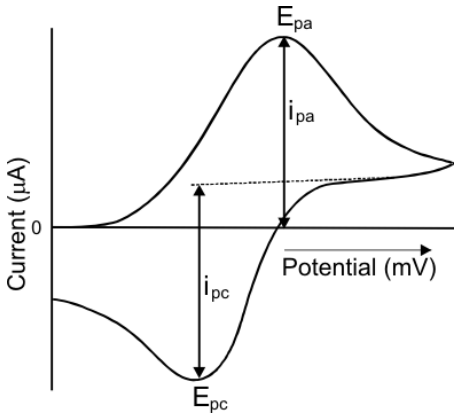

Figure 2. 9. Typical cyclic voltammogram.

From a cyclic voltammogram certain quantitative parameters are important for analysing the electrochemical behaviour of a chemical sample. For electrochemical reversibility, the rate of the electron transfer process of the oxidized and reduced specie with the working electrode is fast

[107] P.T. Kissinger and W.R. Heineman, J. *Chem. Educ*., 1983, **60**, 702.

compared to the diffusion rate of the species in solution. This contrasts electrochemical quasi or irreversible systems where a slow exchange of electrons takes place compared to the diffusion rate of the species in solution. Peak potential differences between the anodic (E_{pa}) and cathodic (E_{pc}) processes gives a measure of the rate of electron transfer between the analyte in solution and the electrode. For *n* electrons transferred the peak separation for electrochemically reversible processes corresponds to

$$\Delta E_p = |E_{pa} - E_{pc}| = \frac{0.059\ V}{n}$$

For one electron transfer process the separation should be 59 mV for an ideal electrochemical reversible reaction but practically due to cell resistance, values of ΔE_p slightly larger than 59 mV may be found. Thus, ΔE_p-values of 90 mV and less are still considered to indicate electrochemical reversibility. Other chemical processes are considered to be electrochemically quasi-reversible when ΔE_p-values are between 90 mV and 150 mV, while ΔE_p-values more than 150 mV are considered to indicate irreversible systems. The value of the redox couple are reported as the formal reduction potential, $E^{o\prime}$, which for an electrochemically reversible system, can be concluded as

$$E^{o\prime} = \frac{E_{pc} + E_{pa}}{2}$$

Peak current ratio (i_{pa}/i_{pc}) can be used to determine the chemical reversibility (or irreversibility) of a system. When the ratio approaches the value of 1, the system is said to be chemically reversible implying that the oxidized specie (or reduced) does not undergo any further reactions before it is reduced in the reverse cycle. Ratios far from 1 imply chemical irreversibility where the specie undergoes additional reaction sequences.

All ferrocene derivatives, **62**, (see **Scheme 2. 15**) exhibit reversible Fc^+/Fc couples although their $E^{o\prime}$ values differ depending on the type of substituent, R. Ferrocene shows great sensitivity towards substituent effect when groups such as alcohol, acids, alkyls and ketones replace the hydrogen.[108] Easily oxidized compounds are those whose R groups are electron-donating in nature leading to negative $E^{o\prime}$ values relative to the Fc^+/Fc couple, while positive values suggest that the R group is more electron-withdrawing that the hydrogen atom.

[108] S. Trupia, A. Nafady and W.E. Geiger, *Inorg. Chem.*, 2003, ***42***, 5480.

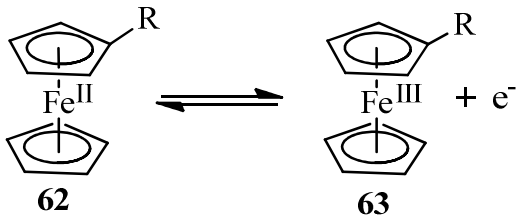

62 63

Scheme 2. 15. The oxidation of ferrocene to the ferrocenium ion represents a reversible couple. The IUPAC internal standard is the above reaction with R = H and assigning $E^{o'} = 0$ V.

2.8.2 Solvents, electrolytes, internal standards

For an electrochemical reaction to be studied a suitable medium is required and the choice of this medium depends on various factors. The solvent must be redox silent, it must be able to dissolve both the analyte of interest and the supporting electrolyte in sufficient quantities, it must have a large enough potential range to observe the redox processes of interest and it must be able to form conducting solutions. Acetonitrile, CH_3CN, is commonly used. However, because a non-coordinating solvent is much better, dichloromethane, CH_2Cl_2, is gaining favour as the solvent of choice.

In an electrochemical reaction the supporting electrolyte imparts conductivity to the medium, ensuring continuous flow of current. The supporting electrolyte must be electrochemically inactive in the potential window of interest. Supporting electrolytes such as the common tetrabutylammonium hexafluorophosphate, $[N^nBu_4][PF_6]$,[109,110] and less commonly, the extremely uncoordinating tetrabutylammonium(tetrakispentafluorophenyl)borate,[111] $[N^nBu_4][B(C_6F_5)_4]$, are used.

Internal standards are used in electrochemical experiments to overcome potential drifts due to cell imperfections.[112] They are used to provide a reference potential standard in redox reactions. In non-aqueous electrochemistry, ferrocene is the IUPAC internal standard[113] but other compounds like decamethylferrocene[114] may be used to avoid overlapping of peaks if the analyte contains a ferrocenyl group.

---

109 J. Conradie and J.C. Swarts, *Dalton. Trans*, 2011, **40**, 5844.

110 D. Lamprecht and G.J. Lamprecht, *Inorg. Chim. Acta*., 2000, **309**, 72.

111 C. Ohrenberg and W.E. Geiger, *Inorg. Chem*., 200, **39**, 2947.

112 C.G. Zoski, *Handbook of Electrochemistry*, 1st edition, Elsevier, Oxford, 2007, p. 94-99.

113 R.R. Gagne, C.A. Koval and G.C. Lisensky, *Inorg. Chem*., 1980, **9**, 19.

114 I. Noviandri, K.N. Brown, D.S. Fleming, P.T. Gulyas, P.A. Lay, A.F. Masters and L. Phillips, *J. Phys. Chem.*, 1999, **103**, 6713.

2.8.3 Examples of cyclic voltammetric studies

An electrochemical study in CH_3CN/2 mM $[N^nBu_4][PF_6]$ on a series of ferrocene-containing β-diketones of the type $FcCOCH_2COR$ has been performed by du Plessis[115] and co-workers. Electrochemical reversibility was observed for the ferrocenyl group on the β-diketones **4-8** with ΔE_p values between 71-92 mV and current ratios approaching 1 (**Figure 2.10**). A linear relationship between $E^{o\prime}$ values and group electronegativities, χ_R, of the R group was observed. χ_R is the measure of the electron density on the R-group of the ferrocene-containing β-diketones **4-8**. The electrochemical data is summarized in **Table 2. 3**.

R	ΔE_p (mV)	$E^{o\prime}$ (mV)	i_{pc}/i_{pa}	χ_R
CH_3	92	236	0.97	2.34
CF_3	74	317	0.97	3.01
CCl_3	83	293	0.97	2.97
Ph	81	231	1.01	2.21
Fc	74; 71	106; 271	0.88; 1.09	1.87

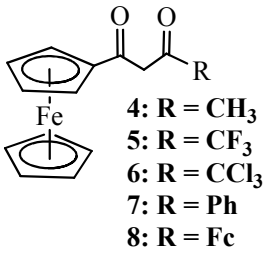

4: R = CH_3
5: R = CF_3
6: R = CCl_3
7: R = Ph
8: R = Fc

Table 2. 3. Electrochemical data obtained from CV's done at a scan rate of 100 mV s^{-1}. Figure 2. 10. Ferrocene-containing β-diketones, $FcCOCH_2COR$, 4-8.

The electrochemistry of rhodium(I) dicarbonyl complexes **23-26** coordinated to ferrocene-containing β-diketones[116] was also studied in CH_3CN/ 0.1 M $[N^nBu_4]$ $[PF_6]$. The complexes possess two redox centres, the rhodium(I) core and the iron centre of the ferrocenyl group. Reversible one electron oxidation of the ferrocenyl group occurs at lower potentials than the irreversible two-electron oxidation of Rh(I) to Rh(III). An acetonitrile adduct also formed in the CV of **24** and it was oxidized at higher potentials than the ferrocenyl group, see **Figure 2. 11**. The electrochemical data is summarized in **., 2005, 358, 2530. Table 2. 4.**

115 W.C. du Plessis, J.C. Erasmus, G.J. Lamprecht, J. Conradie, T.S. Cameron, M.A.S. Aquino and J.C. Swarts, *Can. J. Chem.*, 1999, **77**, 378.

116 J. Conradie, T.S. Cameron, M.A.S. Aquino, G.J. Lamprecht and J.C. Swarts, *Inorg. Chim. Acta.*, 2005, **358**, 2530.

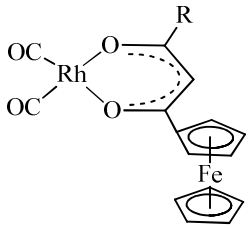

23: R = CH_3
24: R = CF_3
25: R = Ph
26: R = Fc

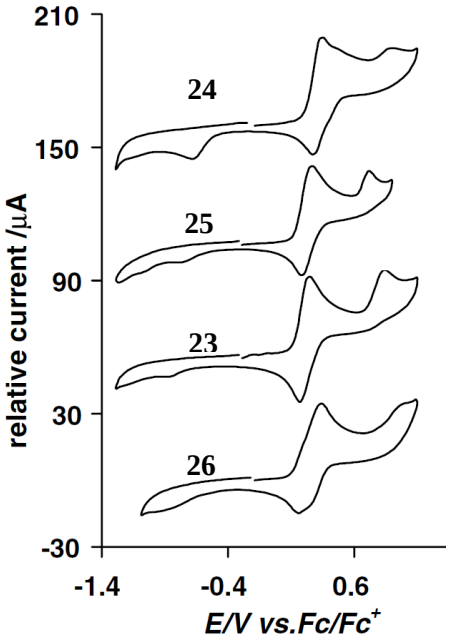

R	$E^{o\prime}_{Fc}$ (mV)	$E_{pa, Fc}$ (mV)	$E_{pa, Rh}$ (mV)
CH_3	190	224	844
CF_3	304	345, 457	901
Ph	199	235	718
Fc	172	207, 312	1022

Figure 2. 11. CV's of [Rh(FcCOCHCOR)$(CO)_2$] complexes 23-26. Diagram duplicated from J. Conradie, T.S. Cameron, M.A.S. Aquino, G.J. Lamprecht and J.C. Swarts, *Inorg. Chim. Acta.*, 2005, 358, 2530. Table 2. 4. Summary of the electrochemical data of [Rh(FcCOCHCOR)$(CO)_2$] complexes.

For the reversible Fe^{2+}/Fe^{3+} couple, $\Delta E_p \leq 90$ mV and current ratios were in the range $0.83 < i_{pc}/i_{pa} < 1$, while formal reduction potentials, $E^{o\prime}$ values were independent of the scan rates in the range 50 – 250 mV s^{-1}. The oxidation and reduction peaks were not clearly resolved for **26** having two ferrocenyl groups on the β-diketone. Better resolution was obtained by square wave voltammetry to confirm two independent one electron transfer process for each of the two ferrocenyl ion centre. The rhodium centres in the complexes, although oxidized, did not exhibit any electrochemical reversibility. A low intensity peak was observed for the reduction of Rh(III) to Rh(I) at lower potentials compared to the formal oxidation potential of the ferrocenyl group. The low intensity is due to the instability of the newly oxidized Rh(III) specie, that is, by the time it gets reduced to Rh(I) a large concentration has decomposed or diffused. That this was indeed the case was confirmed by using higher scan rates (250 mV s^{-1}), where an increase in the size of the cathodic peak was observed since more Rh(III) specie becomes available for reduction.

The relationship between the Gordy scale group electronegativities, χ_R, of the side groups on a β-diketone and the electrochemical oxidation potential of the rhodium core for rhodium(I) carbonyl phosphine complexes coordinated to ferrocene-containing β-diketones,

[Rh(FcCOCHCOR)(CO)(PPh_3)], **27-30** (see **Figure 2. 12**) was investigated.[117] Unlike complexes **23-26** the rhodium(I) centre of **27-30** undergoes two-electron oxidation at much lower potentials compared to the ferrocenyl oxidation potential. This observation is expected given that introducing a phosphine ligand increases the density substantially.

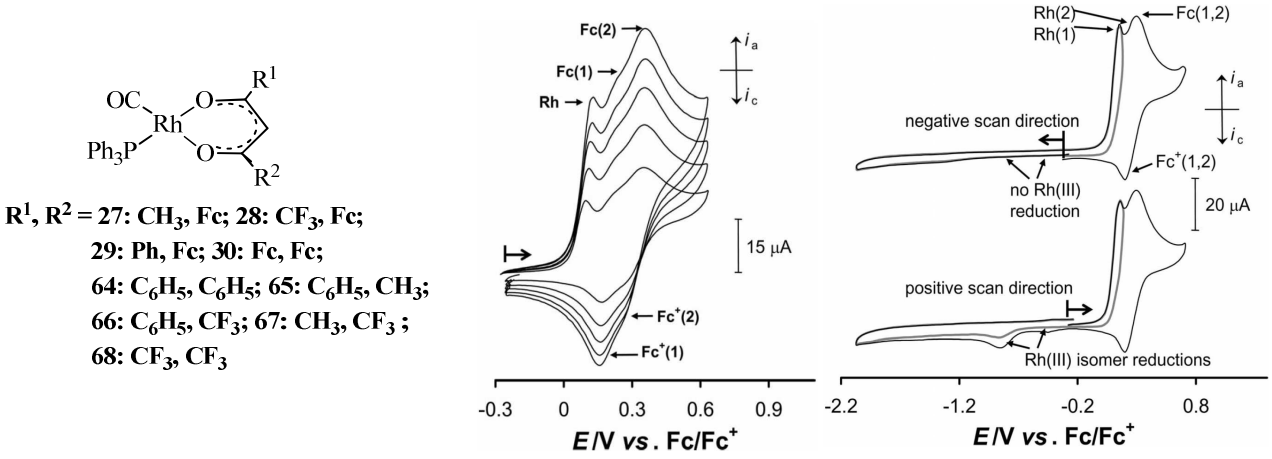

Figure 2. 12. CV's of rhodium(I) carbonyl phosphine complexes attached to ferrocene-containing β-diketones, [Rh(FcCOCHCOR)(CO)(PPh_3)]. Diagram duplicated from J. Conradie and J.C. Swarts, *Eur. J. Inorg.*

The ease with which the rhodium centre is oxidized (E_{pa}) was also shown to have a linear dependency with the group electronegativity sum, $\chi_R^1 + \chi_R^2$. That is, the more electron-donating the side groups are, the more electron rich the rhodium centre is and the easier oxidation takes place. Lamprecht[118] studied complexes **64-68** under the same conditions and similar observations were made. However, one-electron electrochemical oxidation process for the rhodium metal rather than two-electron oxidation was shown to take place when the solvent and supporting electrolyte were changed from CH_3CN and $[N^nBu_4][PF_6]$ to CH_2Cl_2 and $[N^nBu_4][BF_4]$[119] or $[N^nBu_4][B(C_6F_5)_4]$.[120]

This concludes the literature survey of aspects related to this study that the author deems as important. What follows in the rest of this thesis (Chapter 3, 4 and 5) is the research performed by the author on new polysiloxane functionalized in such a way that they possess side chains to which a rhodium(I) centre could be coordinated.

---

117 J. Conradie and J.C. Swarts, *Eur. J. Inorg. Chem*., 2011, 2439.

118 D. Lamprecht and G.J. Lamprecht, *Inorg. Chim. Acta*, 2000, **309**, 72.

119 M. Fátima, C.G. da Silva, A.M. Trzeciak, J.J. Ziólkowski and A.J.L. Pombeiro, *J. Organomet. Chem*., 2001, **620**, 174.

120 H.J. Geriecke, N.I. Barnard, E. Erasmus, J.C. Swarts, M.J. Cook and M.A.S. Aquino, *Inorg. Chim. Acta.*, 2010, **363**, 2222; J.C. Swarts, A. Nafady, J.H. Roudebush, S. Trupia and W.E. Geiger, *Inorg. Chem*., 2009, **48**, 2156.

3 Results and Discussion

3.1 Introduction

In this chapter, the author's own research is presented. The synthesis of ferrocene-containing β-diketones, 1-ferrocenyl-3-methylbutane-1,3-dione, **4**, and 1-ferrocenyl-4,4,4-trifluorobutane-1,3-dione, **5**, rhodium(I) complexes of the type [Rh(FcCOCHCOR)(cod)] and [Rh(FcCOCHCOR)(CO_2)] with Fc = ferrocenyl, R = CF_3 and CH_3 is described first. Thereafter the synthesis of several derivatized polysiloxanes will be described to ultimately end with the successful synthesis of $\{(OSiMe_2)_2OSiMe\{(CH_2)_mPPh_2(CO)(FcCOCHCOR)Rh\}\}_n$. Where possible, compounds were characterized by spectroscopic methods (NMR, FTIR, UV/vis), elemental analyses, electrochemistry (cyclic, square-wave, linear sweep voltammetry) and viscosity measurements.

3.2 Synthesis

3.2.1 Ferrocene-containing β-diketones

Two ferrocene-containing β-diketones, **4** and **5**, were prepared in 16 and 53 % yield by Claisen condensation under Schlenk conditions, **Scheme 3. 1**. Acetyl ferrocene, **2**, was deprotonated by lithium diisopropylamide (LDA) base to form a nucleophillic specie, $FcCOCH_2^-$ to react with the appropriate ester, ethyl acetate (R = CH_3) or ethyl trifluoroacetate (R = CF_3).

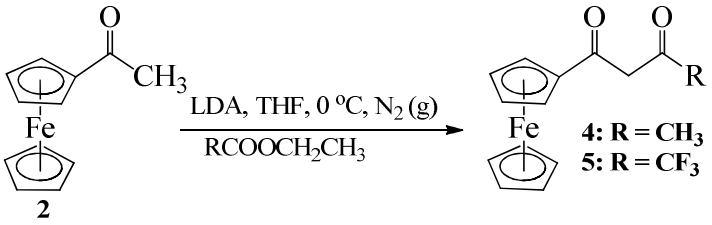

Scheme 3. 1. Synthesis of ferrocene-containing β-diketones 4 and 5, LDA = lithium diisopropylamide.

Complexes **4** and **5** are wine-red powders. Drying of ethylacetate (CH_3COOEt) with chemical methods was essential for this ester because of its large water content. Simple distillation does not dry it as an azeotrope containing 8.1 % water distills. Water, therefore was removed by distillation over K_2CO_3. The reactive $FcCOCH_2^-$ specie and LDA are destroyed by moisture. All β-diketones were purified on silica gel by chromatographic separation using ether/hexane mixture as eluent in 1:1.

3.2.2 Complexation of rhodium to ferrocene-containing β-diketones

The ferrocene-containing β-diketonato dicarbonyl rhodium(I) complexes **23** and **24** were synthesized according to **Scheme 3. 2**. Di-μ-chloro-bis(η^4-cycloocta-1,5-diene)dirhodium(I), $[Rh_2Cl_2(cod)_2]$, **18**, was first prepared by refluxing $RhCl_3.xH_2O$ in ethanol in 26 % yield. The rhodium-chloro-cod dimer, **18**, was converted to [Rh(FcCOCHCOR)(cod)], **19** and **20**, in very good yields (>95%) by reacting it with the appropriate β-diketone, **4** or **5**, in DMF at room temperature. Compound **19** and **20** were purified on silica gel by chromatography.

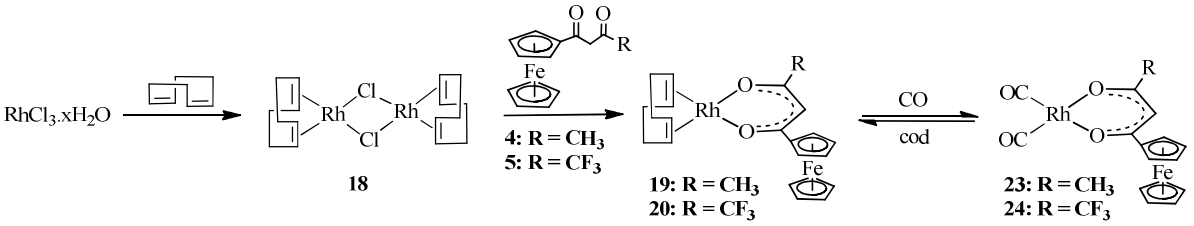

Scheme 3. 2. Synthetic route used for the synthesis of rhodium(I) dicarbonyl β-diketonato complexes.

To obtain the dicarbonyl complexes **23** and **24**, an acetone solution of [Rh(FcCOCHCOR)(cod)], **19** or **20**, was saturated with carbon monoxide gas to induce cod-carbonyl ligand exchange to liberate pure $[Rh(FcCOCHCOR)(CO)_2]$. The pure product was precipitated from the solvent with cold water and filtered to prevent conversion of complex **23** back to **19** or **24** to **20**. The desired red compound separated from the aqueous reaction mixture and settled to the bottom. Rhodium(I) dicarbonyl β-diketonato complexes, **23** and **24,** were synthesized at room temperature at 42 and 48 % yields respectively.

3.2.3 Siloxane and Silane monomers

3.2.3.1 Disodium Tetramethyldisiloxane-1, 3-diolate

Disodium tetramethyldisiloxane-1,3-diolate, **36**, was synthesized by gradually heating a stoichiometric mixture of octamethylcyclotetrasiloxane, **35**, and aqueous NaOH to boiling in methanol, **Scheme 3. 3**. The solvent and excess water were removed under vacuum to give a white powder containing several waters of crystallization as product in good (79 %) yield.

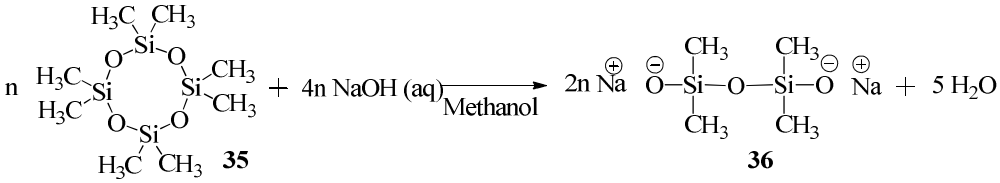

Scheme 3. 3. Synthesis of disodium tetramethyldisiloxane-1, 3-diolate.

Because of large quantities of water that coprecipitated with the disodium salt,[121] extensive drying had to be employed. The compound was dried in an Abderhalden drying pistol using phosphorus pentoxide (P_4O_{10}) as the drying agent and boiling dimethoxy ethane (85 ^oC) as the heat source. Drying took up to 3 days for 36 g of product. The salt, **36**, is highly hydroscopic, therefore its storage needed to be absolutely moisture free and this was ensured by storing it under argon. In the absence of acidic and alkaline traces it can be stored for months without decomposition. Complete dryness of the monomer **36** is highly important for polymerization reaction to obtain polysiloxanes because it determines the quality of the polymeric product obtained. For example, it was noticed that failure to successfully dry the salt resulted in partial homogeneity when the salt is dissolved in 1,4–dioxane in the polymerization step and it formed lumps which needed many long hours of stirring to obtain any useful product.

3.2.3.2 Silane monomers

The alkylhalide-functionalised dichloromethylsilane derivatives (3–chloropropyl)methyldichlorosilane, **73**, (4–bromobutyl)methyldichlorosilane, **74**, and (5–bromopentyl)methyldichlorosilane, **75**, having a different number of carbon atoms, m, between the silicon atom and the halide were synthesized in 31, 63 and 60 % yield respectively via hydrosilylation reactions using $H_2PtCl_6.6H_2O$ as a catalyst as shown in **Scheme 3. 4**. Inert and dry conditions had to be adhered to**.**

[121] Y.T. Struchkov, V. M. Kopylov, A. M. Muzafarov, P. L. Prikhod and A. A. Zhdanov, *Structure*, 1982, **23**, 63.

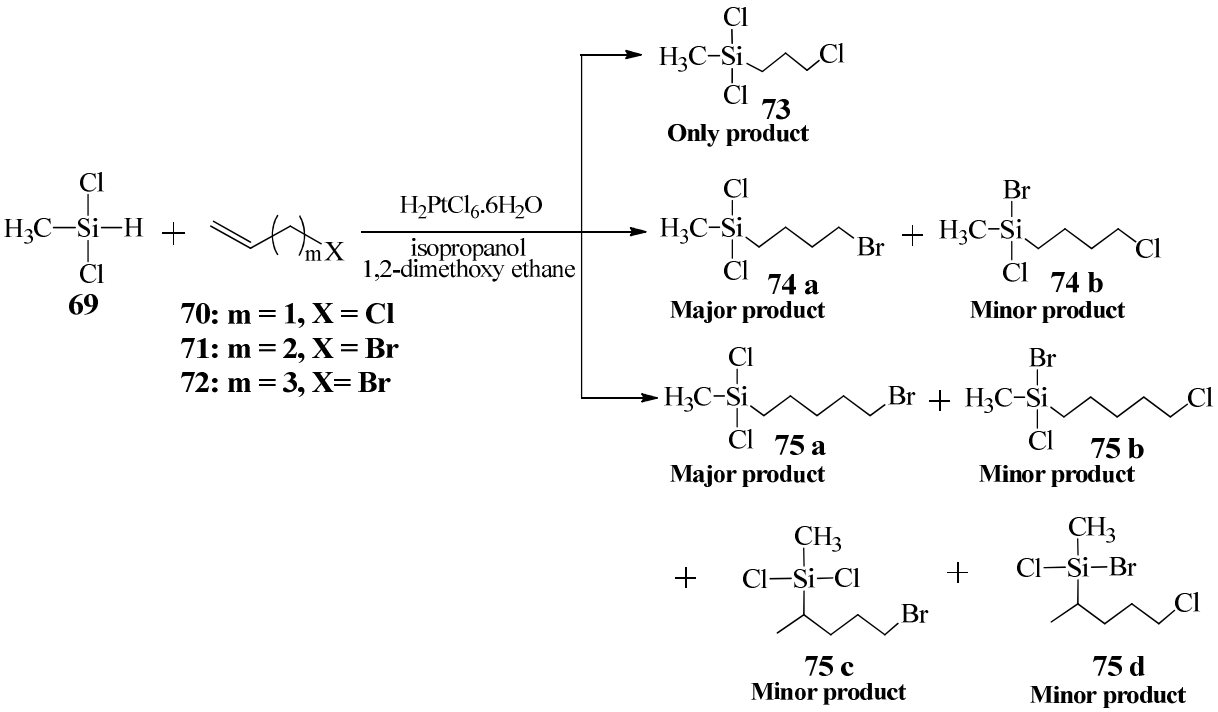

Scheme 3. 4. Hydrosilylation reactions between dichloromethylsilane and different alkenes yielding halo-functionalized silanes 73 with three CH_2 spacers between the Si and Cl atoms, 74 having m = 4 and 75 having five CH_2 spacers between the Si and Br atoms in the main product. Detected side-products are also shown. α-Hydrosilylation occurred in each case to liberate the main product. Only 75 gave noticeable amounts of β-hydrosilation products.

The two shorter chain alkenes, allyl chloride and 4-bromobutene, 70 and 71, gave exclusively α-hydrosilylation while the longer chain alkene 5-bromopentene, 72, gave observable quantities of β-hydrosilylation. Allyl chloride 70, gave only one detectable dichloromethylsilane derivative, 73 as product. The reaction between dichloromethylsilane, 69, and 71 gave a minor product in 19 % yield (see ^{1}H NMR in **Figure 3. 1**) which in principle could either be the β-hydrosilylation product, similar to 75 c, or it could represent an isomer of the major product, 74 b, where a chloride and a bromide atom exchanged positions. However in subsequent reactions, 74 was polymerized with 36 to give polysiloxane 77, which was thereafter reacted with NaI. In this iodization reaction all halides were replaced with an iodo group (see ^{1}H NMR in **Figure 3. 2**, **paragraph 3.2.5**, compound 80). Only a compound possessing a backbone that was constructed of α-hydrosilylated iodated monomers was obtained. Based on this evidence it may be concluded that during the synthesis of 74, only α-hydrosilylation was obtained and the side product which was observed by ^{1}H NMR must be the isomerized product where chloride and bromide atoms exchanged positions as shown by **Scheme 3. 4**, compound 74 b.

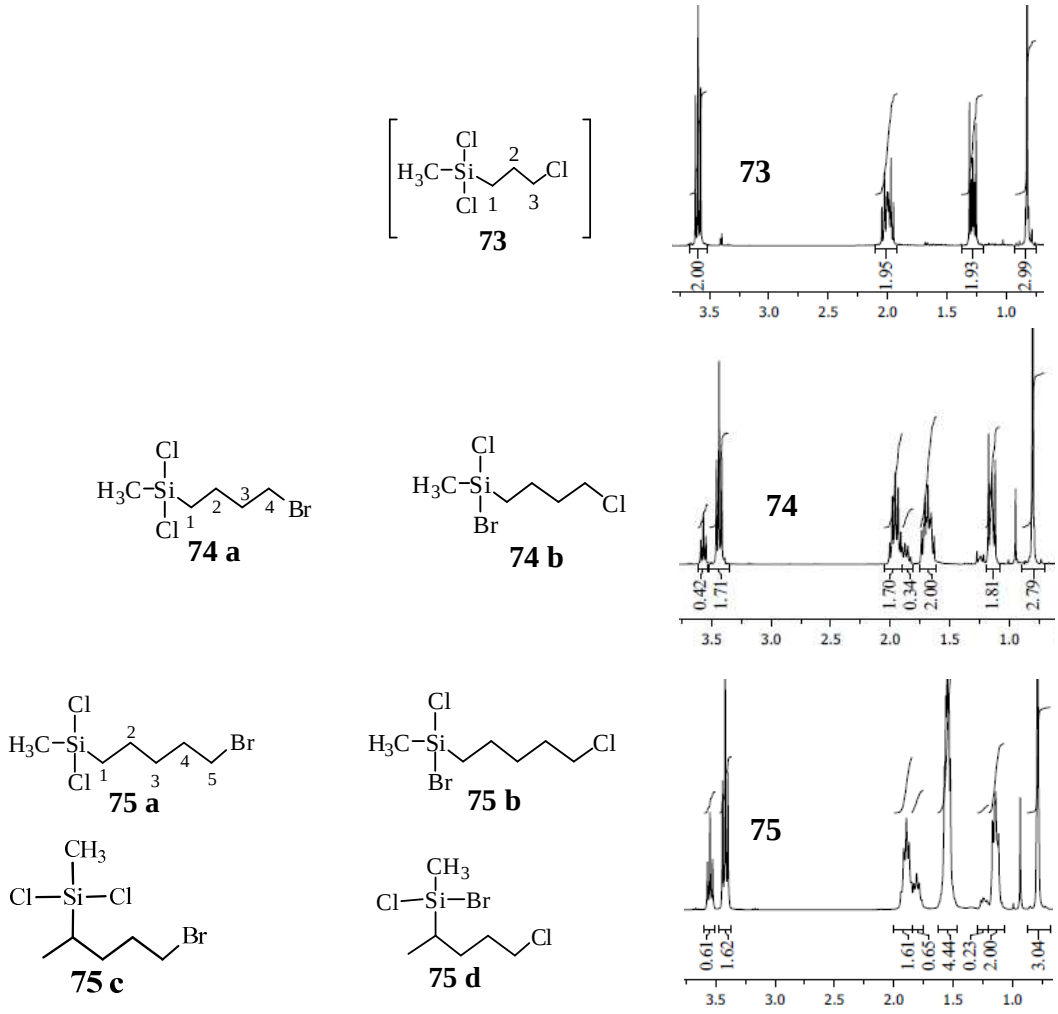

Figure 3. 1. Hydrosilylation reaction products and the ^{1}H NMR spectra of (3–chloropropyl)methyldichlorosilane, 73, (4– bromobutyl)methyldichlorosilane, 74, (5–bromopentyl)methyldichlorosilane, 75, and their isomers.

The difference in ^{1}H NMR spectra for the synthesis of a pure α-hydrosilylation product (compound 73) and a halogen exchanged isomerized product, 74, is shown in **Figure 3. 1**. For the spectrum of silane compound 73, two triplets are observed at δ 1.28 and 3.60 ppm and belong to the CH_2 groups of position 1 and 3 respectively. For 74 a, the multiplet associated with CH_2 at position 3 is observed at δ 1.95 ppm and a well-defined triplet at δ 3.44 ppm, which is associated with the CH_2 of position 4. If Cl-Br exchange occurred as in 74 b the peak at δ 3.57 ppm would be observed as two distinct separate triplets as shown in ^{1}H NMR of 74 in the region δ 3.4-3.7 ppm. If β-hydrosilylation occurred in 74, one would expect to find a doublet in the region δ 0.5-1.5 ppm, but this was not observed. Also, evidence in **paragraph 3.2.5**, **Figure 3. 2**, suggests the total absence of a β-hydrosilylation product.

The ^{1}H NMR spectrum of the silane with the longest carbon chain length, compound 75, shown in **Figure 3. 1**, did show isomerization in the δ 3.3-3.6 and also 1.75-2.0 ppm region, similar to what was found for 74. This is certainly indicative of a Cl-Br exchange reaction, as shown by the

structure of 75 b. However, after polymerization with 36 and an iodide exchange reaction of all halogen ions to give 81 as described in paragraph 3.2.5, a ^{1}H NMR was obtained that still showed two different structures of monomer 75 in the polymer backbone of 81, see **Figure 3. 2** This result causes the author to allow for the possibility of β-hydrosilylation (see **Scheme 3. 4** and **Figure 3. 1**, compound 75 c and 75 d and also **Figure 3. 2**, compound 81).

Care in weighing $H_2PtCl_6.6H_2O$ had to be taken as this complex is highly hygroscopic. To ensure good yields of the silanes **73-74**, care had to be taken on how the reactants are mixed. The dichloromethylsilane was always first mixed with a small amount (about 0.12 equivalents) of the appropriate alkene. This was followed by addition of the catalyst dissolved in 1,2-dimethoxymethane in the presence of a small amount of isopropanol. This addition sequence is important because before hydrosilylation can take place, the catalyst has to be first reduced by isopropanol to the active platinum catalyst before addition of the majority of the stoichiometric amount of the alkene is added to prevent formation of stable, non-catalytic platinum–alkene coordination compounds. After Pt(IV) reduction occurred, the remainder of the alkene was slowly added to the reaction mixture. When the reagents were simply added together, even with slow addition of the alkene, a precipitate having the same colour as the catalyst, $H_2PtCl_6.6H_2O$, was observed and no product formation could be identified. An exothermic reaction occurred for alkenes **71** and **72** with temperature increasing to 60 ^{o}C. Almost no temperature increase was observed for the allyl chloride reaction because allyl chloride, **70**, is less reactive compared to 4-bromobutene, **71**, and 5-bromopentene, **72**.

Dichloromethylsilane derivatives **73-75** are very toxic and moisture sensitive as the Si-Cl moieties are easily hydrolyzed to Si-OH groups with concomitant release of HCl gas. Since the hydrolyzed hydroxysilanes cannot be used for the envisaged polymerization reactions of this study, the hydrochlorosilanes **73-75** had to be stored under dry conditions, preferably under argon. Storage in glass flasks with well-greased airtight glass stoppers ensured stability of these compounds for at least four months.

3.2.4 Polymerization

Polysiloxanes, poly(3–chloropropylpentamethyltrisiloxane), **76**, poly(4-bromobutylpentamethyl-trisiloxane), **77**, and poly(5-bromopentylpentamethyltrisiloxane), **78**, were synthesized *via* a polymerization reaction between the disodium salt, **36**, and halo-organosilanes possessing different lengths of the carbon side chain, (3–chloropropyl)methyldichlorosilane, **73**, (4–

bromobutyl)methyldichlorosilane, **74**, or (5–bromopentyl)methyldichlorosilane, **75**, as shown in **Scheme 3. 5**.

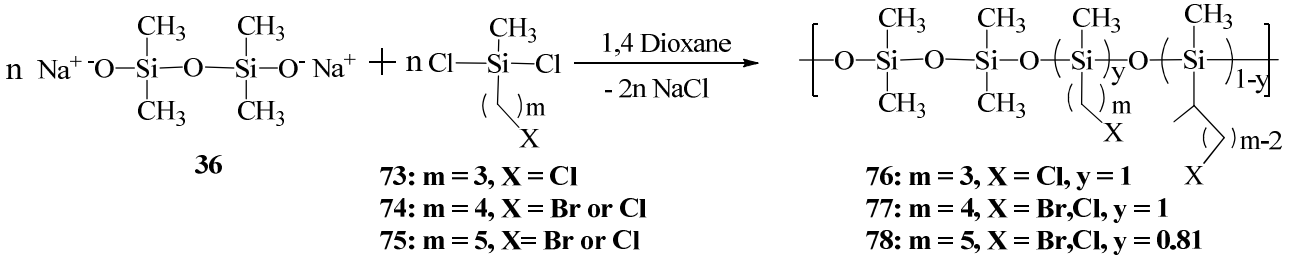

Scheme 3. 5. Synthesis of chlorinated and brominated polysiloxanes.

For all three reactions the volatile organosilane, **73-75**, was dissolved in dry 1,4-dioxane and added dropwise to a stirred white homogeneous suspension of the salt, **36**, in 1,4-dioxane. The fine NaCl precipitate that formed was centrifuged off and removal of the solvent gave polymers **76-78** as pale yellow viscous oils. During the synthesis of polysiloxane **77** and **78**, the temperature of the reaction mixture slightly increased. Yields of 80 and 90 % were obtained for **77** and **78** respectively. Polysiloxane **76** that possesses the shortest carbon side chain was obtained in a yield of 54 %. The ^{1}H NMR of chlorinated polysiloxane **76** showed one product (see Appendix, Spectrum 4.11), while two differently structured products were obtained for polysiloxane **77** and **78** as a result of the isomerized silanes **74** and **75** (see Appendix, Spectrum 4.12 and 4.13).

3.2.5 Iodization of chloro- and bromo-polysiloxanes

The halide group Cl or Br on polysiloxane **76-78** was replaced with a more reactive iodo group by refluxing with a sixty times molar excess of NaI in dry acetone[122] for 6 days to give poly(3-iodopropylpentamethyltrisiloxane), **79**, poly(4-iodobutylpentamethyltrisiloxane), **80** and poly(5-iodopentylpentamethyltrisiloxane), **81**, in 84, 54 and 64 % yields respectively, **Scheme 3. 6**.

[122] H. Finkelstein, *Ber. Deutsch. Chem. Gesell.*, 1910, **43**, 1528.

A.

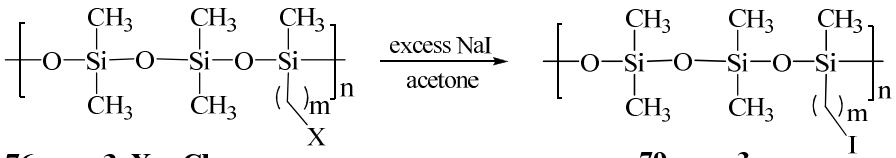

76: m = 3, X = Cl
77: m = 4, X = Br or Cl

79: m = 3
80: m = 4

B.

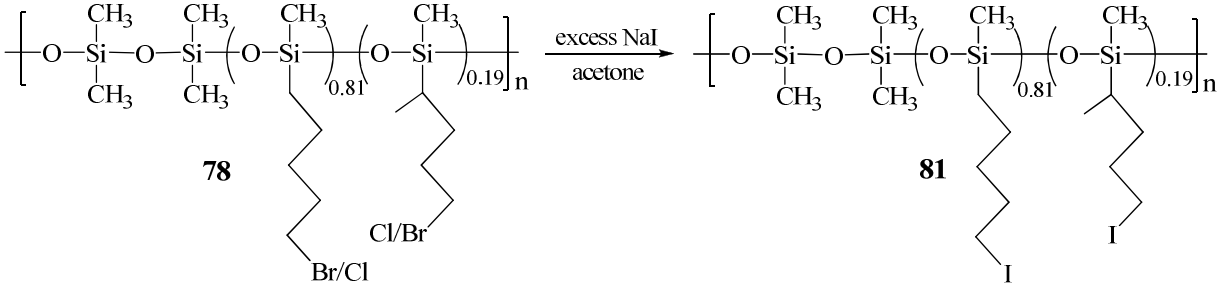

78

81

Scheme 3. 6. Halide conversion reactions for polysiloxanes.

The iodated polysiloxanes, **79**-**81**, were recovered by extensive extraction with dichloromethane and washing with copious amounts of water to remove the excess NaI and the NaCl or NaBr that precipitated during the conversion reaction. The iodated polymers were all viscous oils. ^{1}H NMR analysis of these polymers showed halogen conversion in excess of 95 % for all three polymers **79**-**81**. The ^{1}H NMR of **79**-**81** showed a triplet resonance for the new I-CH_2 molecular fragment at δ 3.11-3.33 ppm (the peak is labeled a′ in **Figure 3. 2**). The disappearing Cl-CH_2 or Br-CH_2 resonances are found at δ 3.35-3.60 ppm and they are labeled a while a' represents the newly formed I-CH_2 peaks.

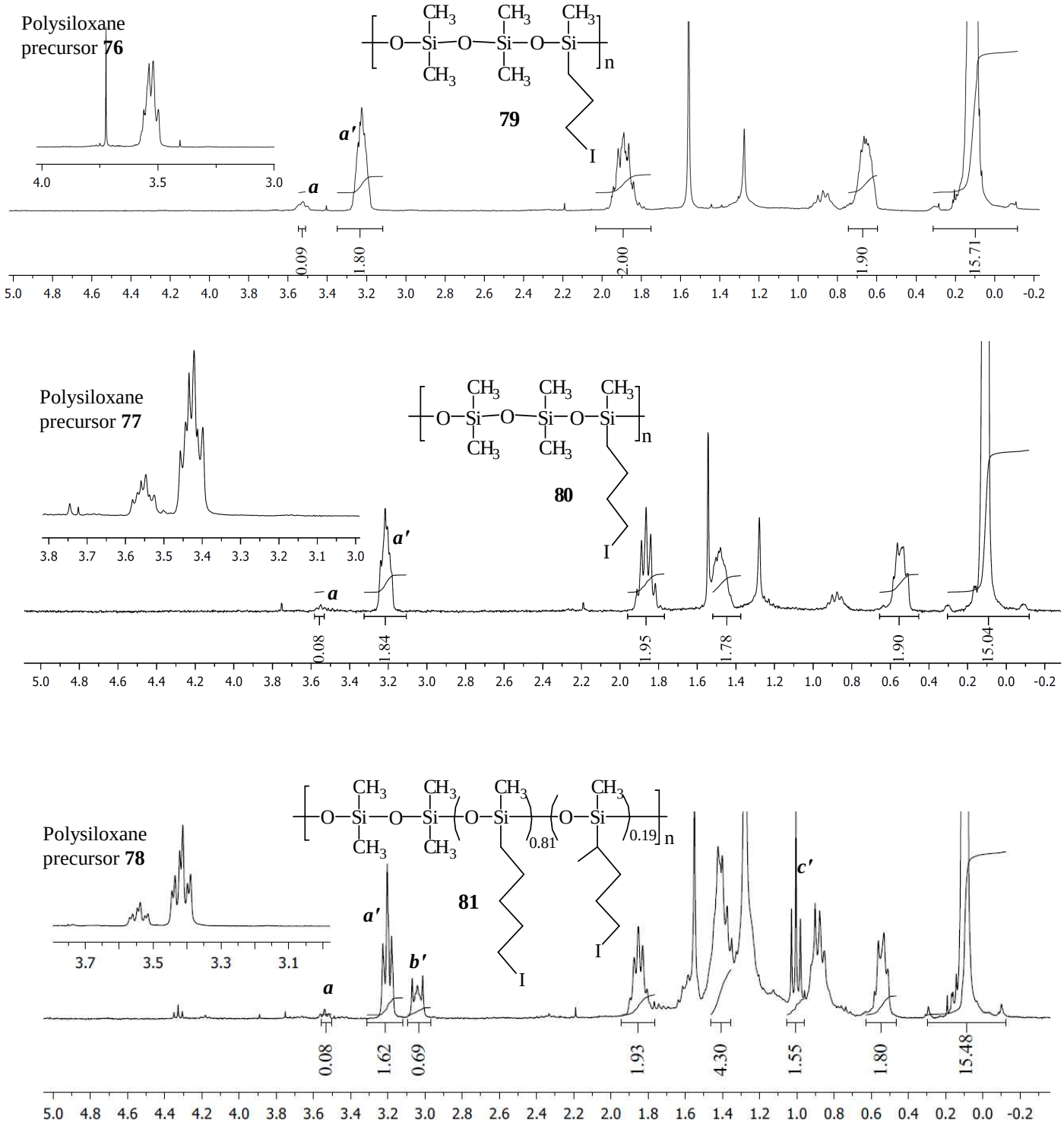

Figure 3. 2. [1]NMR of the iodized polysiloxanes, 79, 80 and 81.

As previously discussed in paragraph 3.2.3.2, no β-hydrosilylation occurred at position 2 of the silanes, **73** and **74**, therefore there can only be one iodated polysiloxane product. This is observed by comparing the ^{1}H NMR spectrum of the iodated polysiloxanes **79** and **80** with those of the precursor polysiloxane, **76** and **77** respectively. The halogen exchange reaction of the chlorinated polysiloxane

76 gave exclusively one iodated polysiloxane, **79**. For the isomerized brominated/chlorinated polysiloxane, **77**, the two peaks in the region δ 3.35-3.60 ppm resulting from these two isomer products collapse into a single I-CH_2 peak at 3.21 ppm to give the iodated polysiloxane **80** as the only product. However for iodated polysiloxane **81** (see **Scheme 3. 6**, reaction B), due to the occurrence of β-hydrosilylation at carbon position 2 of the silane **75**, two peaks are observed in the polysiloxane precursor **78** in the region 3.35-3.6 ppm. It is concluded therefore that the Cl/Br active site of both α- and β-isomers in polysiloxane **78** are iodated in the polymer backbone to form polysiloxane **81**. This is evident on the ^{1}H NMR of **81** which shows an I-CH_2 signal from the main iodated polymer product at 3.20 ppm and the appearance of two new triplets at δ 1 ppm and 3.05 ppm (labelled c′ and b′ respectively) which represent an isomer of **81** with a β-substituted alkyl chain as shown in **Figure 3. 2.**

3.2.6 Phosphination of iodo-polysiloxanes and complexation with rhodium(I) complexes

Six new carbonyl rhodium(I) complexes, **85-90**, containing a phosphinated polysiloxane ligand have been synthesized, **Scheme 3. 7**. The synthesis was accomplished in moisture and oxygen free conditions first by displacing the iodide group on polymers **79-81** with a PPh_2 group utilizing a stoichiometric amount of $LiPPh_2$ as reagent in dry and deoxygenated THF. All the phosphinated polysiloxanes **82-84** are air sensitive and are oxidized when exposed to open air atmosphere. Hence they were synthesized “in situ” and not isolated, except a small portion to perform an NMR analysis of **82-84**.

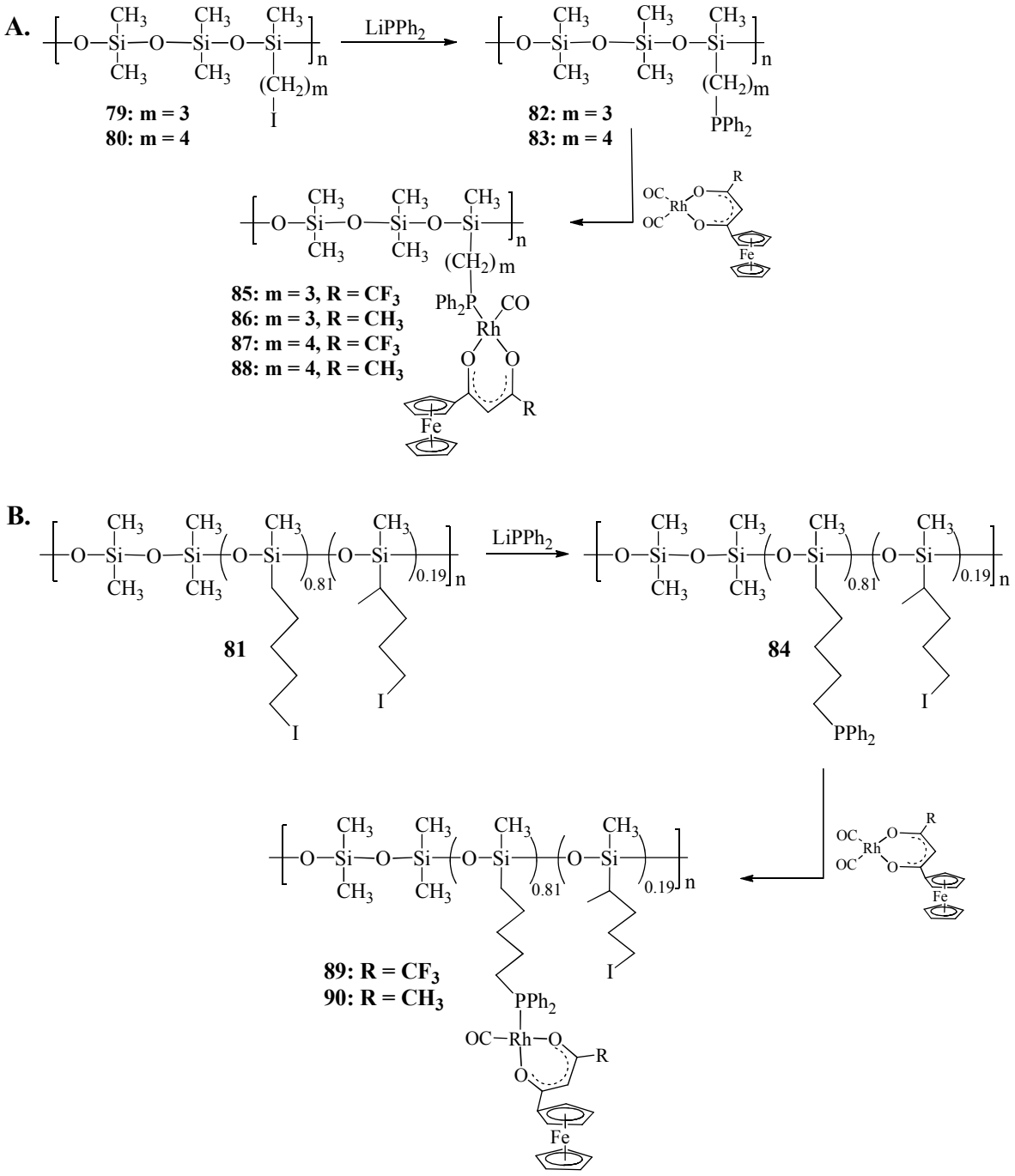

Scheme 3. 7. Complexation of [Rh(FcCOCHCOR)(CO)$_2$] with the phosphine polysiloxane, 82-84.

They were then immediately treated with either [Rh(FcCOCHCOCH$_3$)(CO)$_2$] or [Rh(FcCOCHCOCF$_3$)(CO)$_2$] to obtain complexes **85-90**. However, spectrums 4.17, 4.18 and 4.18 in the Appendix show the ^{1}H NMR of phosphinated polymers **82, 83** and **84** that were obtained by removing a sample of the reaction mixture under reduced pressure and quickly dissolving the residue in CDCl$_3$ just to characterize the product by ^{1}H NMR. As can be seen, traces of THF still remained, but all the important peaks could be clearly identified from the crude reaction mixture. ^{31}P NMR of the phosphinated polymers **82-84** (see Appendix, Spectrum 4.26) showed a phosphorus peak at δ -16 to -17 ppm relative to the external standard, 85 % H$_3$PO$_4$ at 0 ppm.

To obtain the rhodium-containing polymers, a warm phosphinated polysiloxane solution in $CDCl_3$ was added slowly to a warm solution of [Rh(FcCOCHCOR)$(CO)_2$]. Bubbling was observed due to the release of CO ligand as a gas. In general phosphine substitution was allowed to continue by stirring the reaction mixture for 5 minutes to ensure complete reaction. After complexation, the new rhodium(I) phosphine polysiloxanes could be handled in an open air atmosphere without decomposition. The solubility in $CDCl_3$ decreased for longer alkyl chained phosphine polysiloxanes **83** and **84**, thus THF was used as a solvent for the synthesis of complexes **87-90** (**Scheme 3. 7**). All the new rhodium(I) polysiloxane complexes were purified by extracting the reaction mixture with water. For compound **87-90** the THF was slowly removed under vacuum before $CDCl_3$ was added prior to extraction with water. In all reactions, the iodated or phosphinated polysiloxanes were always added to $LiPPh_2$ and [Rh(FcCOCHCOR)$(CO)_2$] respectively and not the other way around to reduce the degree of cross linking of the polymer according to the reaction,

$$\text{polymer-I} + \text{polymer-PPh}_2 \rightarrow [\text{polymer-P}^{+}\text{Ph}_2\text{-polymer}]\text{I}$$

The ^{1}H NMR for the new rhodium(I) phosphine polysiloxanes **85-90** showed that rhodium(I) complex, [Rh(FcCOCHCOR)$(CO)_2$], is indeed bound to the polymeric phosphine group. The polysiloxanes and the free complex, **24**, show the existence of two isomers in solution. One isomer has the ferrocenyl group on the same side of rhodium as the CO group and the other has the ferrocenyl and CO groups opposite sides of the rhodium center. They are labeled the C and T isomers respectively, see **Figure 3. 3**. The ^{1}H NMR in $CDCl_3$, **Figure 3. 4**, shows on top the ferrocenyl part of the monomeric precursor [Rh(FcCOCHCOCF$_3$)$(CO)_2$], **24**, in the middle is the authentic free [Rh(FcCOCHCOCF$_3$)(CO)(PPh_3)], **28**, and then the full spectrum of polymer **87** at the bottom.

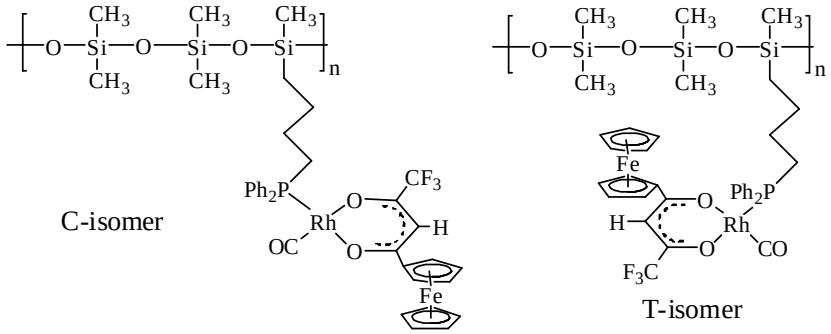

Figure 3. 3. Isomers of the new rhodium(I) phosphine polysiloxane, 87, with the ferrocenyl group on the same side of the CO group (C-isomer) and the other has the ferrocenyl group on the opposite side of the CO group (T-isomer).

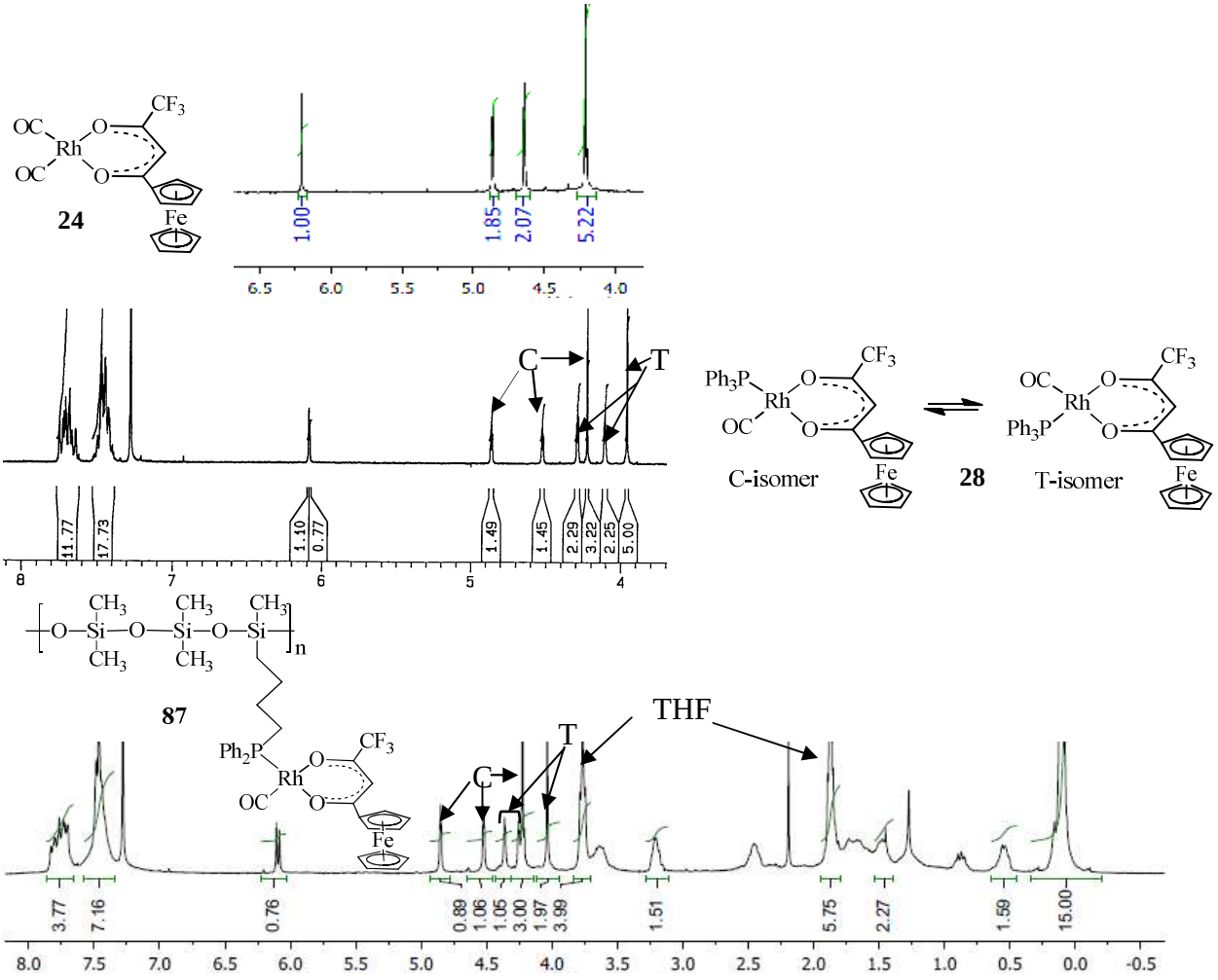

Figure 3. 4. ^{1}H NMR of the monomeric precursor [Rh(FcCOCHCOCF$_3$)(CO)$_2$], 24 (top), the new rhodium(I) carbonyl polysiloxane, 87, (bottom) and the free [Rh(FcCOCHCOCF$_3$)(CO)(PPh$_3$)] complex, 28 (middle) duplicated from J. Conradie, J.C. Swarts, *Organometallics*, 2009, 28, 1018. C and T represent the C-isomer and T-isomer respectively.

From the spectrum of **24**, [Rh(FcCOCHCOR)(CO)$_2$], it is clear the ferrocenyl group resonates at 4.87 (2H, C_5H_4), 4.65 (2H, C_5H_4) and 4.22 (5H, C_5H_5) (see **Figure 3. 4**, top). Conradie and Swarts[123] have shown that the ferrocenyl group of [Rh(FcCOCHCOCF$_3$)(PPh$_3$)], **28**, resonates as two distinct sets due to two isomers in solution. One isomer has the ferrocenyl group trans to the CO group, the other has the ferrocenyl group cis to the CO group. The ^{1}H NMR position of the ferrocenyl signals of these two isomers are 4.25 (2H, C_5H_4), 4.06 (2H, C_5H_4) and 3.98 (5H, C_5H_5) as well as 4.83 (2H, C_5H_4), 4.47 (2H, C_5H_4) and 4.22 (5H, C_5H_5) respectively (see **Figure 3. 4**, middle). The position of the signals of the ferrocenyl group of the two isomers of polymer **87** are 4.36 (2H, C_5H_4), 4.26 (2H, C_5H_4) and 4.03 (5H, C_5H_5) as well as 4.86 (2H, C_5H_4), 4.52 (2H, C_5H_4) and 4.22 (5H, C_5H_5) respectively (see **Figure 3. 4**, bottom). This "*cis*" and "*trans*" isomerization

123 J. Conradie and J.C. Swarts, *Organometallics*, 2009, **28**, 1018.

was also observed for rhodium(I) polysiloxane complex **85**, **86**, **88**, **89** and **90** (see Appendix, Spectrum 4.20, 4.21, 4.23, 4.24 and 4.25).

^{31}P NMR for monomeric rhodium carbonyl triphenyl phosphine complexes is found as doublet at δ 49.05 ppm (C-isomer) and 47.53 ppm (T-isomer) for R = CH_3 and also at δ 48.04 ppm relative to H_3PO_4.[123] The present polymer rhodium-containing complexes showed broad doublets for the two CF_3 isomers of **85** at approximately δ 38.5 and 37 ppm. Peaks were so broad and rounded due to the polymeric nature of these complexes that J-values could not be meaningfully determined. For Rh(I) polymer complexes **87** and **89**, the main signal appeared at approximately δ 40 ppm (see Appendix, Spectrum 4.29 and 4.31,). For the three CH_3 complexes **86**, **88** and **90** the main signal was observed at approximately δ 37.8 ppm, (see Appendix, Spectrum 4.28, 4.30 and 4.32).

3.3 Viscosity measurements

The resistance to flow of dichloromethane solutions containing iodide polymers was determined by measuring the viscosity at different concentrations. Extrapolation of the data to "zero" concentration gave the inherent viscosity (η_{inh}). **Figure 3. 5** demonstrates this for iodated polysiloxane **80** and **81**.

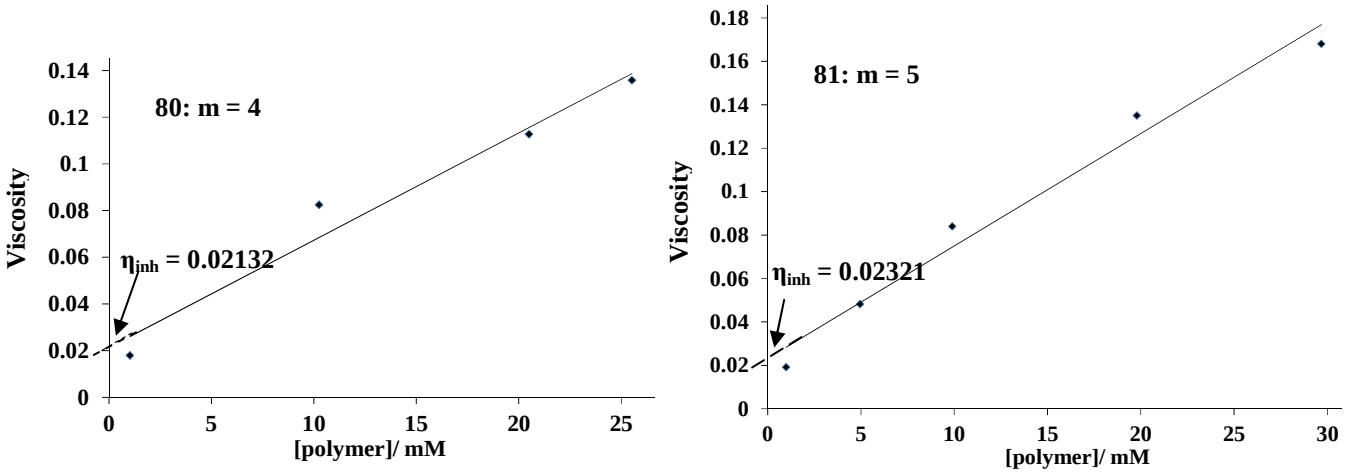

Figure 3. 5. Linear graphs of viscosity, η, as a function of concentration allowed the determination of the inherent viscosity, η_{inh}, at the y-intercept, i.e. at [polymer] = 0 mM.

It was noted that the inherent viscosity and the viscosity of the polymer solution at the lowest concentration (ca. 1.76 mM) was almost the same. Therefore, in accordance with international practice, for the rhodium-containing polymers, the inherent viscosity was approximated by reporting viscosity at polymer concentration 1.76 mM. Results are summarized in **Table 3. 1**.

Table 3. 1. Summary of inherent viscosity measurements.

Compound	η (η_{inh} at c = 0)[a]
76: n = 3, X = Cl	0.021 (-)
77: n = 4, X = Br	0.014 (-)
76: n = 5, X = Br	0.013 (-)
79: n = 3, X = I	0.05 (0.02)
80: n = 4, X = I	0.019 (0.021)
81: n = 5, X = I	0.021 (0.023)
85: n = 3, R = CF_3	0.016 (-)
86: n = 3, R = CH_3	0.012 (-)
87: n = 4, R = CF_3	0.019 (-)
88: n = 4, R = CH_3	0.017 (-)
89: n = 5, R = CF_3	0.011 (-)
90: n = 5, R = CH_3	0.028 (-)

[a] The first value is the approximate value at [polymer] = 1.76 mM while the value in brackets represent the experimentally determined value from concentration data extrapolated to "zero" concentration as per **Figure 3. 5**.

3.4 XPS analysis

The rhodium-containing polymer samples **85-90** were submitted for X-ray photoelectron spectroscopic (XPS) analysis at the Department of Physics, University of the Free State. The samples were not sputtered during measurement and as a result the composition of the sample as determined by XPS had large C and O contents. It also meant the atom percentages of Si, P, F, I, Rh and Fe were not accurate. The elemental analyses results presented in Chapter 4 are, however reliable to determine the success of each reaction. However from the analyses of the freshly prepared samples it was shown that a residual amount of iodide was still in it. It was found that up to 10 % of the available iodated sites were not phosphinated and this complicated the kinetic analysis that is described later in this chapter. For illustrative purposes the wide scan of rhodium polymer **85** (with m =3 and R = CF_3) is shown in **Figure 3. 6** while the high resolution XPS signals for Si, P, F, I, Rh and Fe are shown in **Figure 3. 7**. **Table 3. 2** summarizes the measured binding energies of each element. The data for the elements C and O is not included because sputtering of the samples was not performed by the analyst. Therefore large amounts of surface adsorbed carbon (from CO_2) and oxygen (from O_2) made the data and spectrums irrelevant.

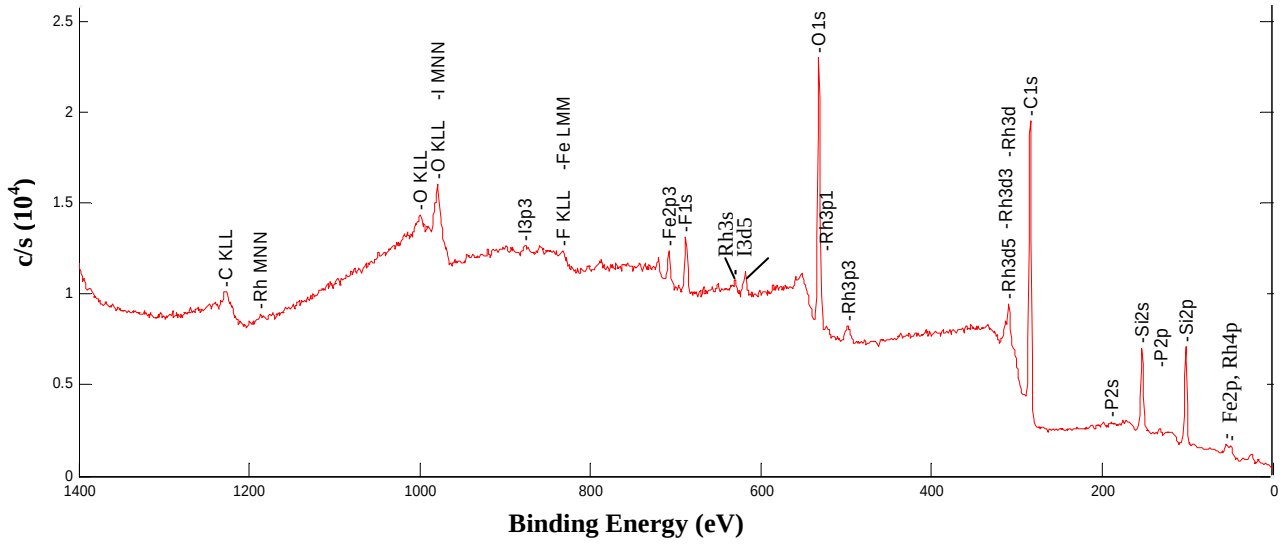

Figure 3. 6. XPS wide scan survey of polymer 85.

The measured silicon peak in **Figure 3. 7** shows to be the compliment of two separate peaks (it was fitted to two separate peaks) and is probably the result of two different types of Si in each polymer from the 2p orbital. The Fe signal appears as two peaks because of the $2p_{1/2}$ and $2p_{3/2}$ orbitals. The two peaks observed for rhodium are due to interactions of the $3d_{3/2}$ and $3d_{5/2}$ orbitals. The binding energies of the rhodium and iron imply that Rh^{I} and Fe^{II} species are present in the compounds.

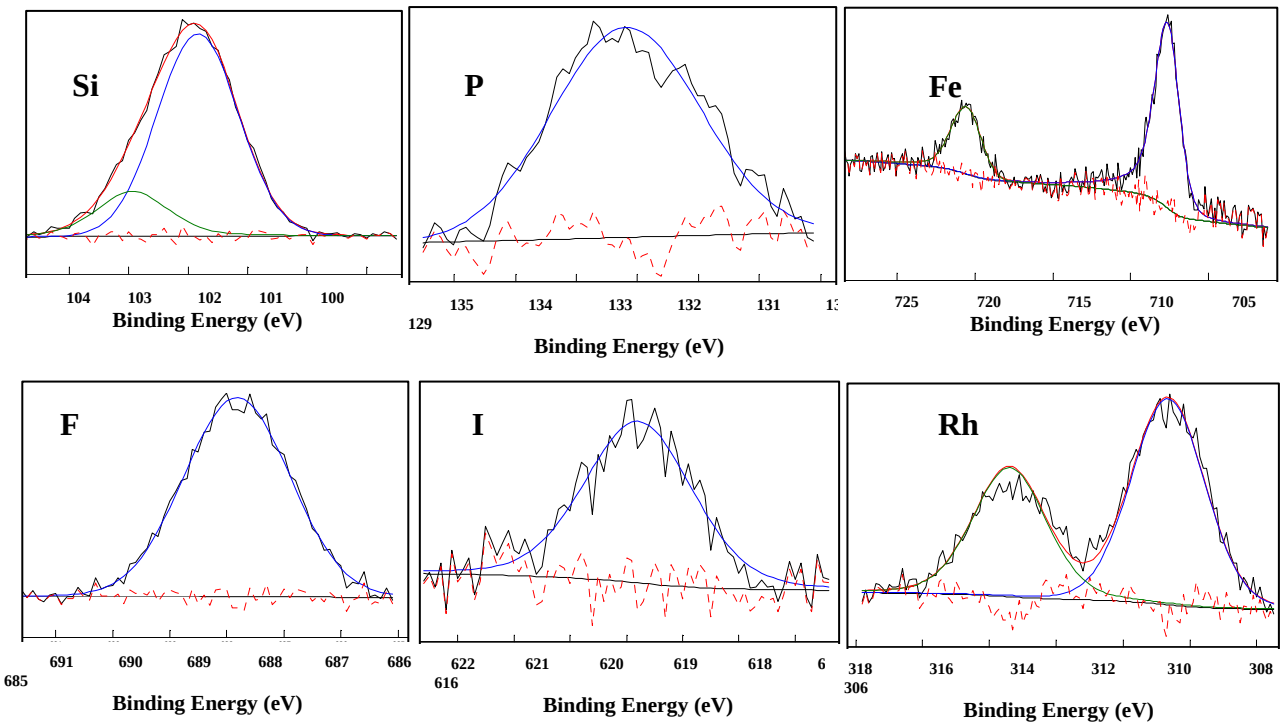

Figure 3. 7. Narrow XPS scan of polymer 85 measured for Si, P, Fe, F, I and Rh elements. I is measured in very low quantities and is the result of trace amounts of iodated polymer sites that were not phosphinated during the

Elements	Orbital	Binding energy
Si	2p	102.93; 101.84
P	$2p_{3/2}$	132.18
Fe	$2p_{1/2}$; $2p_{3/2}$	720.55; 707.63
F	1s	687.82
I	$3d_{5/2}$	618.78
Rh	$3d_{3/2}$; $3d_{5/2}$	313.39; 308.65

Table 3. 2. Summary of the elemental binding energies.

3.5 Electrochemistry

3.5.1 Introduction

Cyclic voltammetry (CV), Oster Young square wave voltammetry (SWV) and linear sweep voltammetry (LSV) were performed on selected rhodium complexes (see **Goal 5 – Chapter 1**). The effect of the group electronegativity (χ_R) of substituents and the presence of the polysiloxane backbone on the formal reduction potential of the redox active metallic nuclei of the complexes were determined.

The rhodium(I) and ferrocenyl metallic redox-active centres in the synthesized complexes were studied. The Rh^I/Rh^{II} and Fc/Fc^+ redox-active couples were found to vary from being electrochemically reversible (theoretically this implies $\Delta E_p = 59$ mV but experimentally it was taken as $\Delta E_p \leq 90$ mV in this study), quasi-reversible (assigned to experimental values between $90 < \Delta E_p < 150$ mV) to irreversible (experimental values of $\Delta E_p > 150$ mV). The peak current ratios were calculated as $i_{pc\ (reverse\ sweep)}/i_{pa\ (forward\ sweep)}$. All potentials are reported *vs* ferrocene, $FcH/(FcH)^+$, although they were experimentally measured *vs* a Pt wire reference electrode. Decamethylferrocene (Fc^*) was utilized as internal standard since ferrocene overlapped with signals of the compounds analyzed. Under the conditions of this study $E°'$ of Fc^* = -610 mV *vs* FcH/FcH^+. In order to minimize solvent and electrolyte interactions, CH_2Cl_2 was used as solvent and $[N^nBu_4][B(C_6F_5)]$ as supporting electrolyte.

3.5.2 Electrochemistry of Rhodium(I) Dicarbonyl Complexes

First, an electrochemical study was done on the two rhodium(I) dicarbonyl complexes $[Rh(FcCOCHCOR)(CO)_2]$ where Fc = ferrocenyl, R = CH_3, 23, and CF_3, 24. These complexes have

previously been studied in CH_3CN using $[N^nBu_4][PF_6]$ as an electrolyte.[124] It was found in that study[124] that the rhodium(I) oxidation peak overlaps with the reversible one electron transfer oxidation peak of the ferrocenyl group. The Rh^I centre was in that study electrochemically irreversibly oxidized to Rh^{III} and a small reduction wave of electrochemically generated Rh^{III} was observed with ΔE_p > 1000 mV. The authors of the CH_3CN study also found that at oxidation potentials larger than the overlapping ferrocenyl/rhodium wave, a second rhodium species was oxidized. This was proposed to be the Rh^I/Rh^{III} oxidation of the solvent-associated complex, $[Rh(FcCOCHCOR)(CO)_2(CH_3CN)]$.

In this study, using the non-coordinating solvent CH_2Cl_2 and $[N^nBu_4][B(C_6F_5)_4]$ electrolyte system, only one poorly resolved oxidation wave was observed for all possible electron transfer steps. In analogue to the CH_3CN study, therefore, it is proposed that the electrochemically reversible oxidation wave of the ferrocenyl group and that of the rhodium centre overlaps. The obtained electrochemical data are summarized in **Table 3. 3** and the cyclic voltammograms (CV's), linear sweep voltammograms (LSV's) and square-wave voltammograms (SWV's) are shown in **Figure 3. 8.**

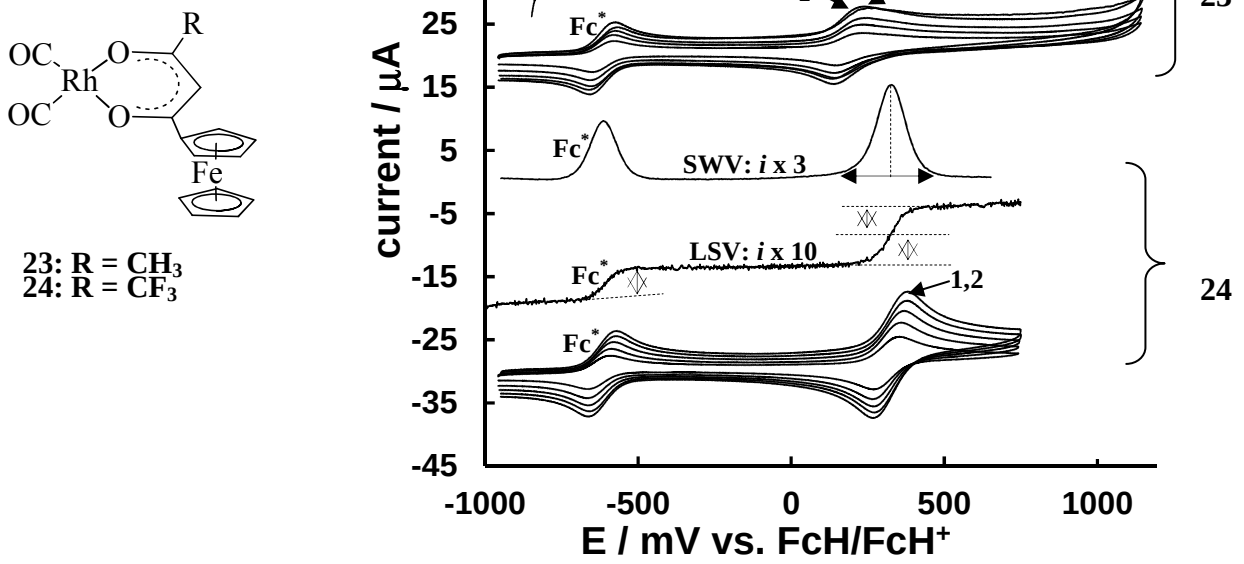

Figure 3. 8. Cyclic voltammograms of a 0.25 mmol dm^{-3} solutions of 23 and 24 measured in CH_2Cl_2/0.1 M $[N^nBu_4][B(C_6F_5)_4]$ at a glassy carbon-working electrode and a scan rate of 100, 200, 300, 400 and 500 mV s^{-1} together with the SWV's at 40 Hz and the LSV's at 1 mV s^{-1}. The current of the LSV (*i* x 10) as well as that of SWV (*i* x 3) were enlarged for clarity.

[124] J. Conradie, T.S. Cameron, M.A.S. Aquino, G.J. Lamprecht and J.C. Swarts, *Inorg. Chim. Acta*, 2005, **358**, 2530-2542.

For complex **23** where R = CH_3, a broad electrochemically reversible oxidation wave is observed at 246 mV with ΔE_p < 90 mV at slow (100 mVs^{-1}) scan rates. The broadness of the peak suggests this wave represents two closely overlapping peaks, labelled 1 and 2 in **Figure 3. 8**. Wave 1 is assigned to a Rh^{I}/Rh^{II} couple and wave 2 is assigned to the electrochemically reversible Fc/Fc^{+} couple, the same as in the acetonitrile study.[124]

Table 3. 3. Electrochemical data obtained for 0.25 mM solutions of rhodium(I) dicarbonyl complexes 23 and 24 in CH_2Cl_2/0.1 M $[N^nBu_4][B(C_6F_5)_4]$ at 25 °C.

v /mVs^{-1}	**E_p /mV**	**ΔE_p**	**$E°'$ /mV**	**i_{pa} /mA**	**i_{pc}/i_{pa}**
[Rh(FcCOCHCOCH$_3$)(CO)$_2$], **23**					
100	246	87	203	2.77	0.90
200	250	99	201	4.04	0.89
300	244	106	191	5.10	0.92
400	244	109	190	6.35	0.89
500	259	115	202	6.89	0.91
[Rh(FcCOCHCOCF$_3$)(CO)$_2$], **24**					
100	366	84	324	4.10	0.91
200	373	97	325	5.90	0.93
300	377	111	321	6.67	0.92
400	376	100	326	8.01	0.94
500	390	130	325	7.95	0.92

The CV of **24** where R = CF_3, shows even less resolution than the CV of **23** for peak 1 and 2. This is consistent with the ferrocenyl and rhodium(I) centers being oxidized at almost the same potential. SWV did not assist in resolving the peaks better than the CV, but it did show a more broadened peak base for **23**, **Figure 3. 8**, consistent with more than one oxidation process taking place in this potential range. Since $i_{pc}/i_{pa} \approx 1$, both the overlapping oxidation wave of the rhodium and ferrocenyl are assigned to be a chemically reversible one electron transfer process. A one-electron transfer process for the rhodium couple is decided on because ΔE_p = 87 or 84 mV at slower scan rates (100 mV s^{-1}) rather than ΔE_p < 30 mV for $2e^-$ transfer process. We conclude, therefore, that in $CH_2Cl_2/[N^nBu_4][B(C_6F_5)_4]$ Rh^{I} is oxidized to Rh^{II} and not Rh^{III} as was observed in the acetonitrile study.[124] From the LSV study of these compounds, it was confirmed that there is indeed two oxidation processes taking place when the number of electrons transferred during the oxidation process was compared. At the same concentrations, the ratio of the number of electrons transferred for decamethyl ferrocene to the sum of the overlapped ferrocenyl group and the rhodium center of

23 and **24** (waves 1 and 2 combined) gave approximately a ratio of 1:2 (see LSV's in **Figure 3. 8**), thus showing a one-electron oxidation process for each redox-active center. A Rh^{I}/Rh^{II} couple has also previously been observed elsewhere when a solvent such as CH_2Cl_2 is used instead of CH_3CN.[125]

The oxidation for **23** where R = CH_3 occurs at lower potentials (E°′ = 203 mV) than **24** where R = CF_3 (E°′ = 324 mV). This observation is explained using Gordy group electronegativities, a parameter that quantifies the attraction of a group of atoms on the bonding electrons. It is observed that the formal reduction potentials (E°′) of the ferrocene peak increases as the group electronegativities of the different R-substituents of the β-diketonato ligand in [Rh(FcCOCHCOR)$(CO)_2$], **23** (R = CH_3, χ_R = 2.34) to **24** (R = CF_3, χ_R = 3.01) increases. Since the CF_3 substituent in **24** is more electron-withdrawing than CH_3 in **23**, more electron-density is removed from its Fe and Rh centers making these metals more difficult to oxidize. Hence larger oxidation potentials were observed for **24** than for **23**. This large difference in oxidation potential implies good electronic communication between the R-substituent and the Fe and Rh centers exists through the β-diketone backbone.

3.5.3 Electrochemistry of new polysiloxane-bound Rhodium(I) Phosphine Complexes

Six new rhodium(I) phosphine polysiloxanes of the type $\{(OSiMe_2)_2OSiMe\{(CH_2)_mPPh_2(CO)(FcCOCHCOR)Rh\}\}_n$ where R = CF_3 and m = 3 **(85)**, m = 4 (**87**) and m = 5 (**89**) or where R = CH_3 and m = 3 (**86**), m = 4 (**88**) and m = 5 (**90**) were studied in CH_2Cl_2/0.1M $[N^nBu_4][B(C_6F_5)_4]$ at 25 °C.

It was previously shown in Chapter 2 that two isomers of monomeric complexes of the type [Rh(FcCOCHCOR)(CO)$(PPh_3]$ exist.[126] In the electrochemistry of these isomers, Rh(I) is first oxidized, sometimes as two distinct peaks (not always observed), followed by the oxidation of the ferrocenyl group at two different peaks. However the peaks are not always resolved. The existence of two isomers (shown in **Scheme 3. 8**) was also observed on the ^1H NMR spectrums for complexes of the type $\{(OSiMe_2)_2OSiMe\{(CH_2)_mPPh_2(CO)(FcCOCHCOR)Rh\}\}_n$ (see Appendix, Spectrum 4.20 to 4.25,).

---

125 M. Fatima, G.C. da Salva, A.M. Trzeciak, J.J. Ziolkowski and A.J.L. Pombeiro, *J. Organomet. Chem*., 2001, **620**, 174.

126 J. Conradie and J.C. Swarts, *Eur. J. Inorg. Chem*., 2011, 2439

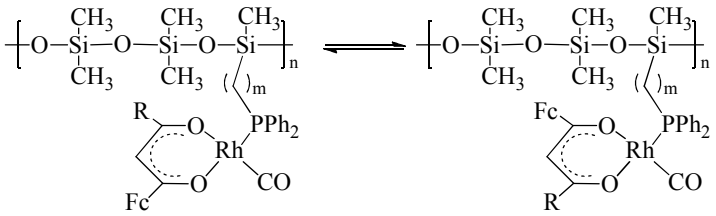

85: m = 3, R = CF_3
86: m = 3, R = CH_3
87: m = 4, R = CF_3
88: m = 4, R = CH_3
89: m = 5, R = CF_3
90: m = 5, R = CH_3

Scheme 3. 8. The isomeric structures of rhodium(I) phosphine polysiloxane complexes 85-90.

From these isomeric structures, the CV's of the polysiloxane complexes are thus expected to exhibit two electrochemically irreversible rhodium(I) oxidation peaks and two oxidation peaks due to the two ferrocenyl groups on the β-diketonato ligand from each isomer. For polysiloxane complexes **85**, **87** and **89** these peaks were actually almost completely resolved (see **Figure 3. 9** and **Table 3. 4**). All CV's showed electron transfer activity in the region 100-600 mV. Only rhodium peak 1 and 2 could not with certainty be identified separately.

From the CV's of **85** (shown in **Figure 3. 9**, (a), bottom) a shoulder wave at 152 mV on the anodic cycle can be attributed to the electrochemically irreversible one electron oxidation of the Rh^{I} center to Rh^{II} of isomer 1 (labeled Rh (1)). The second rhodium oxidation from isomer 2 could not be identified because it was obscured under the first Fc(1) wave and could not be resolved. Two electrochemically reversible oxidation peaks for the ferrocenyl groups with $\Delta E_p < 90$ mV (at slow scan rates) are observed at a more positive potential for each isomer. The first appears at 303 mV and is associated with the Fc group Fc(1) of isomer 1 and the second, Fc(2), is observed at higher oxidation potential of 404 mV because of the trans-effect it has with the CO group. The peak at 588 mV is identified as an impurity at this stage and does not form part of the compound system. In support to this, this "impurity" peak could not be observed for the other two complexes, **87** and **89**.

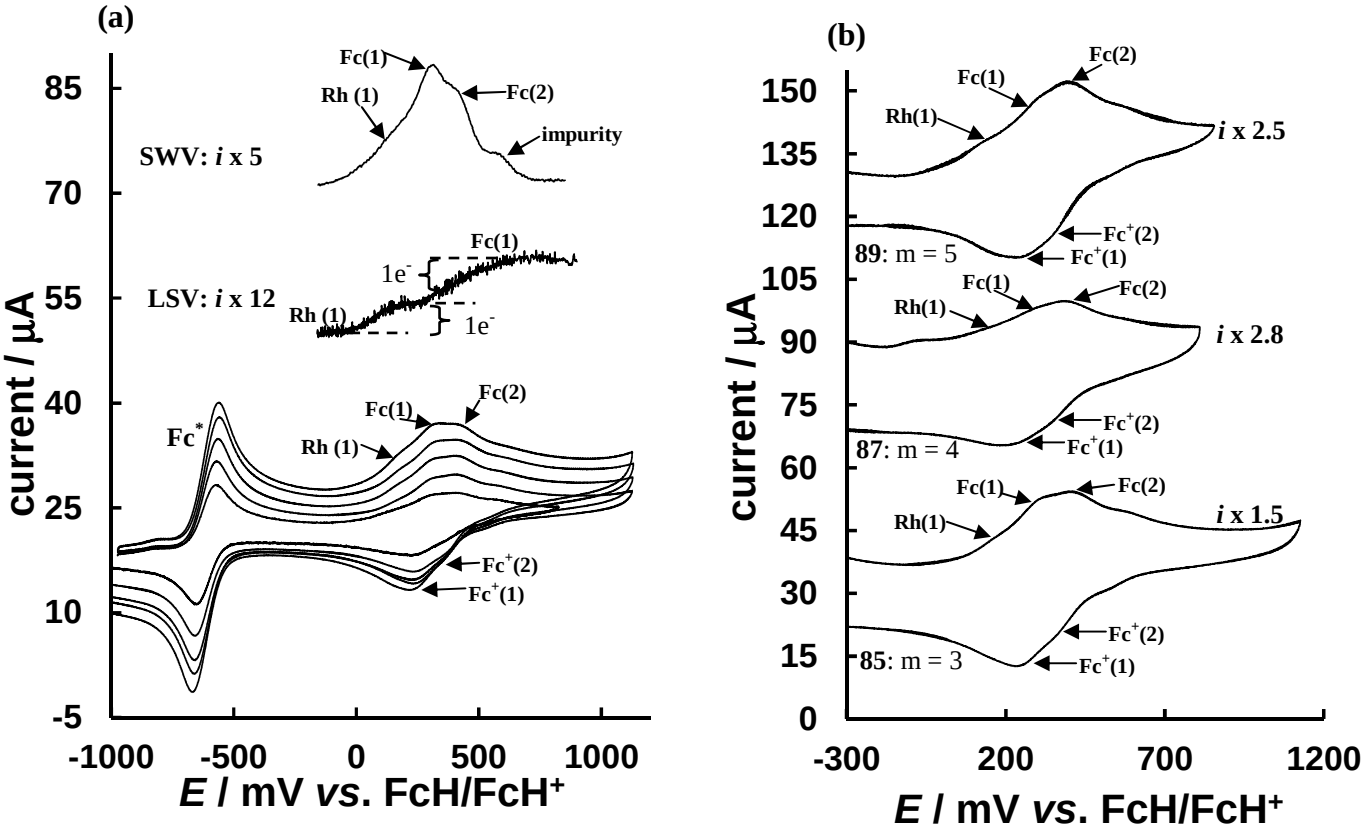

Figure 3. 9. (a) CV's of ɬ$(OSiMe_2)_2OSiMe\{(CH_2)_3PPh_2(CO)(FcCOCHCOCF_3)Rh\}$ɭ$_n$, 85, at 100, 200, 300, 400 and 500 mVs^{-1} scan rates (bottom), LSV (middle) and SWV (top). The LSV was multiplied by 12 and the SQW by 5 for better clarity (b) CV's of ɬ$(OSiMe_2)_2$ $OSiMe\{(CH_2)_mPPh_2(CO)(FcCOCHCOCF_3)Rh\}$ɭ$_n$ where m = 3, 85, m = 4, 87 and m = 5, 89, at 200 mVs^{-1} scan rate in CH_2Cl_2/0.1M $[N^nBu_4][B(C_6F_5)_4]$ at 25 °C.

In the SWV of the complex **85** (shown **Figure 3. 9**, **(a)**), the ferrocenyl peak waves were more clearly resolved than the CV. From the LSV two oxidation processes are shown to be taking place, one for Rh^I to Rh^{II} oxidation and the second for Fc to Fc^+ oxidation of the two closely overlapped ferrocenyl groups of each isomer. Since a ferrocenyl group is known to be a one-electron oxidation transfer process, it is concluded that rhodium undergoes a one-electron and is therefore oxidized from Rh^I to Rh^{II} and not Rh^{III} as was observed in the acetonitrile study.[124] The oxidation of Rh^I to Rh^{II} has also been observed for rhodium(I) metallocene-containing phosphines in CH_2Cl_2.[127]

The CV's of **86**, **88** and **90** where R = CH_3 showed similar behavior as the complexes where R = CF_3. In all three cases a broad oxidation peak was observed in the region 100-500 mV. The polysiloxane complex with the shortest carbon chain, m = 3, **86**, is discussed in detail. The electrochemical data is summarized in **Table 3. 4** and the CV's, LSV's and SWV's are shown in **Figure 3. 10**.

[127] E. Fourie, Thesis: *A structural, electrochemical and kinetic investigation of fluorinated and metallocene-containing phosphines and their rhodium complexes*, 2008.

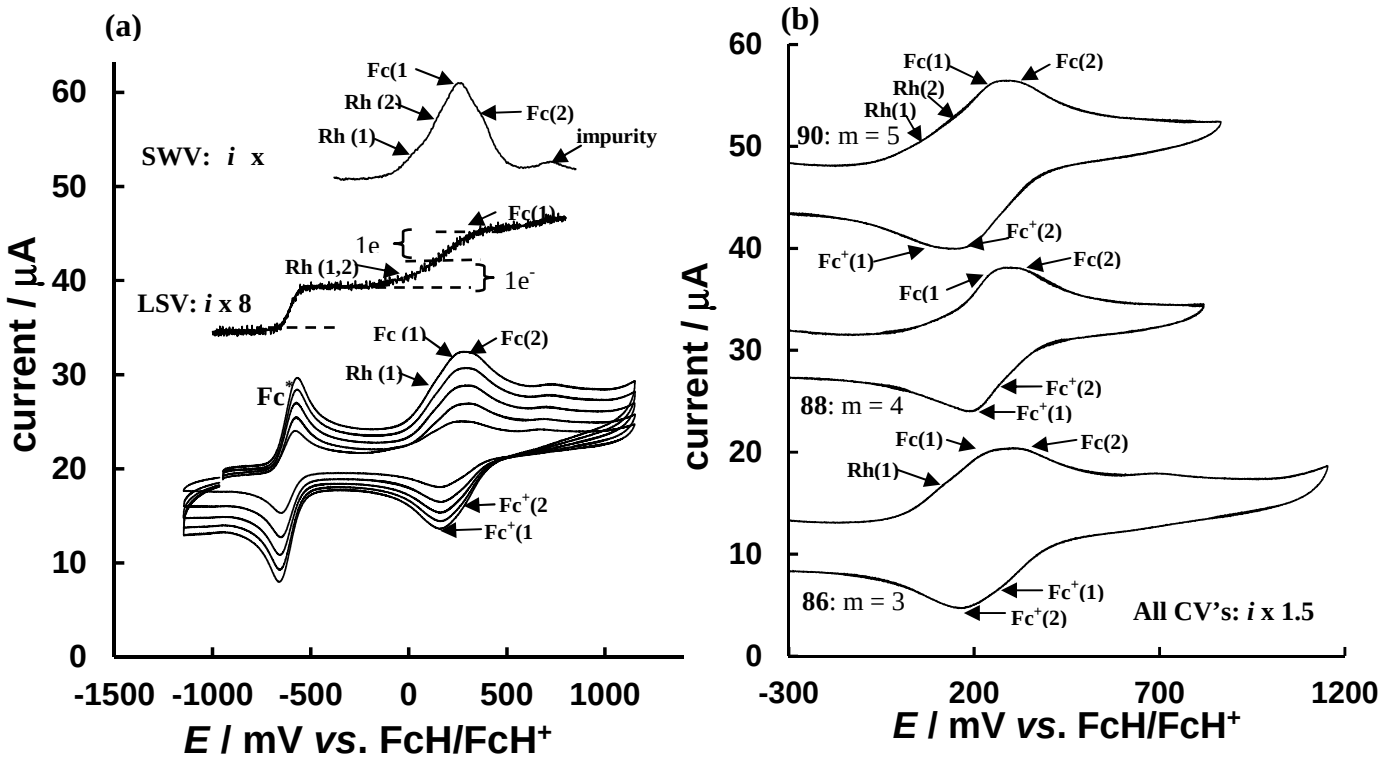

Figure 3. 10. (a) CV of $\{(OSiMe_2)_2OSiMe\{(CH_2)_3PPh_2(CO)(FcCOCHCOCH_3)Rh\}\}_n$, 86, at 100, 200, 300, 400 and 500 mVs^{-1} scan rates (bottom), LSV (middle) at 1 mVs^{-1} at and SWV (top) at 40 Hz. The LSV was multiplied by 8 and the SWV by 4 for better clarity. (b) CV's of complexes 86, 88 and 90 at 200 mVs^{-1} scan rate in CH_2Cl_2/0.1 M $[N^nBu_4][B(C_6F_5)_4]$ at 25 °C.

From the CV's of polysiloxane rhodium(I) complex **86** (see **Figure 3. 10**, **(a)**), the rhodium oxidation of isomer 1 is less clearly visible compared to polysiloxane complexes with R = CF_3 as a result of peak broadening. As was observed in **85** the second rhodium oxidation Rh(2) for isomer 2 could not be identified because of lack of resolution. The oxidation of the first rhodium oxidation Rh(1) could be identified at 114 mV. Two ferrocenyl group oxidation from isomer 1, Fc(1), and isomer 2, Fc(2), were detected during the anodic cycle at 230 and 327 mV respectively. However two shoulders at 75 and 131 mV appeared when SWV was performed. They are consistent with rhodium oxidation peaks Rh(1) and Rh(2) from the possible isomers. From the SWV two iron oxidations at waves Fc(1) and Fc(2) could be identified. Due to the lack of resolution, peak potentials reported in **Table 3. 4** are estimates only. As was observed in **85** the impurity shoulder at 671 mV for polymer **86** was not present for **88** (m = 4) and **90** (m = 5).

Table 3. 4. Electrochemical data obtained for 0.25 mM solutions of rhodium(I) phosphine polysiloxane complexes, $\{(OSiMe_2)_2\ OSiMe\{(CH_2)_mPPh_2(CO)(FcCOCHCOR)Rh\}\}_n$ in CH_2Cl_2/0.1M $[N^nBu_4][B(C_6F_5)]$ at 25 °C.

Compound	v/ mVs^{-1}	E_p/[a,b] mV	i_{pa}/[a] μA	E_p[a] /mV	ΔE_p	E°′ /mV	i_{pc}[a,b] /μA	E_p[a] /mV	ΔE_p	E°′ /mV	i_{pc}[a,b] /μA
	Rh (1,2)		Fc (1)					Fc (2)			
(85): R = CF_3, m = 3	100	152	1.31	303	74	266	2.33	404	60	374	1.44
	200	154	2.40	305	79	266	2.95	409	66	376	2.05
	300	156	3.00	309	84	267	3.70	414	72	378	2.75
	400	158	3.50	313	89	269	4.32	418	78	379	2.95
	500	159	3.70	315	93	269	5.19	421	84	379	3.18
(86): R = CH_3, m = 3	100	114	1.34	230	66	197	-	327	-[d]	293	-
	200	115	1.82	231	67	198	-	329	-[d]	294	-
	300	119	3.28	234	63	203	-	336	-[d]	297	-
	400	123	3.36	238	74	201	-	338	-[d]	300	-
	500	125	3.97	243	79	204	-	339	-[d]	303	-
(87): R = CF_3, m = 4	100	128	0.18	277	84	235	0.7	375	60	345	0.50
	200	129	0.33	278	88	234	1.33	375	63	345	1.00
	300	130	0.33	280	92	234	1.42	376	66	344	1.22
	400	130	0.33	281	96	233	1.56	377	67	345	1.37
	500	131	0.61	283	100	233	1.67	378	68	344	1.44
(88): R = CH_3, m = 4	100	109	2.02	246	58	217	4.79	327	-[d]	287	-
	200	110	2.30	248	60	218	5.53	328	-[d]	288	-
	300	111	2.56	258	75	221	6.70	329	-[d]	294	-
	400	111	2.94	249	71	214	7.53	330	-[d]	290	-
	500	111	3.21	249	72	213	8.64	330	-[d]	290	-
(89): R = CF_3, m = 5	100	175[e]	2.80	296	61	266	1.74	397	52	371	1.14
	200	176[e]	3.64	297	61	267	2.02	400	55	373	1.43
	300	179[e]	3.92	302	66	269	2.38	402	59	373	1.79
	400	179[e]	4.38	301	64	269	2.50	404	63	373	2.18
	500	180[e]	5.11	303	66	270	2.74	405	65	373	2.26
(90): R = CH_3, m = 5	100	98[c]	-	240	65	208	-[d]	324	65	292	-
	200	97[c]	-	247	77	209	-[d]	329	77	291	-
	300	94[c]	-	254	87	211	-[d]	333	87	290	-
	400	92[c]	-	258	91	213	-[d]	339	91	294	-
	500	87[c]	-	265	101	215	-[d]	340	101	290	-

[a] Due to the weak peak resolution, all potentials were estimated, therefore currents are not accurate.
[b] Meaningful measurement of anodic and cathodic peaks was impossible due to poor resolution of peaks.
[c] E_{pc} values.
[d] E°′ estimated by using same ΔE_p as for peak Fc(1).
[e] a secondary shoulder to the left of this peak was observed at ca. 68 mV. This shoulder may be associated with peak Rh(1) then the shoulder at 175-180 mV will be peak Rh(2).

When the carbon chain lengths were compared for all complexes, no meaningful difference in oxidation potentials could be discovered when moving from m = 5 to m = 3 except the increase in broadening of the oxidation peak. This observation is expected because as the chain decreases, the

steric hindrance of the polymeric backbone increases, which hence leads to more profound peak broadening.

When the electrochemistry of the non-polymer bound complex [Rh(FcCOCHCOR)(CO)(PPh_3)] was studied,[126] (previously described in paragraph 2.8.3, Chapter 2) all oxidation and reduction peaks of the two possible isomers were clearly resolved unlike in the polymeric complexes **85-90**. This is because the diffusion constants in solution of the polymeric and that of the free complex cannot be compared. In a polymer, the rate at which one isomer converts to the other in solution is much slower than the rate at which current flows through the solution and therefore a small concentration of the isomeric specie is oxidized and cannot be observed in the anodic cycle. The small ΔE_p values ($\Delta E_p \leq 84$ mV at 100 mVs^{-1} scan rate) for the ferrocenyl group from the shortest to the longest carbon chain is consistent with electrochemical reversibility.

The electrochemical data in **Table 3. 4** show that the formal reduction potentials (E°′) of the ferrocene peak in all polymer-bound rhodium(I) complexes increases as the group electronegativities of the different R-substituents of the β-diketonato ligand increases. For example, the E°′ value for a more electronegative substituent in **85** where n = 3, R = CF_3 is 303 mV compared to 230 mV (at a scan rate of 100 mVs^{-1}) of **86** where n = 3, R = CH_3. This implies that even when polymer-bound, good electronic communication exists between the R-substituent and the redox-active centers, Fe and Rh, through the β-diketone backbone. Good electronic communication was also observed for the free rhodium(I) dicarbonyl complexes, [Rh(FcCOCHCOR)$(CO)_2$], **23** and **24** as reported in paragraph 3.5.2.

3.6 The Beer Lambert law

A UV/vis spectroscopic study was done on the new rhodium(I) phosphine polysiloxanes, ⁞(OSiMe$_2$)$_2$ OSiMe{(CH$_2$)$_m$PPh$_2$(CO)(FcCOCHCOR)Rh}⁞$_n$, **85-90**. **Figure 3. 11** and **Figure 3. 12** show the UV/vis spectra of the rhodium(I) phosphine polysiloxanes grouped according to their R-substituent, R = CF_3 or CH_3, on the ferrocene-containing β-diketonato ligand. All polysiloxane complexes showed three prominent bands, two in the UV region and one in the visible region. In the 260-380 nm region, spectra were observed to vary for all complexes.

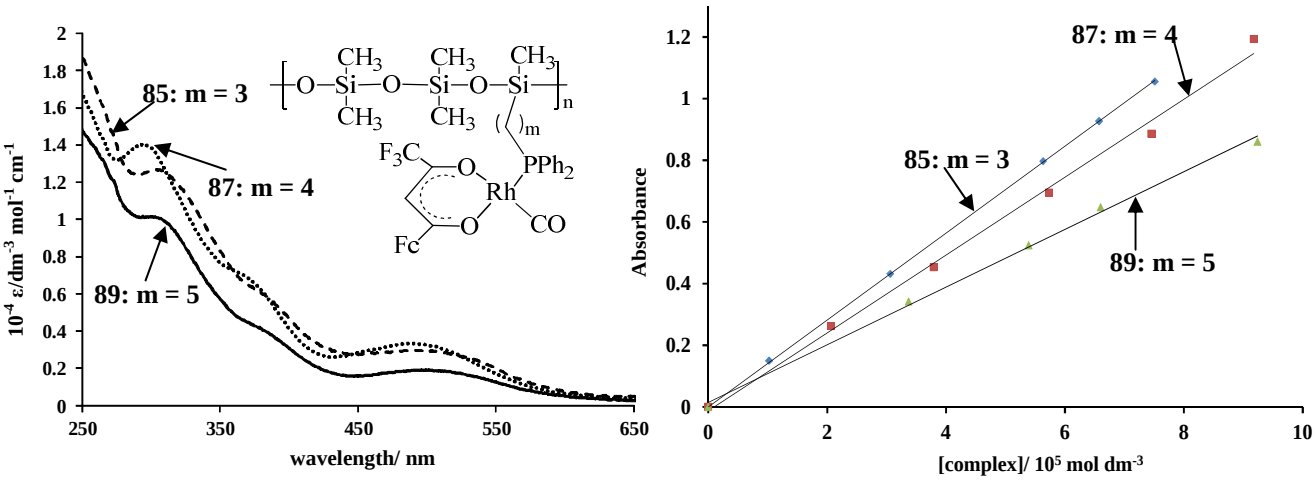

Figure 3. 11. Left: UV spectra of ⁞(OSiMe$_2$)$_2$ OSiMe{(CH$_2$)$_m$PPh$_2$(CO)(FcCOCHCOCF$_3$)Rh}⁞$_n$ where m = 3, 85, m = 4, 87, and m = 5, 89, in dichloromethane at 25 °C. Right: Beer Lambert law is confirmed by the linear relationship between concentration and absorbance of the rhodium polysiloxane compound series. Wavelengths

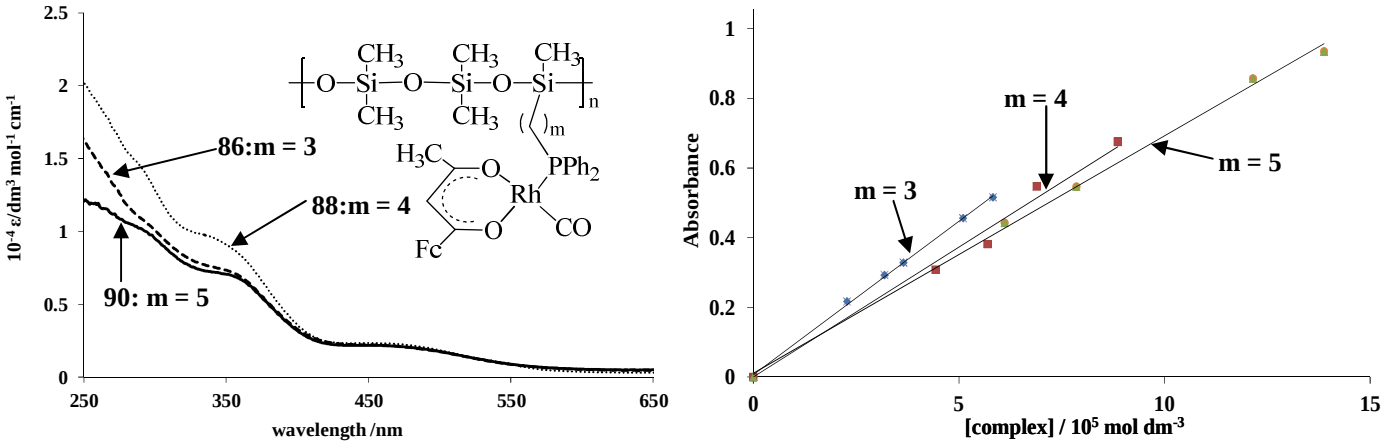

Figure 3. 12. Left: UV spectra of ⁞(OSiMe$_2$)$_2$OSiMe{(CH$_2$)$_m$PPh$_2$(CO)(FcCOCHCOCH$_3$)Rh}⁞$_n$ where m = 3, 86, m = 4, 88 and m = 5, 90, in dichloromethane at 25 °C. Right: Beer Lambert law is confirmed by the linear

A linear relationship between the absorbance, A, and the concentration, c, for the rhodium-containing polysiloxanes as predicted by Beer Lambert law ($A = \varepsilon c l$, with ε = extinction coefficient and l = cell path length = 1 cm) was confirmed (see **Figure 3. 11** and **Figure 3. 12**). A summary of ε-values and wavelengths for peak maximums for all complexes **85-90** are shown in **Table 3. 5**.

Table 3. 5. Extinction coefficients at associated wavelengths, ε, of the rhodium(I) polysiloxane complexes 85-90.

Compound	λ_{max}/nm [a] (ε /mol^{-1} dm^3 cm^{-3})	λ_{max} /nm [a] (ε /mol^{-1} dm^3 cm^{-3})	λ_{max} /nm [a] (ε /mol^{-1} dm^3 cm^{-3})
85: R = CF_3, m = 3	308 (13 0872)	384 (5841)	494 (2985)
87: R = CF_3, m = 4	292 (12 522)	376 (6512)	488 (3359)
89: R = CF_3, m = 5	301 (10 112)	387 (3771)	500 (1919)
86: R = CH_3, m = 3	295 (13 679) [b]	353 (8842)	453 (2348) [c]
88: R = CH_3, m = 4	295 (9896) [b]	362 (6794)	453 (2222) [c]
90: R = CH_3, m = 5	300 (9490) [b]	360 (6716)	455 (2184) [c]

[a] The wavelengths (λ_{exp}) and the associated extinction coefficient at which the kinetics of oxidative addition according to the reaction $\{(OSiMe_2)_2OSiMe\{(CH_2)_mPPh_2(CO)(FcCOCHCOR)Rh\}\}_n$ + MeI → $\{(OSiMe_2)_2OSiMe\{(CH_2)_mPPh_2(CO)(FcCOCHCOR)(Me)(I)Rh\}\}_n$ was studied is also tabulated.

[b] Shoulder before main peak.

[c] Shoulder on the main peak

The reddish colour of all compounds is associated with the peak visible in the wavelength range 450-500 nm. In the UV region, the CF_3 complexes has a definite λ_{max} at 295-301 nm, but a shoulder at ca. 370 nm is also identifiable. The CH_3 complexes showed shoulders at *ca.* 360 and 453 nm.

3.7 Kinetics

Because of the time limitations of an Msc study, only rhodium-containing polysiloxane **85** was chosen to investigate the kinetics of oxidative addition of methyl iodide to the rhodium centre. The reaction was first monitored by UV in the wavelength region 300-600 nm. Two consecutive reaction steps labelled stage 1 and 2 were identified. Because stage 1 was found to be first-order dependant on MeI and stage 2 had a zero-order dependence on MeI, these reaction stages were initially presumed to be as shown in **Scheme 3. 9**.

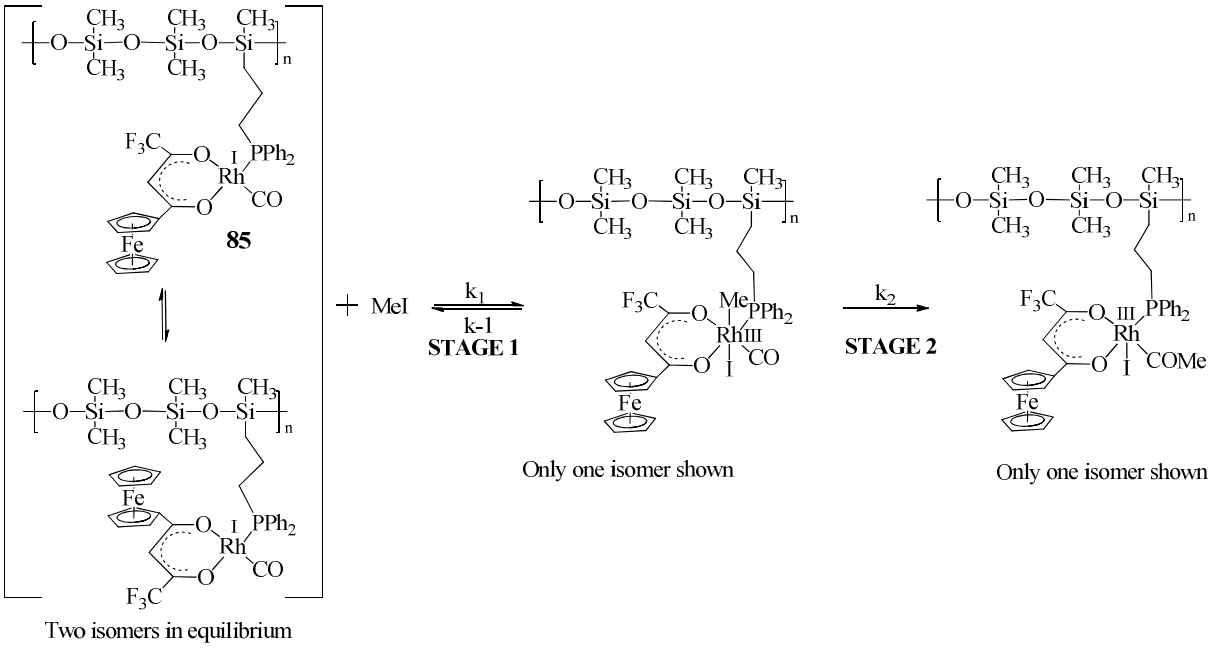

Scheme 3. 9. Two presumed reaction stages that may take place during oxidative addition of MeI to ⁞(OSiMe$_2$)$_2$OSiMe{(CH$_2$)$_3$PPh$_2$(CO)(FcCOCHCOCF$_3$)Rh}⁞$_n$, 85, in chloroform.

The reaction was studied in chloroform using pseudo first-order kinetic conditions, utilizing a 100-2000 fold concentration excess of MeI over the rhodium content (1.53 x 10^{-5} M) of polysiloxane **85**. From time base overlay spectra, significant changes in absorbance were identifiable at 325 and 520 nm. Stage 1 was conveniently monitored by measuring the absorbance change at 325 nm as a function of time, and stage 2 was monitored at 520 nm. **Figure 3. 13** shows overlay spectra of the 2000 fold excess ([MeI] = 0.0306 M) reaction of some of the spectra obtained for stage 1 before 1000 minutes of reaction time expired. This stage corresponds to the disappearance of the starting Rh(I) polysiloxane complex and the simultaneous formation of Rh(III)-alkyl specie due to the oxidative addition step. The insert shows some of the spectra obtained between 2000 – 5000 minutes for stage 2 when the reaction was performed utilizing a 500 fold MeI excess ([MeI] = 0.00765 M) over the Rh(I) content.

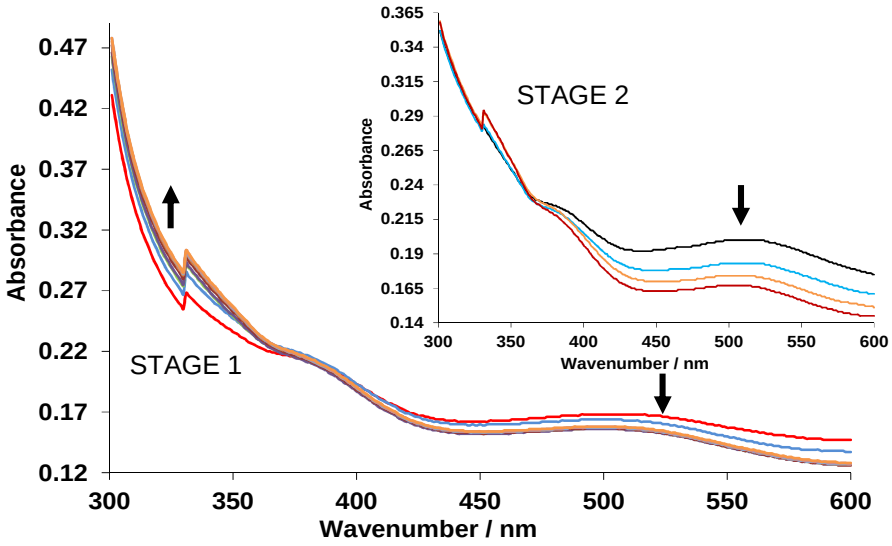

Figure 3. 13. Main diagram: Overlay UV/vis spectra for the oxidative addition of MeI to the rhodium centers of polysiloxane complex 85 recorded at 80, 100, 160, 200, 300, 400, 500, 600 and 700 minutes, [Rh content in polymer 85] = 1.53 x 10^{-5} M and [MeI] = 0.0306 M (a 2000 fold excess). Insert: Overlay UV/vis spectra for the same reaction at times 2010, 2995, 4012 and 4965 minutes, [Rh content in polymer 85] = 1.53 x 10^{-5} M and [MeI] = 0.00765 M (a 500 fold excess).

The obtained absorbance *vs* time kinetic data was plotted in order to determine the observed rate constant, k_{obs}, see **Figure 3. 14**. The left graph shows a rapid increase in absorbance at 325 nm that corresponds to the disappearance of Rh(I)-alkyl species that was complete within 600 minutes, and corresponds to stage 1 of the reaction as proposed in **Scheme 3. 9**. Thereafter, a decrease in absorbance at 520 nm was clearly identified between 2000-5000 minutes of reaction time; this is shown on the right of **Figure 3. 14**. This decrease corresponds to the appearance of a Rh(III)-acyl specie as suggested in **Scheme 3. 9**. Rate constants were obtained from a least square non-linear fit of these absorbance-time data.

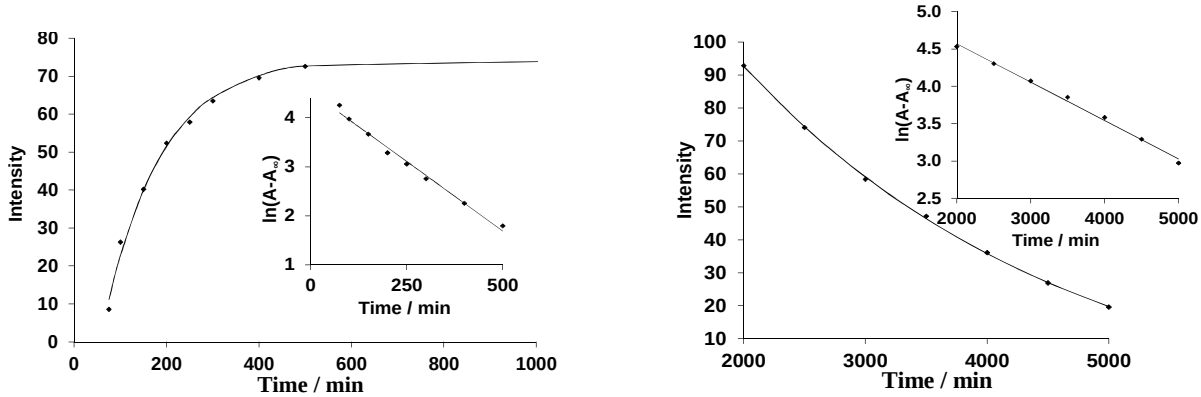

Figure 3. 14. UV-vis absorbance *vs* time data for the oxidative addition reaction of MeI and polymer complex 85 at 325 nm during stage 1 (left) and at 520 nm during stage 2 (right) in chloroform at 25 °C. The y-axis is labeled "intensity" because the observed changes in absorbance were scaled by a convenient factor to enhance observed spectral differences during the reaction. Both inserts show the linearity of a ln(A-A_∞) *vs* time plot (A = absorbance) which confirms the first-order dependence of the reaction on [Rh content in polymer 85].

The rate of reaction in stage 1 was found to be first-order dependant on the MeI concentration and stage 2 was independent of MeI (i.e. zero-order), as illustrated on right in **Figure 3. 15**. Individual k_{obs} rate constants are summarized in the Appendix after Spectrum 4.32 (see **Table A.1**).

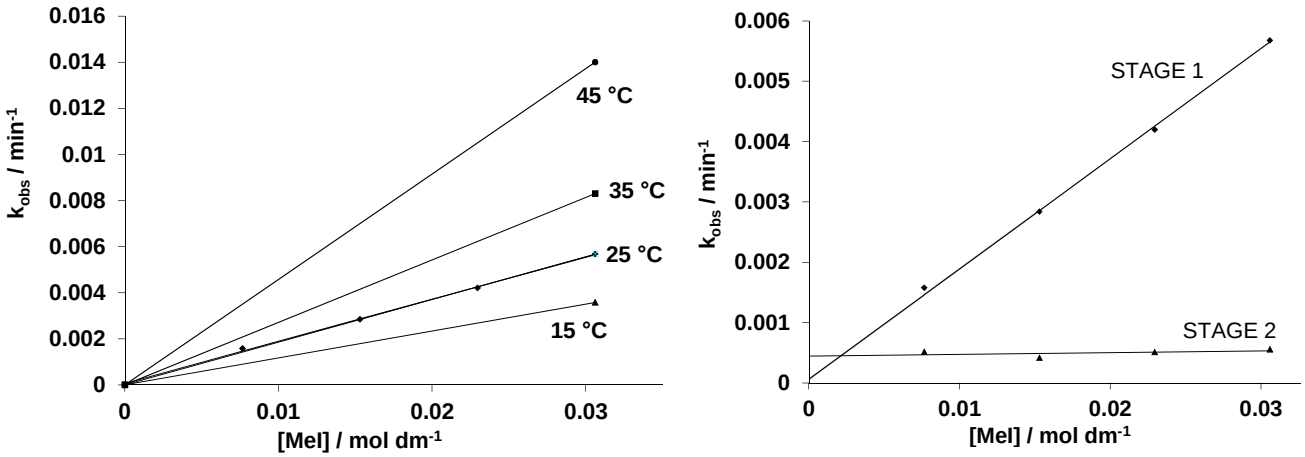

Figure 3. 15. Left: A plot of k_{obs} *vs* [MeI] at 15, 25, 35 and 45 °C during the first 1000 minutes of reaction time (i.e. stage 1). Right: Stage 1 is first-order MeI concentration dependent and stage 2 is independent of MeI concentration

These results fit a rate law equation of

$$R = k_{obs}\,[\text{Rh content in polymer } \mathbf{85}] = k_1\,[\text{MeI}][\text{Rh content in polymer } \mathbf{85}]$$
$$\text{with } k_{obs} = k_1\,[\text{MeI}]$$

for stage 1 where [MeI] and [Rh content in polymer **85**] is the concentration of the methyl iodide, and the Rh(I) content in polysiloxane complex **85**, $\{(OSiMe_2)_2OSiMe\{(CH_2)_3PPh_2(CO)(FcCOCHCOCF_3)Rh\}\}_n$, respectively. k_1 is the second-order rate constant for stage 1. The rate law for stage 2 can be written as

$$R = k_2[\text{Rh content in polymer } \mathbf{85}]$$

Here $k_2 = k_{obs}$ is the first-order rate constant for stage 2 of the reaction. That both stages were first order in the polymer is confirmed by the linear plots of $\ln(A-A_\infty)$ *vs* time in the inserts of **Figure 3. 14**. By repeating the reaction with [Rh content in polymer **85**] = 1.53 x 10^{-5} M and [MeI] = 0.0306 M (2000 fold excess) at different temperatures (15, 25, 35 and 45 °C, see **Figure 3. 15**, left), the activation parameters, entropy of activation, ΔS^*, and enthalpy of activation, ΔH^*, could be determined for both stages using the Eyring equation,

$$\ln\left(\frac{k_n}{T}\right) = \ln\left(\frac{k_B}{h}\right) - \frac{\Delta H^*}{RT} + \frac{\Delta S^*}{R} \qquad (k_n = k_1 \text{ for stage 1 or } k_2 \text{ for stage 2})$$

where k_n is the second-order reaction rate, k_B and h are the Boltzman and Planck's constants respectively with $\ln(k_B/h)$ = 23.760 and R = 8.314 $J.K^{-1}.mol^{-1}$ is the gas constant. **Table 3. 6** summarizes the second-order rate constants k_1 obtained for stage 1, the first-order rate constants k_2 for stage 2, as well as the activation parameters. Determined values for ΔS^* were large and negative for stage 1. This observation indicates that the oxidative addition in stage 1 is achieved *via* an associative mechanism. For stage 2, the activation entropy was essentially zero (6 ± 3 $J.mol^{-1}.K^{-1}$ was calculated). This small value is consistent with an isomerization process (i.e. a unimolecular reaction).

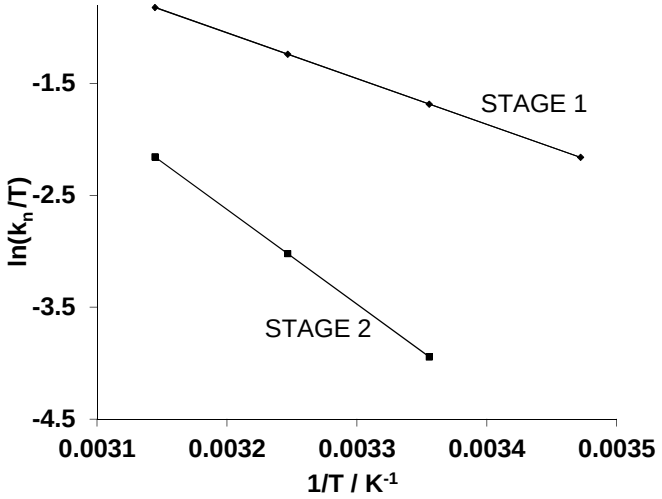

Figure 3. 16. The Eyring equation plot of $\ln(k_n/T)$ vs (1/T) for the formation of Rh(I)-alkyl specie, $\{(OSiMe_2)_2OSiMe\{(CH_2)_3PPh_2(CO)(I)(CH_3)(FcCOCHCOCF_3)Rh\}\}_n$ in stage 1. Stage 2 data does not include a rate constant at low temperature (15 °C) as the reaction becomes too slow at this temperature.

Table 3. 6. Summary of UV/vis kinetic data obtained for methyl iodide oxidative addition to $\{(OSiMe_2)_2OSiMe\{(CH_2)_3PPh_2(CO)(FcCOCHCOCF_3)Rh\}\}_n$ complex with [Rh content in polymer 85] = 1.53 x 10^{-5} M and [MeI] = 0.0306 M at different temperatures in chloroform.

	STAGE 1	STAGE 2
T (K)	**k_1[a] (M^{-1} min^{-1})**	**k_2[b] (min^{-1})**
288.15	0.1170(-)	too slow to measure
298.15	0.1863(4)	0.000443(6)[c]
308.15	0.2710(-)	0.001700(6)
318.15	0.4580(-)	0.003290(6)
	$t_{½}$ = 122 min at 25 °C [MeI] = 0.0306 M	$t_{½}$ = 1565 min [MeI] = 0.0306 M
	ΔH_1^* = 34(2) $kJ.mol^{-1}$ ΔS_1^* = -97(6) $J.mol^{-1}.K^{-1}$	ΔH_2^* = 70(9) $kJ.mol^{-1}$ ΔS_2^* = 6(3) $J.mol^{-1}.K^{-1}$

[a] k_1 is the second-order rate constant for stage 2.
[b] $k_2 = k_{obs}$ is the first-order rate constant.
[c] Rate constant obtained from the y-intercept in **Figure 3.15** (right).

To confirm that stages 1 and 2 in the present oxidative addition reaction represent the reactions shown in **Scheme 3. 9**, the reaction was studied in chloroform at 25 °C utilizing FTIR techniques. The reaction was performed using pseudo first-order kinetic conditions, with [MeI] = 0.0367 M, a 2000 fold excess over the Rh(I) concentration (*ca*. 1.835 x 10^{-5} M). Stage 1 took place during the first 400 minutes. There appears to be two rhodium(I) species, $Rh^{I}(1)$ and $Rh^{I}(2)$ as identified by the FTIR spectrum shown in

, top. The one specie exhibits a CO vibration at 2020 cm^{-1} and the other at 2089 cm^{-1}. The existence of two rhodium(I) species in polymer **85** is surprising but can be explained. Normally Rh^{I}(β-diketonato)(CO)(PPh_3) complexes have a square planar geometry with υ_{CO} in the region 1980-2008 cm^{-1} as shown by Conradie[123] and co-workers when they studied the free (i.e. not polymer-bound) complexes of this study. However Rh(I) can also exist with a planar pyramidal geometry having five coordination bonds[128]. The IR vibration at 2020 cm^{-1} is assigned to the square planar rhodium system on polymer **85** while the IR vibration at 2089 cm^{-1} is at this stage tentatively assigned to a square pyramidal Rh(I) species on **85**. The geometry of this postulated square pyramidal specie and even its exact composition is at this stage not clear, but it *may* look as shown in **Figure 3. 17**. For the kinetics of rhodium(I) disappearance the rate of disappearance of the vibration at υ_{CO} = 2020 cm^{-1} is mutually consistent with the rate of Rh(I) disappearance of the vibration at υ_{CO} = 2089 cm^{-1}.

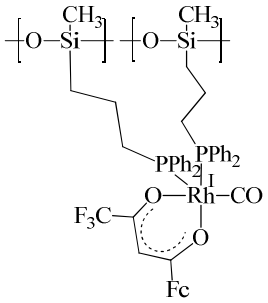

Figure 3. 17. Possible rhodium(I) square bypyramidal diphosphine complex.

During stage 1 then, all Rh(I) carbonyl vibrations disappear with simultaneous appearance of a Rh(III)-alkyl1 specie at *ca.* 2132 cm^{-1} and a Rh(III)-acyl1 specie at 1738 cm^{-1} at the *same* reaction rate, see **Figure 3. 18.**

128 S.S. Basson, J.G. Leipoldt, A. Roodt and J.A. Venter, *Inorg. Chim. Acta*., 1987, **128**, 31.

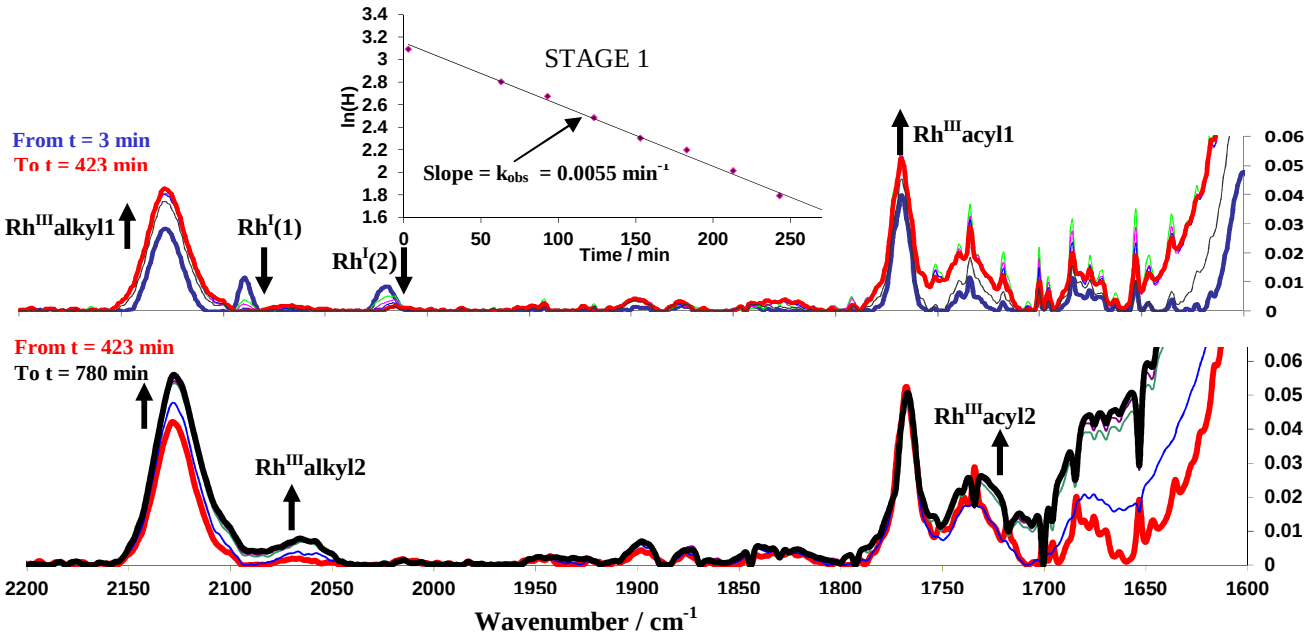

Figure 3. 18. Oxidative addition of MeI to rhodium-containing polysiloxane 85 monitored by infrared in chloroform at 25 °C recorded before 423 minutes expired (top) and between 423-780 minutes (bottom). The insert shows a plot of the decrease in vibration height (at 2089 cm^{-1}) *vs* time which was used to determine k_{obs}.

The surprising results implies that the first formed Rh(III)-alkyl species is in a fast equilibrium with the first formed Rh(III)-acyl species, labelled as Rh(III)-acyl1, and that the postulated reaction sequence shown in **Scheme 3. 9** is wrong. The rate constant of this FTIR-followed reaction is 0.0055 min^{-1}, see the insert of **Figure 3. 18**. To obtain the rate constant, the vibration height (H) of the disappearing vibration of the starting Rh(I) compound was measured in mm by a ruler and a plot of ln(H) versus time was drawn. The slope of this graph gave k_{obs} = 0.0055 min^{-1}. This value replicates the UV/vis determined k_{obs} = 0.0057 min^{-1} very well. By dividing this IR obtained k_{obs} value with the [MeI] used, 0.0367 M, the second order rate constant determined by FTIR is 0.1499 M^{-1}min^{-1}. The UV/vis determined second order rate constant is 0.1863 M^{-1}min^{-1}.

After stage 1, the reaction continued further, with a growth of a new Rh(III)-alkyl2 vibration at 2070 cm^{-1} and a new Rh(III)-acyl2 at 1740 cm^{-1}, but it was only monitored till 800 minutes of reaction time. This represents the initial stages of stage 2 that was detected by UV/vis. These described results that were obtained from the FTIR kinetic study is consistent with an update of the proposed oxidative addition reaction sequence given in **Scheme 3. 10**. This updated sequence replaces **Scheme 3. 9** as a more correct reaction sequence.

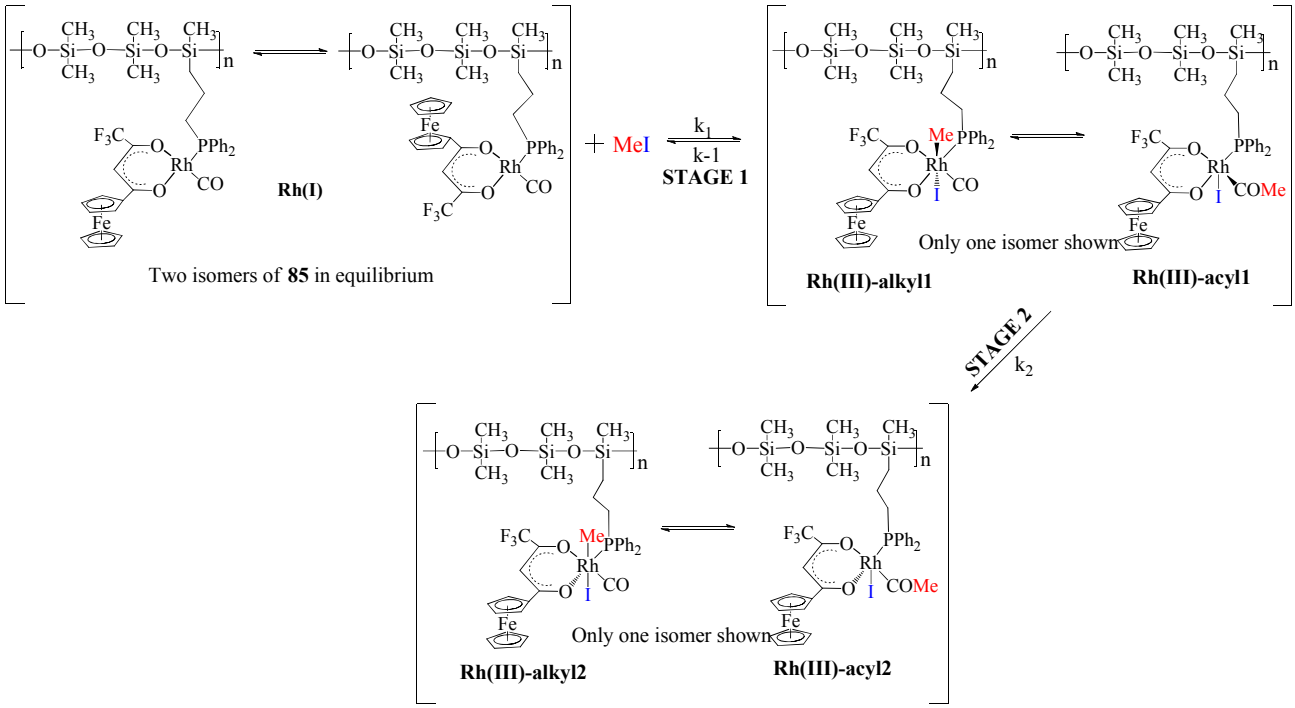

Scheme 3. 10. A more correct reaction sequence of the oxidative addition of MeI to polymer 85. The equilibrium position of stage 2 products is with the present FTIR data not clearly identified.

The indicated geometries of Rh(III)-alkyl1, Rh(III)-alky2, Rh(III)-acyl1 and Rh(III)-acyl2 in **Scheme 3. 10** is not necessarily to be correct. What should be taken from **Scheme 3. 10** is that the geometry of Rh(III)-alkyl1 and Rh(III)-acyl1 are not the same as the geometry of Rh(III)-alkyl2 and Rh(III)-acyl2. The first two compounds Rh(III)-alkyl1 and Rh(III)-acyl1 represent the kinetically favoured products, while the products of stage 2, Rh(III)-alkyl2 and Rh(III)-acyl2 represent the thermodynamically favoured products.

Before the IR kinetic experiment was performed, it was noticed that some Rh(III)alkyl1 and Rh(III)acyl1 species had already formed before any MeI was added by the virtue of the vibrations at 2132 and 1738 cm^{-1} respectively. This suggested that an oxidative addition reaction took place to a limited degree before MeI was added. For oxidative addition to take place, an alkyl group and a halide are required to bind to the rhodium center. The only possible source of such an alkyl halide is the polymeric backbone of polymer **85** itself. A careful analysis of the ^{1}H NMR spectrum of the chlorinated polymer **79** (see **Figure 3. 2**) shows that the chloro groups of polymer **76** were only replaced about 96 % by the iodo groups, **Figure 3. 2**. In addition, an XPS analysis of polymer **85** containing Rh(I) groups showed ca. 7 % iodide content (see **Figure 3. 7**). This means phosphination of **79** to give **82** (see **Scheme 3. 7**) in paragraph 3.2.6 was not quantitative. It follows that the allyl halide side chains could easily oxidatively add to the Rh(I) centre of **85** prior to MeI addition. The way this may have happened is schematically shown in **Scheme 3. 11**.

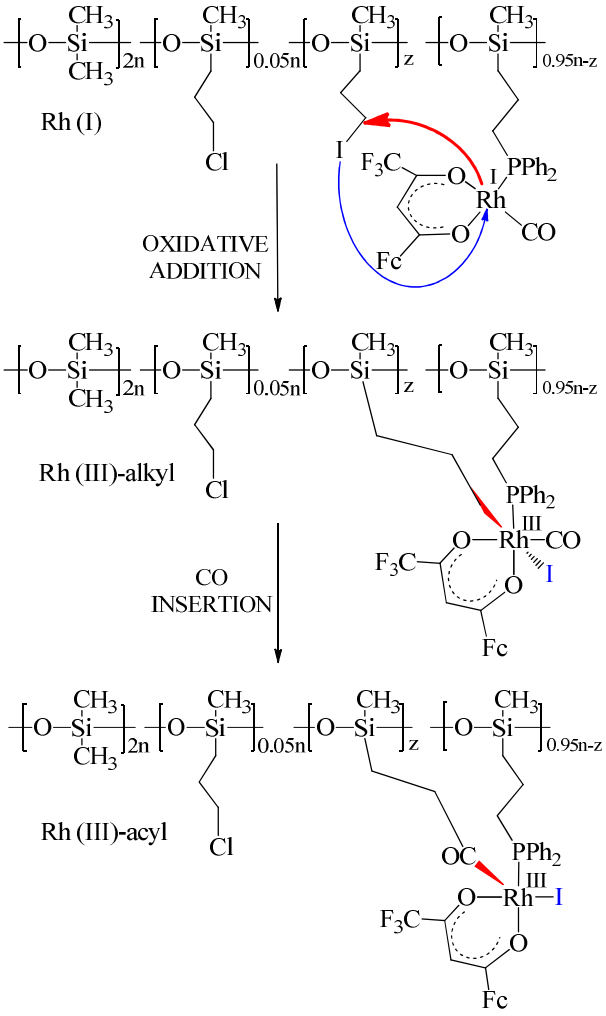

Scheme 3. 11. Unexpected intramolecular oxidative addition of the iodo alkyl chain to the rhodium centre, z represents a fraction of the unreacted iodated polysiloxane monomer and Fc = ferrocene.

This concludes the discussion of the research performed by the author. All goals as defined in Chapter 1 have been met. Chapter 4 gives all the experimental details that were adhered to in obtaining all the research described in this chapter while Chapter 5 summarizes compactly all the results of this study.

4 Experimental

4.1 Introduction

In this chapter, apparatus, experimental procedures and reaction conditions are presented for the synthesis. Spectroscopic characterisation techniques and other studies such as electrochemistry and kinetics of compounds are also included.

4.2 Materials

Solid and liquid reagents from Sigma-Aldrich and Merck Chemicals were used without further purification. Solvents were dried before use according to published methods and double-distilled water was used for all procedures. Melting points of products were determined with an Olympus BX51 polarized microscope, fitted with a LINKAM THRM 600 heating stage (temperatures are uncorrected). Filtration and vacuum evaporation was assisted with a vacuum pump.

4.3 Spectroscopic measurements

Nuclear magnetic resonance (^{1}H and ^{31}P) measurements were recorded on a Bruker Avance DPX 300 NMR spectrometer at 298 K (selected spectrums can be found in the appendix). The ^{1}H chemical shifts were reported relative to $SiMe_4$ at 0.00 ppm and the ^{31}P relative to 85 % H_3PO_4 (0 ppm) as external standards. Fourier transformed attenuated total reflection infrared spectra were recorded on a Bruker Tensor 27 infrared spectrophotometer fitted with a Pike MIRacle single bounce diamond ATR crystal. FTIR adsorption was measured in the solid phase. UV/vis spectra were recorded for dilute solutions in dichloromethane in quartz cuvettes on a Varian Cary 50 UV/vis spectrophotometer. The elemental analysis was performed at the University of the Free State on a Leco Truspec Micro elemental analyzer by the Analytical section of the Chemistry Department and the Canadian Microanalytical Service Ltd.

4.4 XPS measurements

XPS data were recorded on a PHI 5000 Versaprobe system with monochromatic AlK X-ray source. Spectra were obtained using the aluminium anode (Al Kα = 1486.6 eV) operating at 50 μm, 12.5 W and 15 kV energy (97 X-ray beam). The survey scans were recorded at constant pass energy of 187.85 eV and region scans at constant pass energy of 29.35 eV with the analyzer resolution ≤ 0.5 eV. The background pressure was 2 x 10^{-8} mbar. The XPS data were analyzed utilizing Multipak version 8.2c computer software[129] using Gaussian–Lorentz fits (the Gaussian/Lorentz ratios were always > 95%).

4.5 Viscosity measurements

Intrinsic viscosity measurements on polymeric compounds were performed using a suspended level Ubbelholde KPG® Viscometer Ostwald from Schott Geräte Company in dichloromethane at 30 ˚C. Viscosity values were calculated by using the intrinsic viscosity formula,

$$\eta_{inh} = \frac{t - t_0}{t_0}$$

where t_0 is the time taken for the pure solvent to pass through the viscometer and t is the time for the polymer solution. At polymer concentration *ca*. 1.76 mM, the inherent viscosity was measured between 0.011-0.028 g/dL.

4.6 Electrochemical studies

Measurements on *ca*. 0.25 mmol dm^{-3} solutions of the complexes in dichloromethane containing 0.1 mol dm^{-3} $[N^nBu_4][B(C_6F_5)_4]$ as supporting electrolyte were conducted in a glove box at room temperature utilising a PARSTAT 2273 Advanced electrochemical workstation interfaced with a personal computer. A three electrode cell consisting of a Pt auxillary and reference electrode (Pt) and a glassy carbon working electrode with surface area 7.07 mm^2 polished on a Bueler microcloth with 1 micron and ¼ micron diamond paste were employed. Data was worked up on a spreadsheet to be referenced against the Fc/Fc^+ couple at 0 V.

[129] J.F. Moulder, W.F. Stickle, P.E. Sobol and K.D. Bomben, *Handbook of X-ray Photoelectron Spectroscopy*, Japan, 1995, p. 45, 57, 143.

4.7 Kinetic studies

The kinetics for the oxidative addition reaction of methyl iodide was monitored on the FTIR machine at 25 °C in a NaCl liquid cell connected to a water bath by monitoring the disappearance and formation of the carbonyl peak. The reaction was also monitored on the UV-vis spectrophotometer (by monitoring the change in absorbance) at least four different temperatures within the range 15-45 ˚C from which the activation parameters ΔH^* and ΔS^* were obtained. Chloroform was used as solvent and passed through basic alumina just before use to make it acid free. All kinetic measurements were monitored under pseudo first-order conditions with a 500-2000 times molar excess of CH_3I over the concentration of the rhodium polysiloxane content. Pseudo first-order rate constants, k_{obs}, were calculated using MicroMath Scientist 2.0 program.

4.8 Synthesis

4.8.1 1-Ferrocenyl-3-methylbutane-1,3-dione, 4

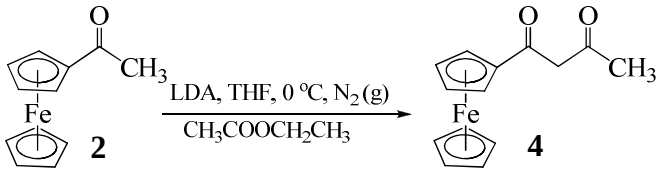

The reaction-vessel was degassed with nitrogen and this inert atmosphere was maintained throughout the duration of the experiment. Acetylferrocene (17.5 mmol, 4 g) was released from a schlenk tube into a three-necked flask and dissolved in dry, deoxygenated THF (35 ml). At 0 °C lithium diisopropylamine (LDA) (21 mmol, 18 ml) was added dry[130] ethyl acetate (17.5 mmol, 1.72 ml) under N_2. The reaction mixture was stirred overnight, and was allowed to slowly warm to ambient temperature. At this point diethyl ether (100 ml) was added to the deep red solution under open atmosphere conditions followed by addition of ice cold 1 M HCl (20 ml) and the mixture was stirred for 30 minutes. The layers were separated and the aqueous layer was extracted with diethyl ether (3 x 100 ml). The organic layer was dried over anhydrous $MgSO_4$ and evaporated under reduced pressure. Pure product was obtained by column chromatography with 1:1 ether and hexane as the eluent. Yield: 16 % (0.78 g), Melting point: 95.6 ˚C, ^{1}H NMR: δ_H (300 MHz, $CDCl_3$)/ppm: 2.11 (enol, 3H, s, CH_3), 3.85 (keto, 2H, s, CH_2), 4.20 (enol, 5H, s, C_5H_5), 4.28 (keto, 5H, s, C_5H_5), 4.51 (enol, 2H, t, C_5H_4), 4.62 (keto, 2H, t, C_5H_4), 4.81 (enol, 2H, t, C_5H_4), 4.86 (keto, 2H, t, C_5H_4) and 5.74 (1H, s, CH), **Spectrum 4.1**.

---

130 L.F. Armarego and C. Li Lin Chai, *Purification of Organic Chemicals*, 6th edition, Butterworth-Heinemann, 2009, p.138.

4.8.2 1-Ferrocenyl-4,4,4-trifluorobutane-1,3-dione, 5

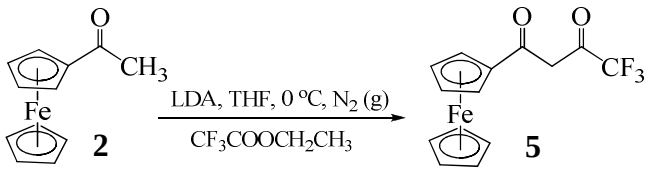

The reaction-vessel was degassed with nitrogen and this inert atmosphere was maintained throughout the duration of the experiment. Acetylferrocene (17.5 mmol, 4 g) was released from a schlenk tube into a three-necked flask and dissolved in dry, deoxygenated THF (35 ml). At 0 °C, lithium diisopropylamine (21 mmol, 2.77 ml) was added and stirred for 30 minutes. To the cold reaction mixture was added dry ethyl trifluoroacetate (17.5 mmol, 2.09 ml) under N_2. The reaction mixture was stirred overnight, and was allowed to slowly warm to ambient temperature. Diethyl ether (100 ml) was then added to the deep red solution under open atmosphere conditions followed by addition of ice cold 1 M HCl (20 ml) and the mixture was stirred for 30 minutes. The layers were separated and the aqueous layer was extracted with diethyl ether (3 x 100 ml). The organic layer was dried over anhydrous $MgSO_4$ and evaporated under reduced pressure. Pure product was obtained by column chromatography with 1:1 ether and hexane as the eluent. Yield: 53 % (3.6 g), Melting point: 99.6 ˚C, ^{1}H NMR: δ_H (300 MHz, $CDCl_3$)/ppm: 4.26 (5H, s, C_5H_5), 4.72 (2H, t, C_5H_4), 4.89 (2H, t, C_5H_4) and 6.10 (1H, s, CH), **Spectrum 4.2**.

4.8.3 Di-μ-chloro-bis[(1,2,5,6-η)1,5-cyclooctadiene]rhodium, 18

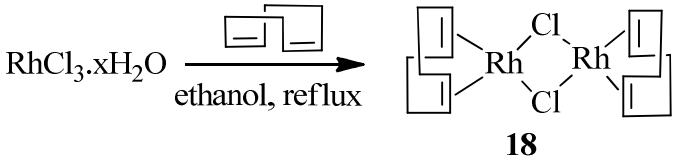

18

In a fumehood, rhodium trichloride (1.5 g, 7.2 mmol) was dissolved in a few drops of water followed by addition of ethanol (33 ml) and dropwise addition of cyclooctadiene (81 mmol, 9.75 ml). The reaction mixture was refluxed while stirring for 2 hours and cooled in an ice bath to form a yellow precipitate. The precipitate was filtered and washed with methanol to yield the pure product. Yield: 26 % (0.94 g), Melting points: 225 ˚C, ^{1}H NMR: δ_H (300 MHz, $CDCl_3$)/ppm: 1.79 (4H, m, ½ x 4CH_2), 2.52 (4H, m, ½ x 4CH_2), 4.26 (4H, m, 4CH), **Spectrum 4.3**.

4.8.4 [Rh(FcCOCHCOCH$_3$)(cod)], 19

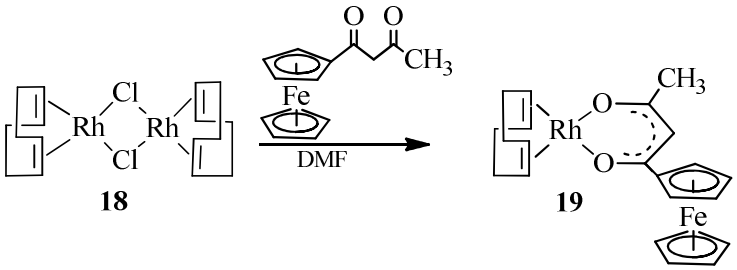

18 19

In a 1-necked round bottomed flask, [$RhCl_2(cod)_2$] (1.22 mmol, 0.6 g) was dissolved in DMF (2 ml). $NaHCO_3$ (1.55 mmol, 0.13 g) was added followed by addition of solid 1-ferrocenyl-3-methylbutane-1,3-dione (2.41 mmol, 0.65 g). The reaction mixture was stirred at room temperature for 16 hours. The product was precipitated with the addition of an excess amount of ice cold water (50ml). The precipitate was filtered off, dissolved in ether and the organic layer washed with water. The ether layer was dried over $MgSO_4$ and evaporated under reduced pressure to give spectroscopically pure product. Yield: 100 % (0.27 g), Melting point: 165.5 ˚C, ^{1}H NMR: δ_H (300 MHz, $CDCl_3$)/ppm: 1.85 (4H, m, ½ x 4CH_2), 2.09 (3H, s, CH_3), 2.55 (4H, m, ½ x 4CH_2), 4.18 (9H, m, 4H of 4CH and 5H of C_5H_5), 4.35 (2H, t, C_5H_4), 4.65 (2H, t, C_5H_4) and 5.65 (1H, s, CH), **Spectrum 4.4**.

4.8.5 [Rh(FcCOCHCOCF$_3$)(cod)], 20

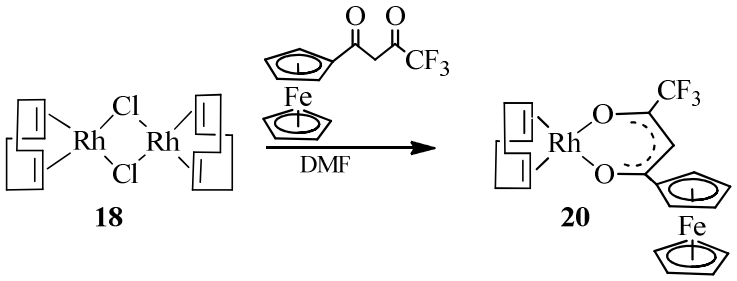

18 20

In a 1-necked round bottomed flask, [$RhCl_2(cod)_2$] (0.51 mmol, 0.25 g) was dissolved in DMF (2 ml). $NaHCO_3$ (1 mmol, 0.085 g) was added followed by addition of solid 1-ferrocenyl-4,4,4-trifluorobutane-1,3-dione (1.01 mmol, 0.39 g). The reaction mixture was stirred at room temperature for 16 hours and the product was precipitated with the addition of an excess amount of ice cold water (50 ml) and filtered off. Extraction was done by dissolving precipitate in ether and washing with water. The ether layer was dried over $MgSO_4$ and evaporated under reduced pressure to give spectroscopically pure product. Yield: 96 % (0.26 g), Melting point: 188.5 ˚C, ^{1}H NMR: δ_H (300 MHz, $CDCl_3$)/ppm: 1.84 (4H, m, ½ x 4CH_2 protons), 2.51 (4H, m, ½ x 4CH_2 protons), 4.18

(9H, m, 4H of 4CH and 5H of C_5H_5), 4.50 (2H, t, C_5H_4), 4.70 (2H, t, C_5H_4) and 5.93 (1H, s, CH), **Spectrum 4.5**.

4.8.6 [Rh(FcCOCHCOCH$_3$)(CO)$_2$], 23

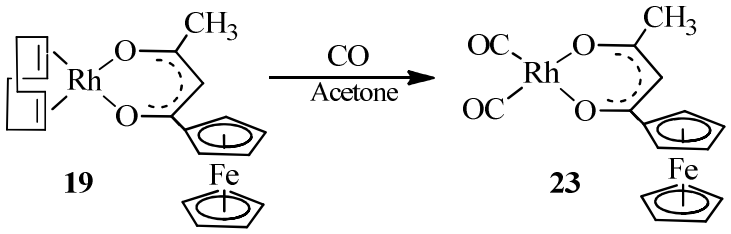

19 **23**

CAUTION: CO is poisonous. [Rh(FcCOCHCOCH$_3$)(cod)] (0.26 g) was dissolved in acetone (80 ml). Working in a fumehood carbon monoxide gas was bubbled through the solution by passing the gas through a sintered glass tube for 15 minutes. Cold water was added to precipitate the product, stirring continued for a further 15 minutes. The precipitate was filtered off, washed with water and dried, giving spectroscopically pure product. Yield: 42 % (0.11 g), Melting point: 161 ˚C, ν(C≡O) = 2008; 2067 cm^{-1}, ^{1}H NMR: δ_H (300 MHz, $CDCl_3$)/ppm: 2.15 (3H, s, CH_3), 4.17 (5H, s, C_5H_5), 4.46 (2H, t, C_5H_4), 4.78 (2H, t, C_5H_4) and 5.88 (1H, s, CH), **Spectrum 4.6**.

4.8.7 [Rh(FcCOCHCOCF$_3$)(CO)$_2$], 24

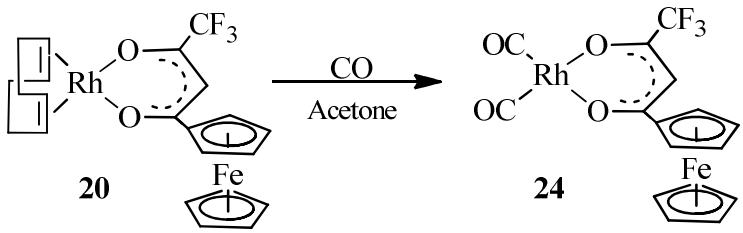

20 **24**

CAUTION: CO is poisonous. [Rh(FcCOCHCOCF$_3$)(cod)] (1.88 mmol, 1 g) was dissolved in acetone. Working in a fumehood carbon monoxide gas was bubbled through the solution by passing the gas through a sintered glass tube for 15 minutes. Cold water was added to precipitate product, stirring continued for a further 15 minutes. The precipitate was filtered off, washed with water and dried, giving spectroscopically pure product. Yield: 48 % (0.48 g), Melting point: 220.5 ˚C, ν(C≡O) = 2016; 2070, cm^{-1}, ^{1}H NMR: δ_H (300 MHz, $CDCl_3$)/ppm: 4.22 (5H, s, C_5H_5), 4.65 (2H, t, C_5H_4), 4.87 (2H, t, C_5H_4) and 6.20 (1H, s, CH), **Spectrum 4.7**.

4.8.8 Disodium tetramethyldisiloxane–1,3–diolate, 36

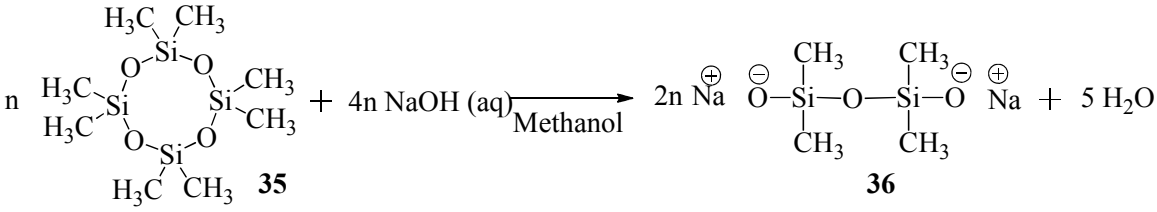

A 50 % NaOH aqueous solution (0.75 mol, 30 g dissolved in 30 ml of H_2O) was added to octamethylcyclotetrasiloxane, **35**, (51 g, 18.73 mmol). Approximately 100 ml of methanol was added and the mixture was stirred and refluxed for 2.5 h. During this time more methanol was added in small amount until a homogeneous solution was obtained. The mixture was cooled and the solvent was removed under reduced pressure. The solid compound was dried at 110 ˚C over phosphorus pentoxide for 72 h below 5 mm Hg in an Abderhalden's drying pistol to remove water from the white crystals. Yield: 79.5% (62.6 g).

4.8.9 3–(Chloropropyl)methyldichlorosilane, 73

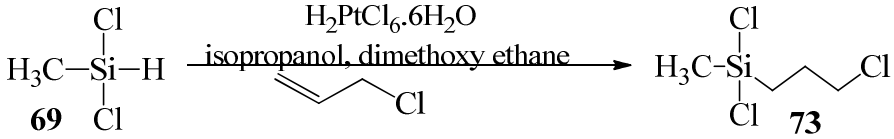

CAUTION: This reaction is very sensitive to moisture. Therefore the catalyst must be solid and in powder form. If it has a liquid appearance, the reaction will fail. Under inert and moisture free atmosphere, dichloromethylsilane (12.45 ml, 119.6 mmol) was added with a small amount of allyl chloride (0.7 ml, 10.37 mmol) in a 3-necked flask. A 1 ml solution of $H_2PtCl_6.6H_2O$ (60 mg), in 20 drops of isopropanol and 1,2–dimethoxy ethane (4 ml)) was added to the reaction mixture while stirring. The rest of the allyl chloride (5.4 ml, 80 mmol) was added dropwise over a period of 30 minutes. After completion of ally chlroride addition, the mixture was refluxed for 4 h at a bath temperature of 110 ˚C. The pure liquid product was distilled at reduced pressure (39 mmHg) at 92.5-94 ˚C. Yield: 31.4 % (6.01 g). ^{1}H NMR: δ_H (300 MHz, $CDCl_3$)/ppm: 0.83 (3H, s, CH_3), 1.28 (2H, t, CH_2), 2.00 (2H, m, CH_2), 3.60 (2H, t, CH_2), **Spectrum 4.8**.

4.8.10 4–(Bromobutyl)methyldichlorosilane, 74

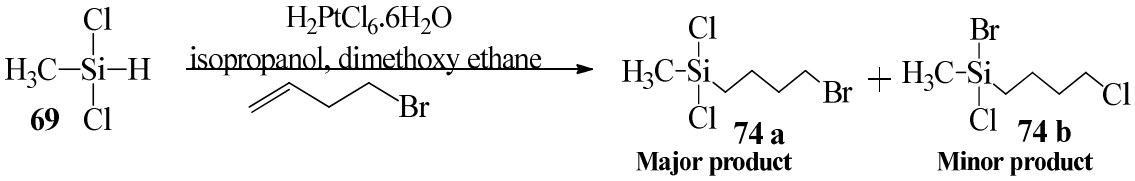

CAUTION: This reaction is very sensitive to moisture. Therefore the catalyst must be solid and in powder form. If it has a liquid appearance, the reaction will fail. Under inert and moisture free atmosphere, dichloromethylsilane (12.45 ml, 119.6 mmol) was added in excess with a small amount of 4-bromobutene (0.7 ml, 6.9 mmol) in a 3-necked flask. A 1 ml solution of $H_2PtCl_6.6H_2O$ (60 mg), in 20 drops of isopropanol and 1,2–dimethoxy ethane (4 ml) was added to the reaction mixture while stirring. The rest of the 4-bromobutene (9.45 ml, 100 mmol) was added dropwise over a period of 30 minutes. During the addition of the alkene a slow temperature rise to 40 ˚C was observed. After completion of 4-bromobutene addition, the mixture was refluxed for 2.5 h at a bath temperature of 110 ˚C. The pure liquid product was distilled at reduced pressure (10 mmHg) at 96-98 ˚C. Yield: 63.2% (15.2 g). 1H NMR: δ_H (300 MHz, $CDCl_3$)/ppm: 0.81 (3H, s, CH_3), 1.15 (2H, t, CH_2), 1.70 (2H, m, CH_2), 1.85 (2H, m, CH_2, 74b), 1.95 (2H, m, CH_2, 74a), 3.44 (2H, t, CH_2, 74a), 3.57 (2H, t, CH_2, 74b). The peaks at 1.85 and 3.57 ppm are due to the Cl/Br exchanged isomer 74b, **Spectrum 4.9**.

4.8.11 5–(Bromopentyl)methyldichlorosilane, 75

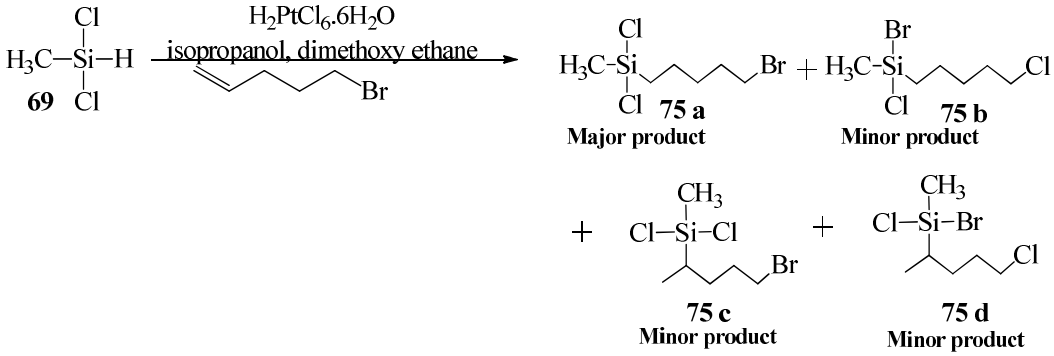

CAUTION: This reaction is very sensitive to moisture. Therefore the catalyst must be solid and in powder form. If it has a liquid appearance, the reaction will fail. Under inert and moisture free atmosphere, dichloromethylsilane (6.4 ml, 61.5 mmol) was added in excess with a small amount of 5-bromopentene (0.7 ml, 5.91 mmol) in a 3-necked flask. A 1 ml solution of solid $H_2PtCl_6.6H_2O$ (60 mg), in 20 drops of isopropanol and 1,2–dimethoxy ethane (4 ml) was added to the reaction

mixture while stirring. The rest of the 5-bromopentene (6.8 ml, 57.4 mmol) was added dropwise over a period of 30 minutes. During the addition of the alkene a slow temperature rise to 55 ˚C was observed. After completion of 5- bromobutene addition, the mixture was refluxed for 2.5 h at a bath temperature of 110 ˚C. The pure liquid product was distilled at reduced pressure (6 mmHg) at 99-101 ˚C. Yield: 59.5% (9.78 g), ^{1}H NMR: δ_H (300 MHz, $CDCl_3$)/ppm: 0.79 (3H, s, CH_3), 1.15 (2H, t, CH_2), 1.55 (4H, m, CH_2), 1.81 (2H, m, CH2, 75b), 1.88 (2H, m, CH_2, 75a), 3.42 (2H, t, CH_2, 75a), 3.55 (2H, t, CH_2, 75b), **Spectrum 4.10**.

4.8.12 Poly(3–chloropropylpentamethyltrisiloxane), 76

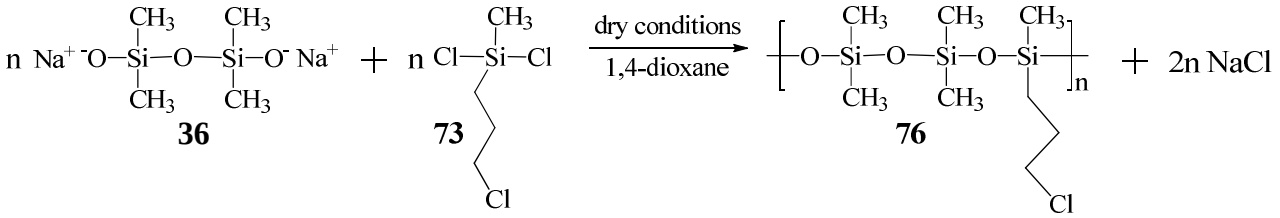

36 **73** **76**

The reaction is sensitive to moisture, therefore the salt, **36**, has to be completely dry as described in paragraph 4.8.8. Disodium tetramethyldisiloxane-1,3-diolate (6.99 mmol, 1.47 g) was dissolved in dry 1,4-dioxane (70 ml) and stirred overnight to form a homogeneous mixture. A solution of 3-(chloropropyl)methyldichlorosilane (9.66 mmol) in dry 1,4-dioxane (4 ml) was added dropwise to the homogeneous mixture. NaCl precipitated while stirring for 2 hours. The NaCl was centrifuged off and a pale yellow oil was obtained after solvent removal under reduced pressure. Yield: 53.6 % (1.07 g), ν(C-Cl) = 796 cm^{-1}, η_{inh} = 0.021 dL/g, ^{1}H NMR: δ_H (300 MHz, $CDCl_3$)/ppm: 0.10 (15H, s, CH_3), 0.66 (2H, t, CH_2), 1.85 (2H, m, CH_2), 3.54 (2H, t, CH_2). Theoretical composition: C, 33.72; H, 7.43. Anal. Found: C, 33.16; H, 7.28, **Spectrum 4.11**.

4.8.13 Poly(4-bromobutylpentamethyltrisiloxane), 77

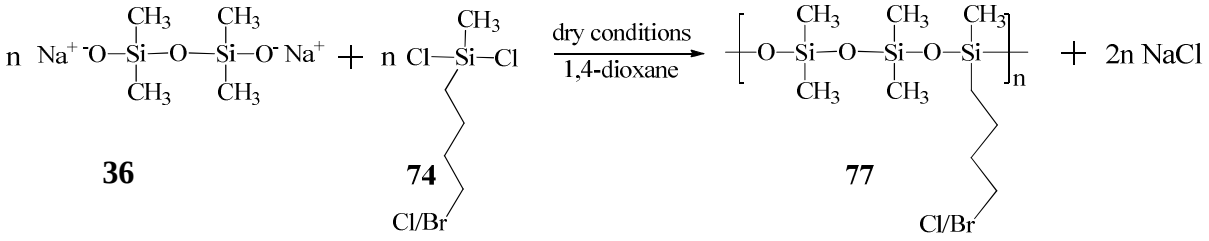

36 **74** **77**

The reaction is sensitive to moisture, therefore the salt, **36**, has to be completely dry as described in paragraph 4.8.8. Disodium tetramethyldisiloxane-1,3-diolate (9.51 mmol, 2 g) was dissolved in dry 1,4-dioxane (70 ml) and stirred overnight to form a homogeneous mixture. A solution of 4-bromopropylmethyldichlorosilane (9.51 mmol) in dry 1,4-dioxane (4 ml) was added dropwise to the

homogeneous mixture. NaCl precipitated while stirring vigorously. During the addition, the temperature of the flask increased to about 55 ˚C. Stirring continued for 2 hours before the NaCl was centrifuged off and a pale yellow oil was obtained after solvent removal under reduced pressure. Yield: 79.5 % (2.54 g), ν(C-Br) = 796 cm^{-1}, η_{inh} = 0.014 dL/g, ^1H NMR: δ_H (300 MHz, $CDCl_3$)/ppm: 0.12 (3H, s, CH_3), 0.56 (2H, t, CH_2), 1.54 (2H, m, CH_2), 1.89 (2H, m, CH_2), 3.40 (2H, t, CH_2). The peaks at 3.56 and the small shoulder at 1.80 ppm is due to the small amount of Cl-Br exchange in silane **74** (see paragraph **4.8.10**). Theoretical composition: C, 31.48; H, 6.75. Anal. Found: C, 32.14; H, 6.38, **Spectrum 4.12**.

4.8.14 Poly(5-bromopentylpentamethyltrisiloxane), 78

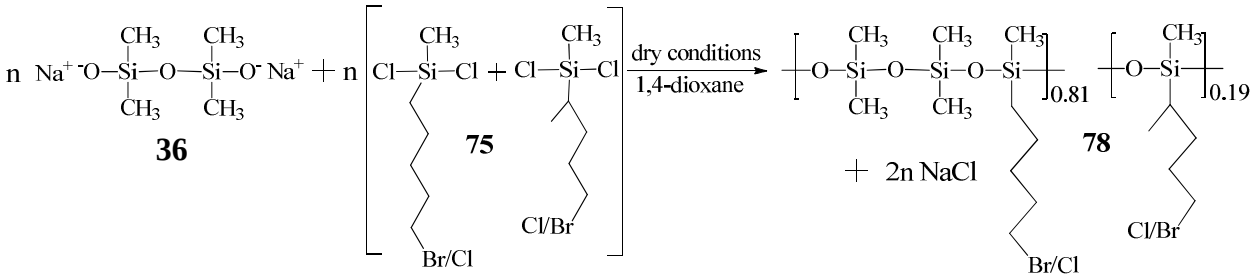

36 **75** **78**

The reaction is sensitive to moisture, therefore the salt, **36**, has to be completely dry as described in paragraph 4.8.8. Disodium tetramethyldisiloxane-1,3-diolate (11.89 mmol, 2.5 g) was dissolved in dry 1,4-dioxane (70 ml) and stirred overnight to form a homogeneous mixture. A solution of 5-bromopropylmethyldichlorosilane (11.89 mmol) in dry 1,4-dioxane (4 ml) was added dropwise to the homogeneous mixture. NaCl precipitated while stirring vigorously. During the addition, the temperature of the flask increased to about 60 ˚C. Stirring continued for 2 hours before the NaCl was centrifuged off to obtain a pale yellow/brown oil after solvent removal under reduced pressure. Yield: 89.5 % (3.85 g), ν(C-Br) = 796 cm^{-1}, η_{inh} = 0.013 dL/g, ^1H NMR: δ_H (300 MHz, $CDCl_3$)/ppm: 0.09 (15H, s, CH_3), 0.54 (2H, , t, CH_2), 1.44 (4H, m, CH_2), 1.77(2H, , t, CH_2, β-isomer), 1.88 (2H, m, CH_2), 3.42 (2H, t, CH_2), 3.55 (2H, t, CH_2, β-isomer). Theoretical composition: C, 33.60; H, 7.05. Anal. Found: C, 34.16; H, 7.48, **Spectrum 4.13**.

4.8.15 Iodization of chloro and bromo polysiloxane 76, 77 and 78 to give iodo polysiloxane 79, 80 and 81.

The general procedure was as follows: The chlorinated/brominated polysiloxane (8 mmol) was dissolved in dry acetone (300 ml) and transferred to a two-necked 500 ml round bottomed flask. A 60 times moler excess (480 mmol) of solid NaI was added and the mixture was refluxed for 5 days. Dichloromethane (300 ml) was added to ensure precipitation of any dissolved NaI. The filtered

organic layer was washed with water until it was clear, dried over MgSO4 and the solvent was removed under vacuum to yield the iodated polysiloxane as oil. The ^{1}H NMR characterization and elemental analysis[131] data follows.

4.8.15.1 Poly[(3-iodopropyl)pentamethyltrisiloxane], 79

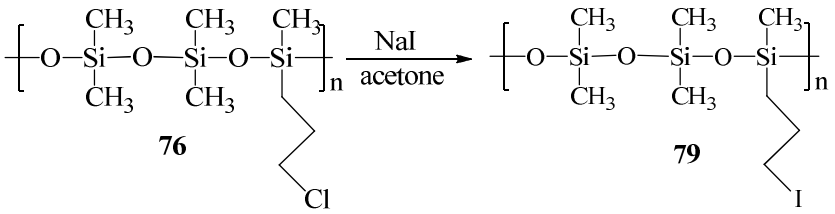

Yield: 84 % (2.53 g), ν(C-I) = 796 cm^{-1}, η_{inh} = 0.05 dL/g, ^{1}H NMR: δ_H (300 MHz, $CDCl_3$)/ppm: 0.11 (15H, s, CH_3), 0.66 (2H, t, CH_2), 1.89 (4H, m, CH_2), 3.22 (2H, t, CH_2). Theoretical composition: C, 25.53; H, 5.62. Anal. Found: C, 25.63; H, 6.05, **Spectrum 4.14**.

4.8.15.2 Poly[(4-iodobutyl)pentamethyltrisiloxane)], 80

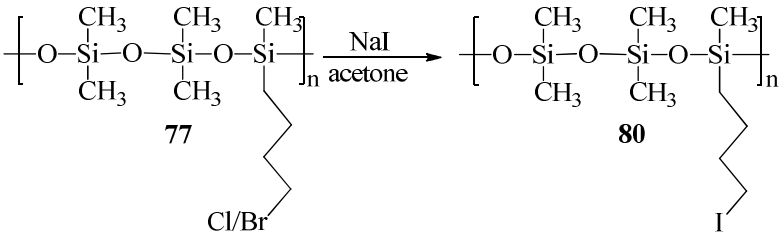

Yield: 54 % (1.71 g), ν(C-I) = 797 cm^{-1}, η_{inh} = 0.019 dL/g, ^{1}H NMR: δ_H (300 MHz, $CDCl_3$)/ppm: 0.13 (15H, s, CH_3), 0.55 (2H, t, CH_2), 1.49 (2H, m, CH_2), 1.87 (2H, m, CH_2), 3.21 (3H, t, CH_2). Theoretical composition: C, 27.69; H, 5.94. Anal. Found: C, 28.21; H, 5.96, **Spectrum 4.15**.

[131] Elementals were first performed in house on a Leco Truspec Micro elemental analyzer, this gave results that were showing big discrepancies from what was expected and contradicted all other characterization techniques. A repeat analysis of one sample was performed at Canadian Microanalytical Service Ltd and was consistent with what was expected. The discrepancies is attributed to a "too low" combustion temperature in the Leco Truspec instrument as it is known that Si derivatives require combustion temperature in excess of 1200 °C for accurate results (personal communication with Prof H. Lang, Chemnitz University of Technology, Germany).

4.8.15.3 Poly[(5-iodopentyl)pentamethyl-trisiloxane)], 81

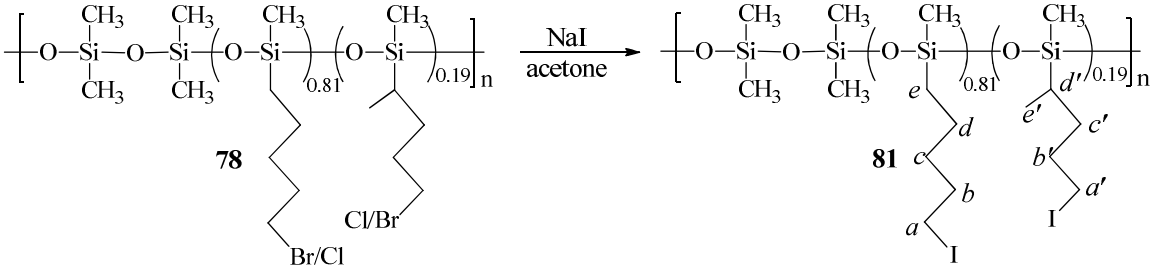

Yield: 64 % (2.08 g), ν(C-I) = 798 cm^{-1}, η_{inh} = 0.021 dL/g, ^{1}H NMR: δ_H (300 MHz, $CDCl_3$)/ppm: 0.12 (15H, s, CH_3), 0.54 (2H, t, CH_2, *e*), 0.8 (2H, t, CH_2, *d'*, *e'*), 1.42 (4H, m, CH_2, *c*,*d*), 1.65 (2H, m, CH2, *b'*), 1.86 (2H, m, CH_2, *b*), 3.04 (2H, t, CH_2, *a'*), 3.32 (2H, t, CH_2, *a*). Theoretical composition: C, 29.70; H, 6.23. Anal. Found: C, 21.4; H, 6.03, **Spectrum 4.16**.

4.8.16 Rhodium-containing polymers 85 and 86

4.8.16.1 Polymer 85

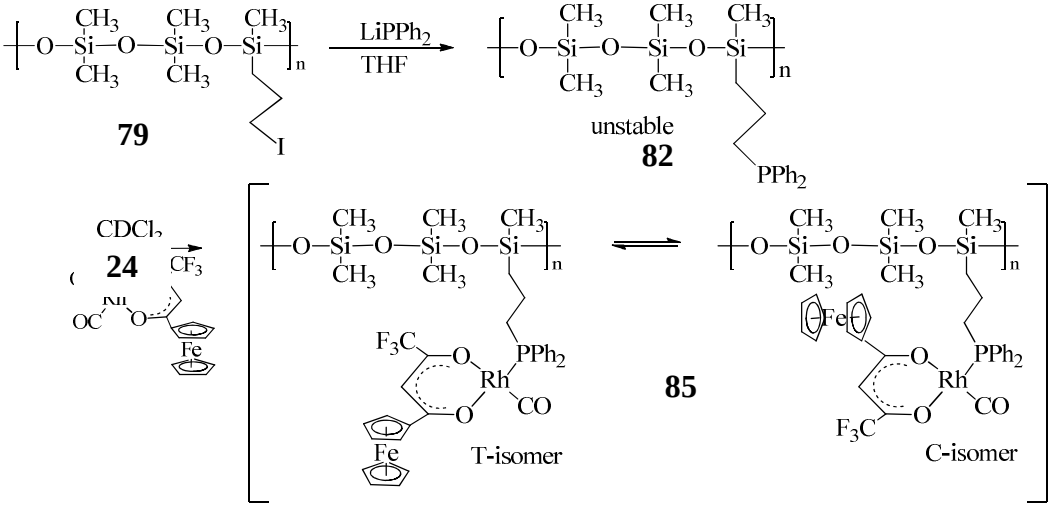

All reaction-vessels were degassed and charged with a nitrogen atmosphere that was maintained throughout the duration of the experiment. $LiPPh_2$ (2.39 mmol, 4.78 ml of a 0.5 M solution) was transferred to a 3-necked flask followed by drop wise addition of a solution of polymer **79** (2.66 mmol of I functional groups, 1 g) in 2 ml dry, deoxygenated THF. Stirring continued for an hour. The solvent was removed at reduced pressure. Dry deuterated chloroform, $CDCl_3$ (4 ml) was added to dissolve the unstable white gel-like phosphine polymer **82** while leaving the LiI precipitated. In another flask, the dicarbonyl rhodium complex **24** (2.93 mmol, 1.15 g) was dissolved in $CDCl_3$ (7 ml) and heated to 60 ˚C. The phosphine solution containing polymer **82** was sucked up in a syringe

under nitrogen leaving the LiI behind and added dropwise to the warm rhodium complex solution. It is important to note the order of addition cannot be changed. This is done to reduce or prevent cross linking and other undesired products. Bubbling was observed due to the release of CO gas. Stirring continued until all gas evolution ceased. The reaction mixture was washed with water (3 x 20 ml) and the organic layer was dried over anhydrous $MgSO_4$ and evaporated under reduced pressure to give the rhodium-containing polymer **85** as a solid hard gum-like red polymer.

Phosphine polymer **82** was unstable. Yield was assumed to be 100 %. A sample solution from the syringe was characterized by ^{1}H NMR: δ_H (300 MHz, $CDCl_3$)/ppm: 0.00 (15H, s, CH_3), 0.70 (2H, t, CH_2), 1.70 (2H, m, CH_2), 3.34 (2H, t, CH_2), 7.35-8.1 (10H, m, C_6H_5), **Spectrum 4.17**.

Characterization of polymer **85**. Yield: 47 % (0.99 g), Melting point: 148 °C, ν(C≡O) = 1982 cm^{-1}, η_{inh} = 0.016 dL/g, ^{1}H NMR: δ_H (300 MHz, $CDCl_3$)/ppm: 0.08 (15H, s, CH_3), 0.84 (2H, t, CH_2), 1.60 (2H, m, CH_2), 3.13 (2H, t, CH_2), 4.03 (5H, t, C_5H_5, C-isomer), 4.25 (5H, t, C_5H_5, T-isomer), 4.36 (2H, t, C_5H_4, C-isomer), 4.36 (2H, t, C_5H_4, C-isomer), 4.65 (2H, t, C_5H_4, T-isomer), 4.87 (2H, t, C_5H_4, T-isomer), 6 .0-6.24 (1H, s, CH), 7.33-7.86 (10H, m, 2 x C_6H_5). Theoretical composition: C, 47.25; H, 4.76; P, 3.48; Fe, 6.28. Anal. Found: C, 44.26; H, 4.06; P, 2.08; Fe, 7.66, **Spectrum 4.20**.

4.8.16.2 Polymer 86

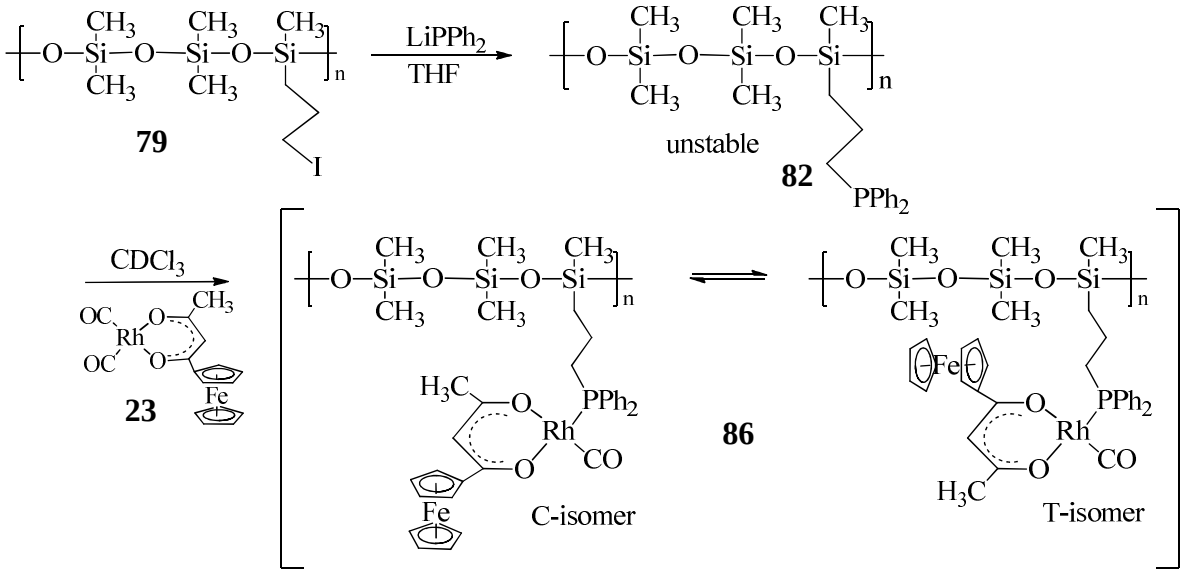

Phosphine polymer **82** and rhodium containing polymer complex **86** were obtained in an analogous manner as paragraph 4.8.16.1 using iodated polymer **79** (0.54 mmol, 204 mg), $LiPPh_2$ (0.54 mmol, 1.09 ml of a 0.5 M solution) and rhodium dicarbonyl complex **23** (0.54 mmol, 260 mg).

Characterization of polymer **86**. Yield: 44 % (0.2 g), Melting point: 137 °C, ν(C≡O) = 1975 cm^{-1}, η_{inh} = 0.012 dL/g, NMR: δ_H (300 MHz, $CDCl_3$)/ppm: 0.08 (15H, s, CH_3), 0.84 (2H, t, CH_2), 1.73 (2H, m, CH_2), 1.86 (2H, m, CH_2), 2.15 (3H, s, CH_2), 3.13 (2H, t, CH_2), 4.03 (5H, t, C_5H_5, T-isomer), 4.25 (5H, t, C_5H_5, C-isomer), 4.26 (2H, t, C_5H_4, T-isomer), 4.36 (2H, t, C_5H_4, C-isomer), 4.65 (2H, t, C_5H_4, C-isomer), 4.87 (2H, t, C_5H_4, C-isomer), 6.22 (1H, s, CH, C-isomer), 7.37-7.94 (10H, m, 2 x C_6H_5). Theoretical composition: C, 50.3; H, 5.43; P, 3.71; Fe, 6.68. Anal. Found: C, 45.50; H, 4.71; P, 2.97; Fe, 6.25, **Spectrum 4.21**.

4.8.17 Rhodium-containing polymers 87-90.

Rhodium-containing polysiloxane polymers **87-90** were obtained in the same manner with the appropriate iodated polymers and rhodium dicarbonyl complex used for each as shown in the reactions. The synthesis given below uses rhodium-containing polysiloxane polymer **87** as an example.

4.8.17.1 Polymer 87

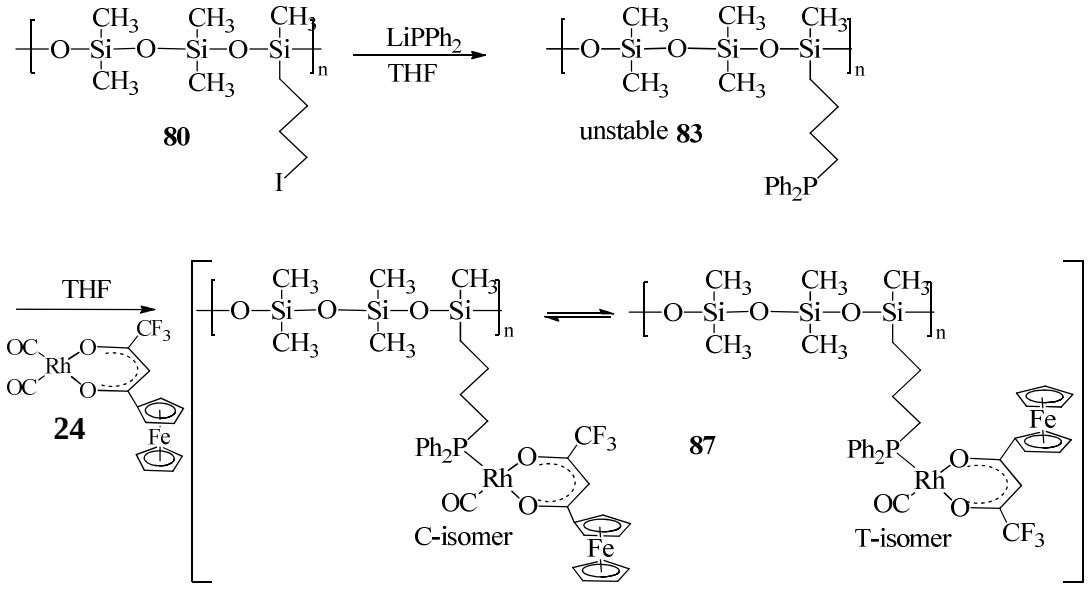

All reaction-vessels were degassed and charged with a nitrogen atmosphere that was maintained throughout the duration of the experiment. $LiPPh_2$ (0.18 mmol, 0.36 ml of a 0.5 M solution) was transferred to a 3-necked flask followed by drop wise addition of the iodated polymer **80** solution (0.18 mmol of I functional groups, 63 mg) in 2.5 ml dry, deoxygenated THF. This sequence of addition cannot be changes. Stirring continued for an hour. The solvent was removed at reduced pressure. Dry, deoxygenated THF (4 ml) was added to dissolve the white unstable gum-like

phosphine polymer **83** while leaving the LiI precipitated. In another flask, the dicarbonyl rhodium complex **24** (0.18 mmol, 87 mg) was dissolved in 3.5 ml THF and heated to 60 ˚C. The unstable phosphine **83** solution was sucked up in a syringe and added dropwise to the warm rhodium complex solution. Bubbling was observed due to the release of CO gas. Stirring continued until all gas evolution ceased. The solvent was removed from the reaction mixture until dryness under reduced pressure and the precipitate was dissolved in $CDCl_3$ (4 ml) and washed with water (3 x 10 ml) and the organic layer was dried over anhydrous $MgSO_4$ and evaporated under reduced pressure to give the rhodium-containing polymer **87** as a solid hard gum-like red polymer.

Phosphine polymer **83** was unstable. Yield was assumed to be 100 %. A sample solution from the syringe was characterized. ^1H NMR: δ_H (300 MHz, $CDCl_3$)/ppm: 0.07 (15H, s, CH_3), 0.52 (2H, t, CH_2), 1.56 (2H, m, CH_2), 1.85 (2H, m, CH_2), 3.26 (2H, t, CH_2), 7.32-8.04 (10H, m, 2 x C_6H_5), **Spectrum 4.18**.

Characterization of polymer **87**. Yield: 60 % (97 mg), Melting point: 166 °C, $\nu(C{\equiv}O)$ = 1989 cm^{-1}, η_{inh} = 0.019 dL/g, NMR: δ_H (300 MHz, $CDCl_3$)/ppm: 0.08 (15H, s, CH_3), 0.53 (2H, t, CH_2), 1.46 (2H, m, CH_2), 1.86 (2H, m, CH_2), 3.22 (2H, t, CH_2), 4.03 (5H, t, C_5H_5, T-isomer), 4.22 (5H, t, C_5H_5, C-isomer), 4.26 (2H, t, C_5H_4, T-isomer), 4.36 (2H, t, C_5H_4, T-isomer), 4.52 (2H, t, C_5H_4, C-isomer), 4.86 (2H, t, C_5H_4, C-isomer), 6.10 (1H, s, CH, C-isomer), 7.33-7.86 (10H, m, 2 x C_6H_5). Theoretical composition: C, 47.85; H, 4.91. Anal. Found: C, 44.05; H, 4.49, **Spectrum 4.22**.

4.8.17.2 Polymer 88

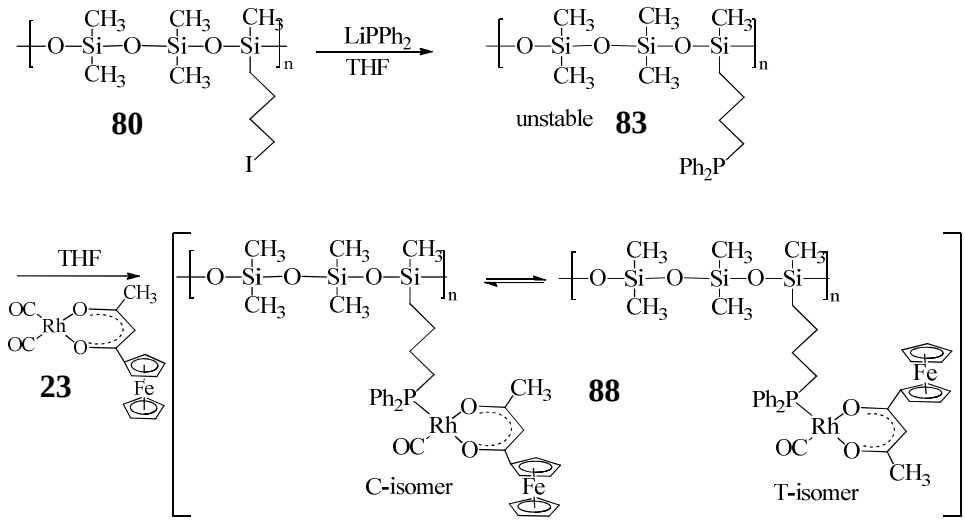

Rhodium-containing polymer complex **88** was synthesized by using iodated polymer **80** (0.49 mmol, 166 mg), $LiPPh_2$ (0.49 mmol, 0.98 ml of a 0.5 M solution) and rhodium dicarbonyl complex **23** (0.49 mmol, 240 mg). Phosphine polymer **83** was unstable and the yield was assumed to be 100 %.

Characterization of polymer **88**. Yield: 57 % (240 mg), Melting point: 155 °C, $\nu(C\equiv O)$ = 1970 cm^{-1}, η_{inh} = 0.017 dL/g, NMR: δ_H (300 MHz, $CDCl_3$)/ppm: 0.10 (15H, s, CH_3), 0.57 (2H, t, CH_2), 1.67 (2H, m, CH_2), 2.10 (2H, m, CH_2), 4.00 (5H, t, C_5H_5, T-isomer), 4.17 (5H, t, C_5H_5, C-isomer), 4.28 (2H, t, C_5H_4, T-isomer), 4.36 (2H, t, C_5H_4, T-isomer), 4.44 (2H, t, C_5H_4, C-isomer), 4.82 (2H, t, C_5H_4, C-isomer), 5.92 (1H, s, CH, C-isomer), 7.33-7.86 (10H, m, 2 x C_6H_5). Theoretical composition: C, 50.89; H, 5.58; P, 3.65; Fe, 6.57. Anal. Found: C, 45.49; H, 4.70; P, 2.58; Fe, 5.82, **Spectrum 4.23**.

4.8.17.3 Polymer 89

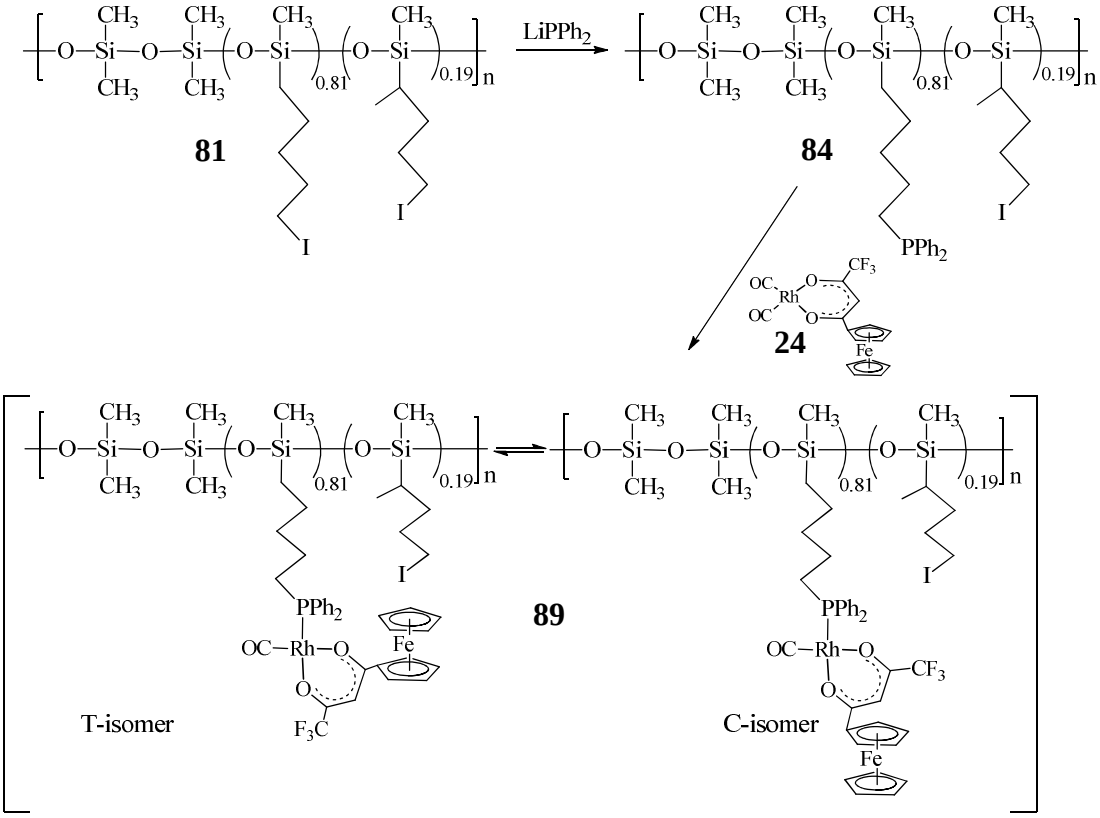

Rhodium-containing polymer complex **89** was synthesized by using iodated polymer **81** (0.38 mmol, 154 mg), $LiPPh_2$ (0.38 mmol, 0.76 ml of a 0.5 M solution) and rhodium dicarbonyl complex **24** (0.38 mmol, 183 mg). Phosphine polymer **84** was unstable and the yield was assumed to be 100 %. A sample solution from the syringe was characterized. ^{1}H NMR:δ_H (300 MHz, $CDCl_3$)/ppm: 0.08 (15H, s, CH_3), 0.42 (2H, t, CH_2), 1.52 (2H, m, 2 x CH_2), 1.69 (2H, m, CH_2), 3.22 (2H, t, CH_2), 7.32-8.01 (10H, m, 2 x C_6H_5).

Characterization of polymer **89**: Yield: 59 % (206 mg), Melting point: 146 °C, ν(C≡O) = 1975 cm^{-1}, η_{inh} = 0.011 dL/g, ^{1}NMR: δ_H (300 MHz, $CDCl_3$)/ppm: 0.08 (15H, s, CH_3), 0.53 (2H, t, CH_2), 1.42 (4H, m, 2 x CH_2), 1.86 (2H, m, CH_2), 3.19 (2H, t, CH_2), 4.03 (5H, t, C_5H_5, T-isomer), 4.21 (5H, t, C_5H_5, C-isomer), 4.26 (2H, t, C_5H_4, T-isomer), 4.36 (2H, t, C_5H_4, T-isomer), 4.53 (2H, t, C_5H_4, C-isomer), 4.85 (2H, t, C_5H_4, C-isomer), 6.10 (1H, s, CH, C-isomer), 7.33-7.86 (10H, m, 2 x C_6H_5). Theoretical composition: C, 48.42; H, 5.05; P, 3.38; Fe, 6.09. Anal. Found: C, 44.33; H, 3.83; P, 2.94; Fe, 4.70, **Spectrum 4.24**.

4.8.17.4 Polymer 90

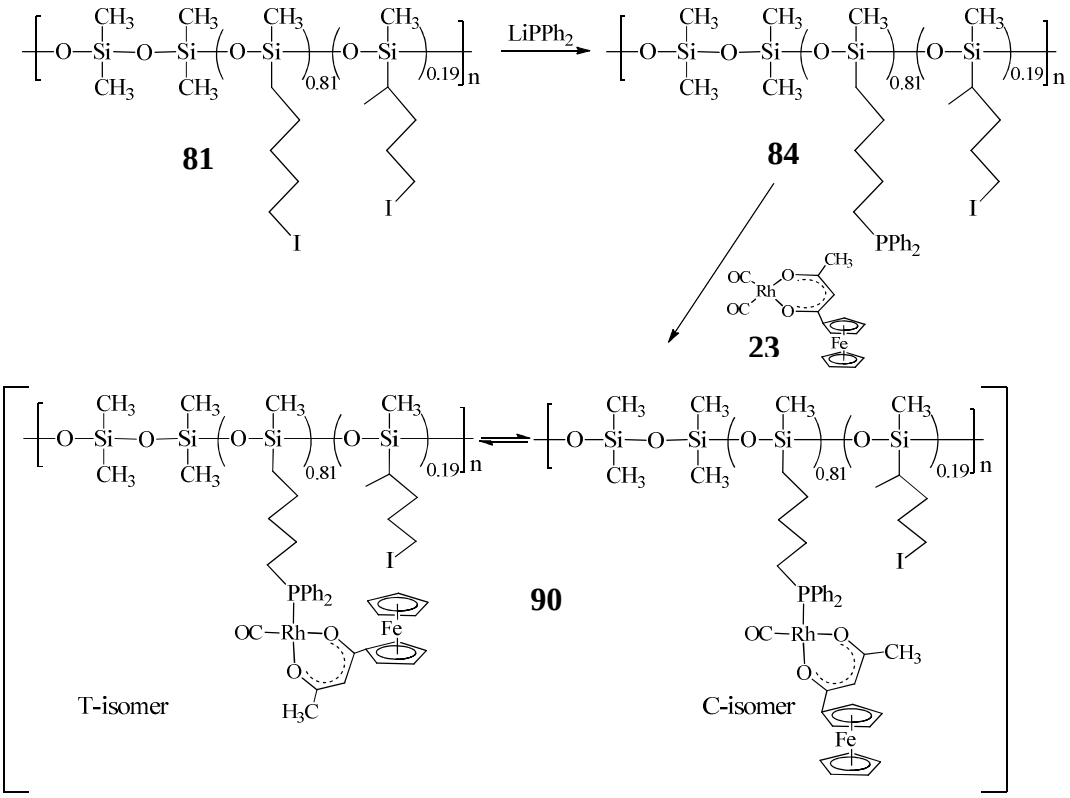

Rhodium-containing polymer complex **90** was synthesized by using iodated polymer **81** (0.23 mmol, 93 mg), $LiPPh_2$ (0.23 mmol, 0.46 ml of a 0.5 M solution) and rhodium dicarbonyl complex **23** (0.23 mmol, 110 mg). Phosphine polymer **84** was unstable and the yield was assumed to be 100 %.

Characterization of polymer **90**. Yield: 50 % (107 mg), Melting point: 164 °C, $\nu(C\equiv O)$ = 1971 cm^{-1}, Melting point = 165 °C, η_{inh} = 0.028 dL/g, ^1H NMR: δ_H (300 MHz, $CDCl_3$)/ppm: 0.11 (15H, s, CH_3), 0.61 (2H, t, CH_2), 1.79 (2H, m, CH_2), 1.89 (2H, m, CH_2), 1.89 (2H, m, CH_2), 2.54 (2H, m, CH_2), 2.91 (2H, t, CH_2), 4.00 (5H, t, C_5H_5, T-isomer), 4.20 (5H, t, C_5H_5, C-isomer), 4.28 (2H, t, C_5H_4, T-isomer), 4.34 (2H, t, C_5H_4, T-isomer), 4.44 (2H, t, C_5H_4, C-isomer), 4.79 (2H, t, C_5H_4, C-isomer), 5.85-6.20 (1H, s, CH), 7.33-7.86 (10H, m, 2 x C_6H_5). Theoretical composition: C, 51.45; H, 5.71; P, 3.59; Fe, 6.46. Anal. Found: C, 46.71; H, 4.88; P, 2.63; Fe, 7.66, **Spectrum 4.25**.

5 Summary and future perspective

Ferrocene-containing β-diketones $FcCOCH_2COR$ with Fc = ferrocenyl and R = CH_3, **4**, or CF_3, **5**, were synthesized by Claisen condensation of acetyl ferrocene with $CH_3COOCH_2CH_3$ or $CF_3COOCH_2CH_3$ under the influence of the base lithiumdiisopropylamide, LDA. In a three-step synthetic sequence, $RhCl_3$ was converted to $[Rh_2Cl_2(cod)_2]$, [Rh(FcCOCHCOR)(cod)] and finally the rhodium dicarbonyl complexes $[Rh(FcCOCHCOR)(CO)_2]$ with R = CH_3, **23**, and CF_3, **24**. Six new rhodium-containing polysiloxanes, $\{(OSiMe_2)_2OSiMe\{(CH_2)_mPPh_2(CO)(FcCOCHCOR)Rh\}\}_n$, where R = CF_3 and m = 3, **85**, m = 4, **87** and m = 5, **89** or where R = CH_3 and m = 3, **86**, m = 4, **88**, and m = 5, **90**, were successfully synthesized and characterized. The complete synthetic pathway towards **85-90** is shown in **Scheme 5. 1**.

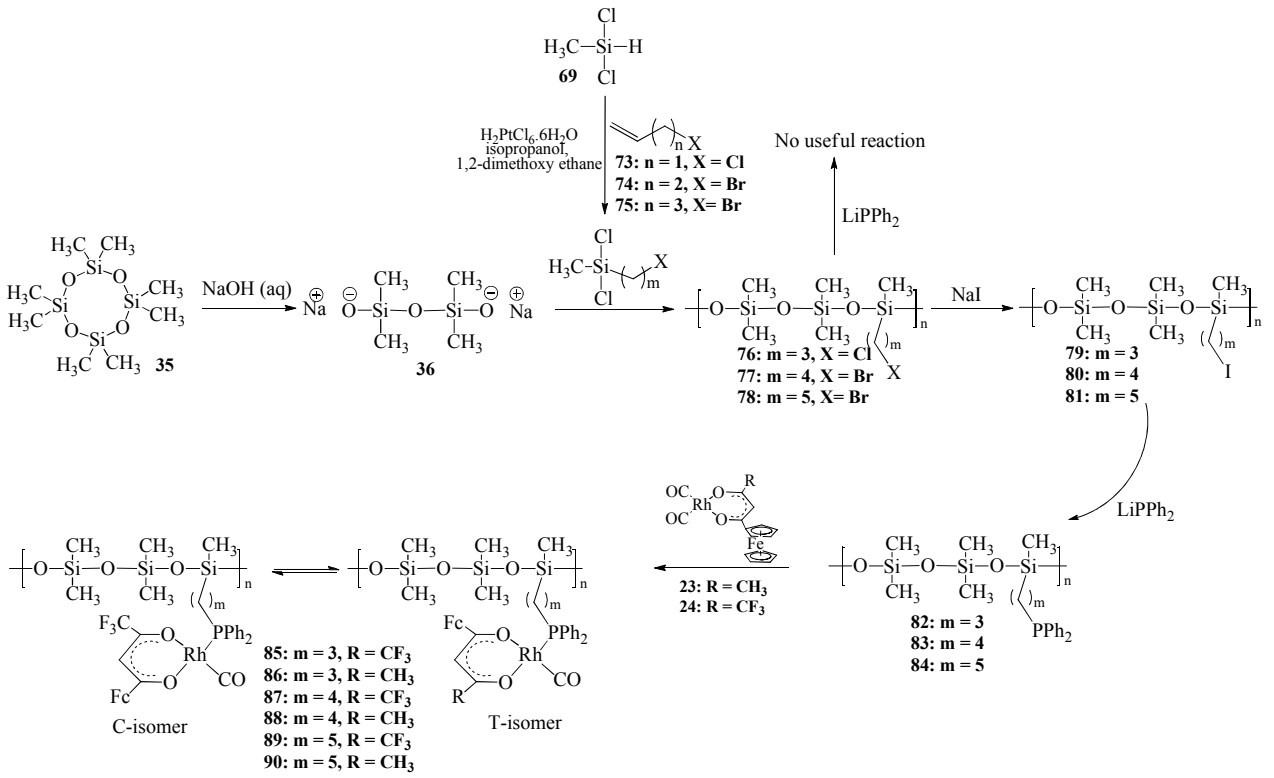

Scheme 5. 1. A complete synthetic pathway for the synthesis of ferrocene- and rhodium-containing carbonyl polysiloxanes, 85-90.

To the knowledge of the author this presents the first successful synthesis of any polysiloxane derivitized in such a way that the [Rh(FcCOCHCOR)(CO)] moiety could be grafted onto side chains of the main polymer.

The synthesis was achieved by first synthesizing a tetramethyldisiloxane-1, 3-diolate monomer, **36**, by a ring-opening reaction of octamethylcyclotetrasiloxane, **35**, by use of NaOH (aq). An exothermic platinum-catalyzed hydrosilylation reaction between dichloromethylsilane and the alkenes, 3-chloropropene, **70**, 4-bromobutene, **71** and 5-bromopentene, **72** yielded α-hydrosilylated 3–(chloropropyl)methyldichlorosilane, **73**, 4–(bromobutyl)methyldichlorosilane, **74** and 5–(bromopentyl)methyldichlorosilane, **75**, as major products. This series of compounds has a different number of carbon atoms, m = 3-5, between the silicon and the active chloride or bromide atom. Halogen-exchanged (for **74** and **75**) and β-hydosilylated (for **75**) isomers were noticeably identified by ^{1}H NMR as side-products. Chlorinated and brominated polysiloxane polymers were synthesized in good yields *via* a condensation reaction between **36** and halosilanes **73**-**75** to give $\{(OSiMe_2)_2OSiMe\{(CH_2)_m\text{-}X\}\}_n$ with m = 3, X = Cl, **76**, m = 4, X = Br, **77**, m = 5, X = Br, **78**.

Neither the chlorinated polymer, **76**, nor the brominated polymers, **77** and **78**, would react with $LiPPh_2$, so the chloro or bromo functional groups were replaced with a more reactive iodo group *via* an iodization reaction utilizing NaI to give $\{(OSiMe_2)_2OSiMe\{(CH_2)_m\text{-}I\}\}_n$ with m = 3, **79**, m = 4, **80**, m = 5, **81**. The reaction was followed by ^{1}H NMR, with the disappearance of the Cl/Br-CH_2 resonance and the appearance of the I-CH_2 resonance at δ 3.33-3.6 ppm and 3.21 ppm respectively. At least 95 % iodization was obtained.

Re-functionalization of the iodo-polysiloxane to phosphinated polysiloxanes was achieved by reacting **79**-**81** under dry and oxygen-free conditions with stoichiometric amount of $LiPPh_2$. These phosphine polymers, $\{(OSiMe_2)_2OSiMe\{(CH_2)_m\text{-}PPh_2\}\}_n$ with m = 3, **82**, m = 4, **83**, m = 5, **84**, were unstable and rapidly oxidized in an open atmosphere. They were, therefore, not isolated after synthesis, but were reacted "in situ" with the rhodium dicarbonyl complex, **23** and **24** to give rhodium-containing polysiloxane complexes **85**-**90**. The phosphine polymers showed a singlet ^{31}P NMR signal at about δ -17 ppm and for the rhodium-containing polysiloxane complexes a broad and rounded doublet signal was observed in the region δ 37-40 ppm in their ^{31}P NMR spectrums. The six polysiloxane complexes existed as two isomers as shown by ^{1}H NMR. One isomer has the ferrocenyl group trans to the CO group (this isomer is labelled the T-isomer), the other has the ferrocenyl group cis to the CO group (isomer labelled the C-isomer).

The degree of polymerization was investigated by measuring the inherent viscosity at repeating unit concentration 1.76 mM in dichloromethane. All polymers showed inherent viscosities within the range $0.011 \leq \eta_{inh} \leq 0.028$ g/dL. The binding energies of all atom types (Si, P, F, I, Rh and Fe) were determined by XPS. Residual amounts (less than 10 %) of unreacted iodo sites which were not phosphinated in the generation of **82**-**84**, were also detected by XPS. Other characterization techniques used included FTIR, elemental analysis, electrochemistry and UV/vis.

The electrochemical behaviour of the rhodium(I) and ferrocenyl redox-active centers in **82**-**90** was studied with cyclic voltammetry (CV), Oster Young square wave voltammetry (SWV) and linear sweep voltammetry (LSV). The experiments were performed using a non-coordinating solvent CH_2Cl_2 and $[N^nBu_4][B(C_6F_5)_4]$ electrolyte system, rather than $CH_3CN/[N^nBu_4][PF_6]$, to minimize solvation and ion pair formation of the type $cation^+\cdots^-anion$. $Fc^+\cdots^-[B(C_6F_5)_4]$ or $[Rh^{II}]^+\cdots^-[B(CF_6)_4]$ interactions, for example are less pronounced than $Fc^+\cdots^-[PF_6]$ or $[Rh^{II}]^+\cdots^-[\ PF_6]$ interactions.

In the CV's of the free rhodium(I) dicarbonyl complexes $[Rh(FcCOCHCOCH_3)(CO)_2]$, **23** and $[Rh(FcCOCHCOCF_3)(CO)_2]$, **24**, the electrochemically reversible one-electron oxidation wave of the ferrocenyl group and that of the electrochemically irreversible rhodium center overlaps. Oxidation takes place at $E^{\circ\prime}$ = 203 mV and 324 mV *vs* FcH/FcH^+ for **23** and **24** respectively. An LSV study confirmed a one electron-transfer process for each metal redox center when decamethylferrocene was used as an internal standard. Decamethyferrocene oxidation is known to be a one-electron transfer process. Thus, in **23** and **24**, Fc is oxidized to Fc^+ and Rh^I to Rh^{II}. The cathodic and anodic peak current ratios were in the range $0.89 \leq i_{pc}/i_{pa} \leq 0.92$ and $\Delta E_p < 90$ mV for the reversible ferrocenyl group. The oxidation for **23** where R = CH_3 occurs at a potential 121 mV lower than **24** where R = CF_3. The formal reductuin potentials are related to the group electronegativity, χ_R, of the different R-groups, where R = CH_3 (χ_R = 2.34) and R = CF_3 (χ_R = 3.01). Because of the higher group electronegativity of the CF_3 substituent in **24**, the Rh and Fe centers of **24** are more difficult to oxidize than those of **23** because more electron-density is removed from the redox centers by the CF_3 group than by the CH_3 group.

For all newly synthesized rhodium-containing polysiloxanes, **85**-**90**, one broad oxidation peak that is the compliment of four closely overlapping peaks in the potential region 100-500 mV was observed in the CV's. Two isomers were detected by CV as previously shown by the ^1H NMR. If one labels Rh(1), Fc(1), Rh(2) and Fc(2) the redox centers of the C and T isomers of **8**5-**90** respectively, then Rh(1) was first electrochemically irreversibly oxidized in a one electron-transfer

process, followed by Rh(2). The Rh(2) peak was either obscured under the first ferrocenyl peak or under the Rh(1)peak. Fc(1) and Fc(2) are then oxidized at more positive potentials in two separate one electron-transfer electrochemically reversible processes. The two processes are observed as peaks with $\Delta E_p \leq 84$ at 100 mV s^{-1} scan rate. The C and T isomers were electrochemically more visible for the polysiloxanes with R = CF_3 than those with R = CH_3 due to better peak resolution. To observe the C and T isomers at all implies the dynamic equilibrium between the C and T isomers must be slow on the CV time scale. SWV was more successful in resolving the peaks than the CV. For polysiloxane complexes where R = CF_3, **85** (m = 3), **87** (m = 4) and **89** (m = 5) the E°' values of the ferrocene group were determined as 374, 345 and 371 mV. When R = CH_3, **86** (m = 3), **88** (m = 4) and **90** (m = 5) formal reduction oxidation potentials were 345, 287 and 292 mV *vs* FcH/FcH^+ respectively. The electrochemical reactivity expressed as E°′ was shown to be directly proportional to the electron-richness of the rhodium metal center, the latter being a function of group electronegativity, χ_R, of the R-groups CH_3 and CF_3. For this to be detectable, good electronic communication must exist between the β-diketonato R = CH_3 and CF_3 side groups, the ferrocenyl moiety and the central rhodium center.

The kinetics of oxidative addition of MeI to **85** was also explored. This reaction is important as it is the rate determining step during the rhodium catalyzed Monsanto synthesis of acetic acid. The reaction sequence was found to exhibit two distinct stages, stage 1 and 2, see **Scheme 5. 2**.

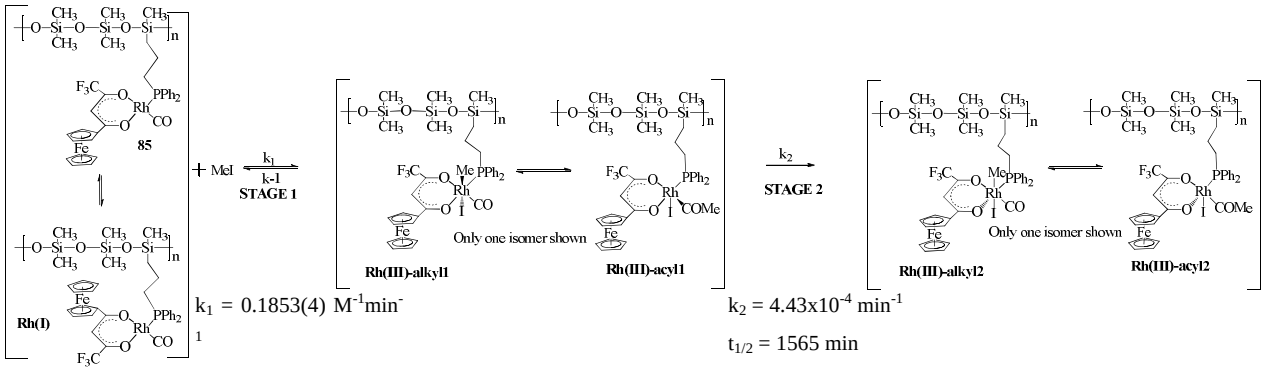

k_1 = 0.1853(4) $M^{-1}min^{-1}$

$t_{1/2}$ = 122 min

[MeI] = 0.0306 M

ΔH^* = 34(2) $kJ.mol^{-1}$

ΔS^* = -97(6) $J.mol^{-1} K^{-1}$

k_2 = 4.43x10^{-4} min^{-1}

$t_{1/2}$ = 1565 min

[MeI] = 0.0306 M

ΔH^* = 70(9) $kJ.mol^{-1}$

ΔS^* = 6(3) $J.mol^{-1} K^{-1}$

Scheme 5. 2. The reaction sequence of oxidative addition of MeI to polymer 85 and a summary of the activation parameters and rate constants.

In stage 1 the rhodium(I) center is oxidized to form two rhodium(III) species that are in rapid dynamic equilibrium with each other, **Scheme 5. 2**. The one specie is a methylated rhodium(III) labelled Rh(III)alkyl1, and the other is an acylated rhodium(III) specie labelled Rh(III)acyl1. During stage 2 these kinetically favoured structures isomerize to a new geometry to form two new species

labelle Rh(III)alkyl2 and Rh(III)acyl2 in **Scheme 5. 2**. These two products are the thermodynamically favoured products and are also in rapid equilibrium with each other. The reaction follows a second-order rate law for stage 1,

$R = k_1$[Rh content of polymer **85**][MeI]

A first-order dependence of MeI concentration was observed for stage 1. However, stage 2 is independent of MeI concentration and follows the first order rate law

$R = k_2$[Rh content of polymer **85**]

The activation parameters ΔH^* and ΔS^* for each stage were determined, and significantly, ΔS^* of stage 1 was -97(6) J.mol.K^{-1}. This indicates that this reaction stage takes place *via* an associative mechanism. Equally significant, ΔS^* for stage 2 approached zero which implies stage 2 involves a unimolecular process, as would be expected for isomerization processes.

The successful synthesis and characterization of the new polymers **85-90** may lead to several new research programs. These may include development of improved methods to actually isolate phosphine-containing polysiloxanes. The polymeric siloxane carrier system may be altered in a number of ways. For example, the siloxane backbone may be changed to be a biodegradable polysiloxane, phosphazene or polyphosphonate. The rhodium metal center may be exchanged for other metals with catalytic properties. For example, other square planar or octahedral complexes with central metals like Pt, Ir, Mn, Ru and Co, or metals that form linear complexes like gold or silver may be anchored onto the carrier polymer. This study only made use of two β-diketonato ligands, one bearing the electron-donating group R = CH_3 and the other bearing the electron-withdrawing CF_3 group. However a much wider range of β-diketonato ligands exist that may be studied. Other ligand systems such as carboxylates, Schiff base systems, catecholates or aminated ligands may substantially alter the behaviour of the new polymeric systems. The phosphine ligand, polymer-PPh_2, can also be changed by replacing one or both the phenyl groups with other groups like long chain alkyl groups or metallocenes. Most important of all, the application of the present "catalyst model" may be tested in several catalytic processes. For example, for **85-90** hydroformylation is a suitable reaction to explore. Other metal systems will catalyze other reactions. Finally, polysiloxanes are well-known to be non-toxic. The non-toxic behaviour of these polysiloxanes may be exploited to launch biological research programs. This may include medical application such as polysiloxane drug delivery systems.

Appendix

^{1}H NMR spectra

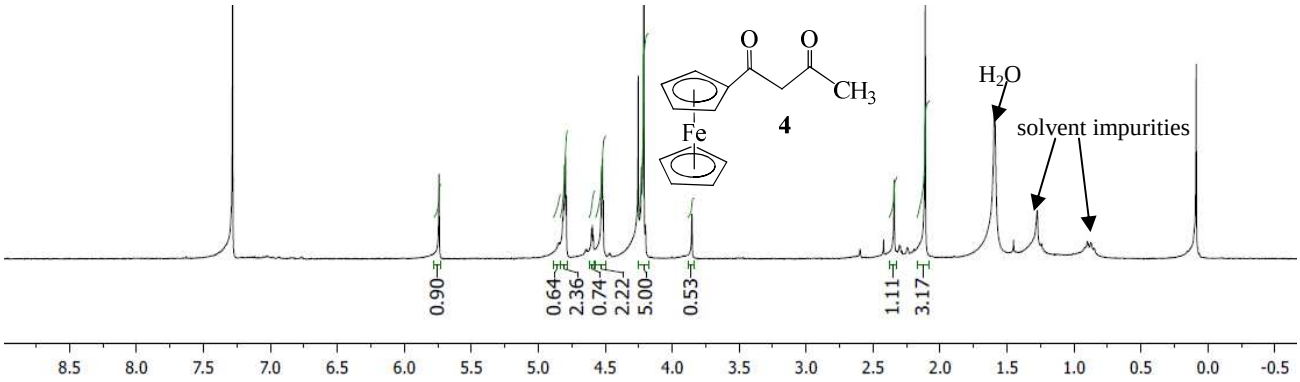

Spectrum 4. 1. 1-Ferrocenyl-3-methylbutane-1,3-dione, 4.

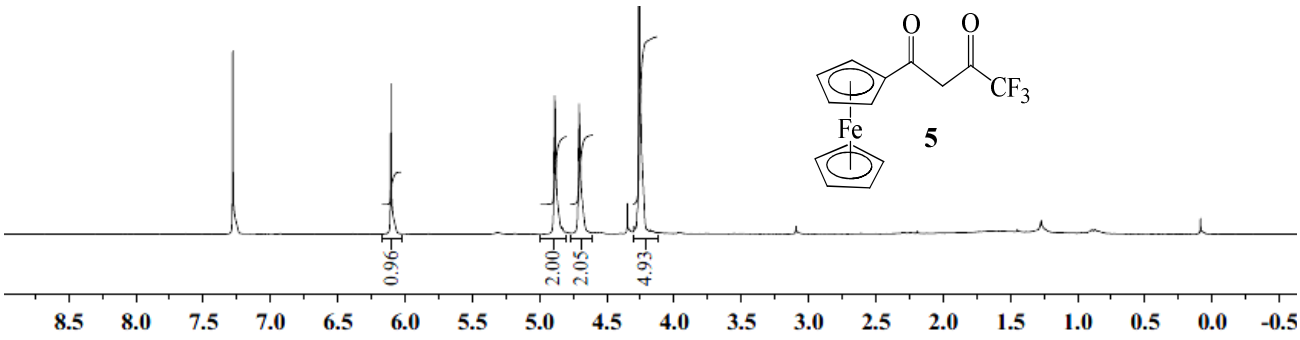

Spectrum 4. 2. 1-Ferrocenyl-4,4,4-trifluorobutane-1,3-dione, 5.

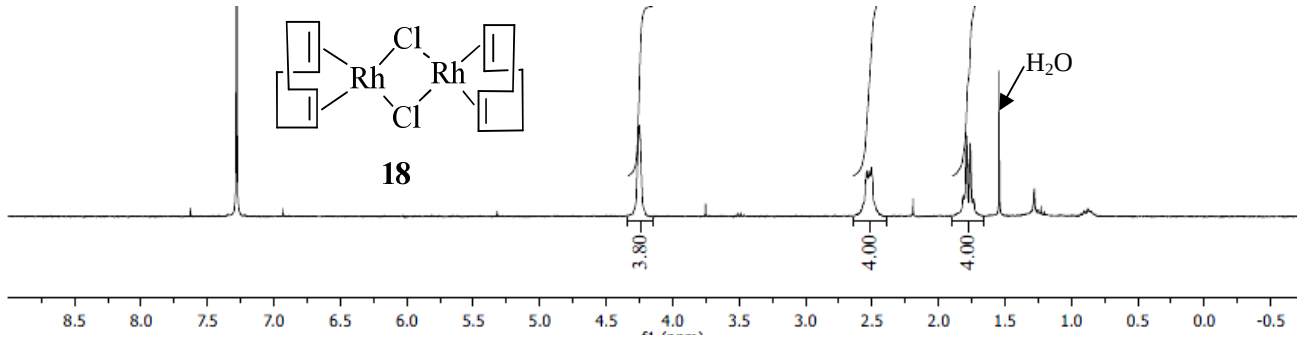

Spectrum 4. 3. Di-μ-chloro-bis[(1,2,5,6-η4)1,5-cyclooctadiene]rhodium, 18.

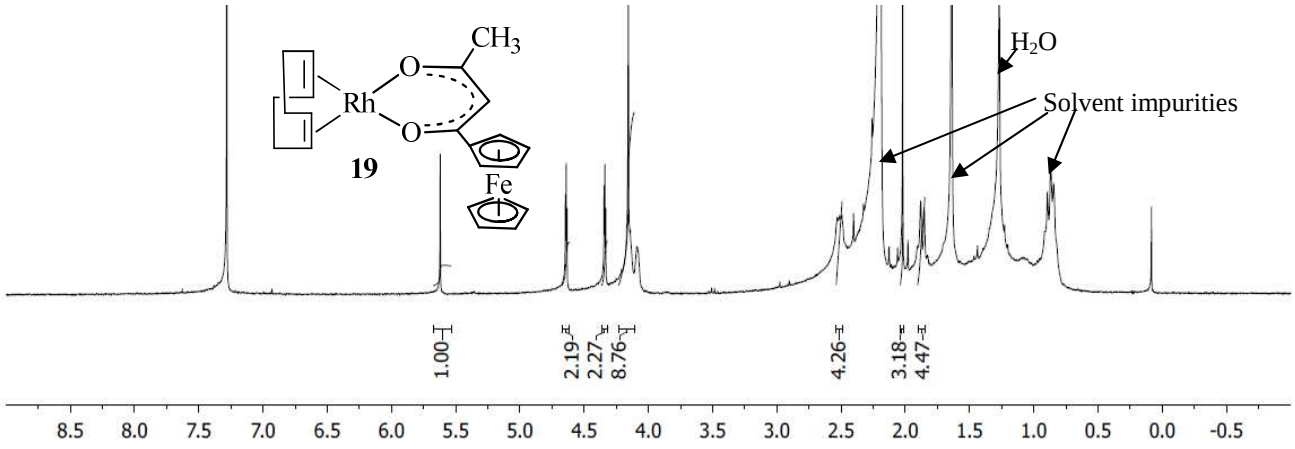

Spectrum 4. 4. [Rh(FcCOCHCOCH$_3$)(cod)], 19.

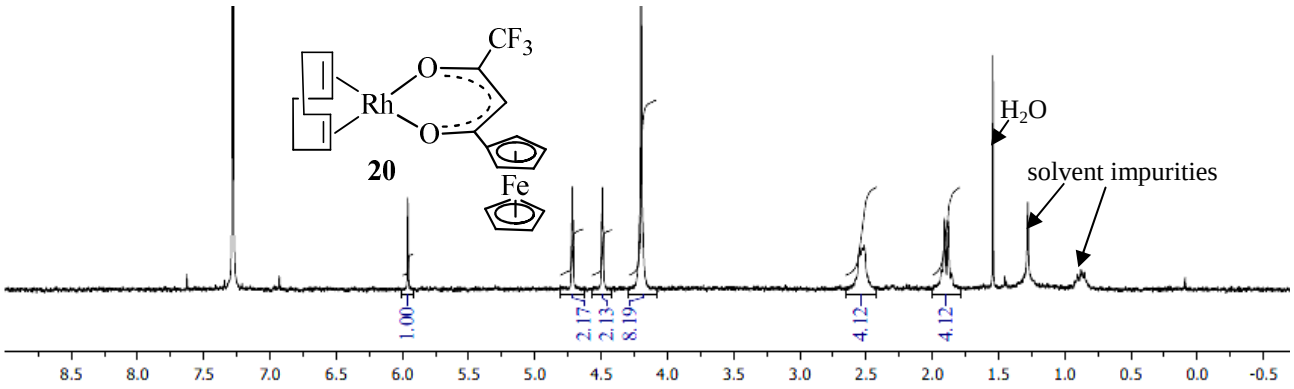

Spectrum 4. 5. [Rh(FcCOCHCOCF$_3$)(cod)], 20.

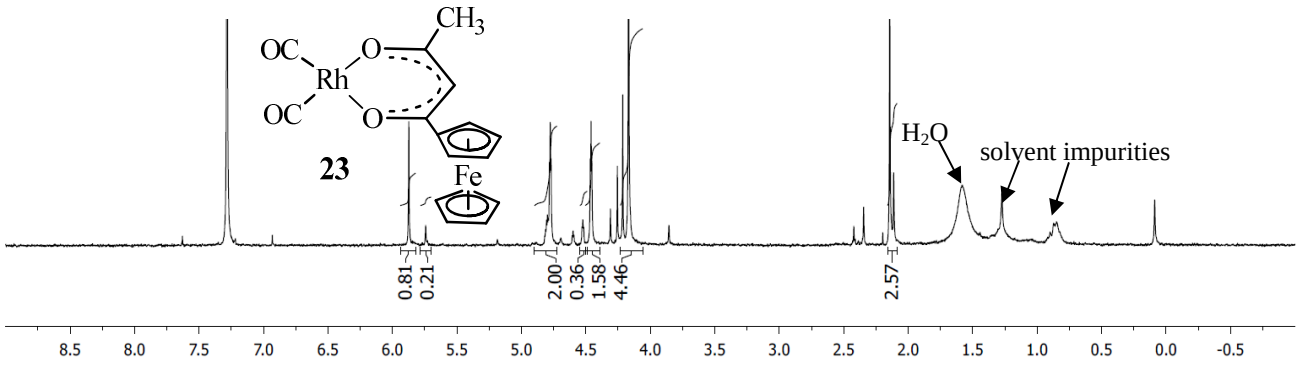

Spectrum 4. 6. [Rh(FcCOCHCOCH$_3$)(CO)$_2$], 23.

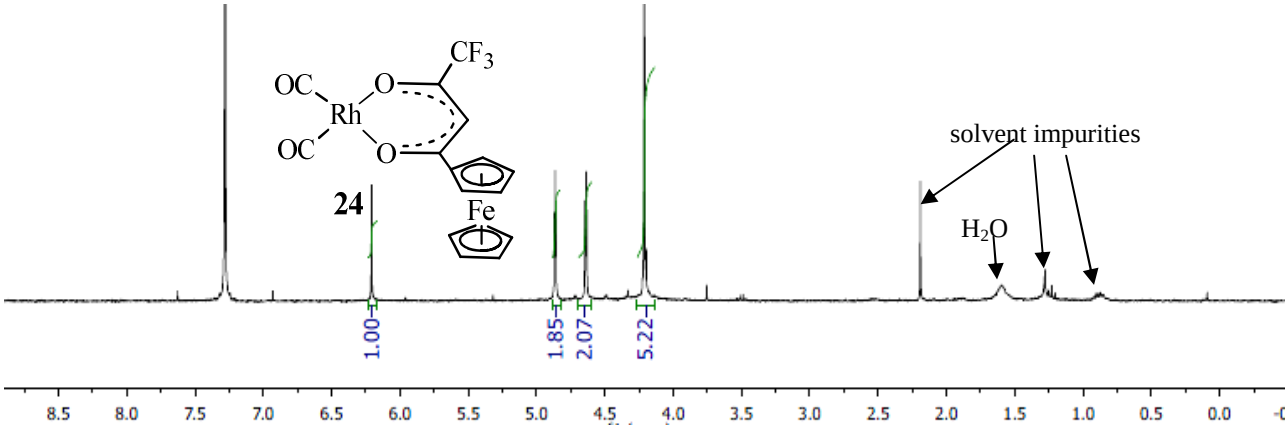

Spectrum 4. 7. [Rh(FcCOCHCOCF$_3$)(CO)$_2$], 24.

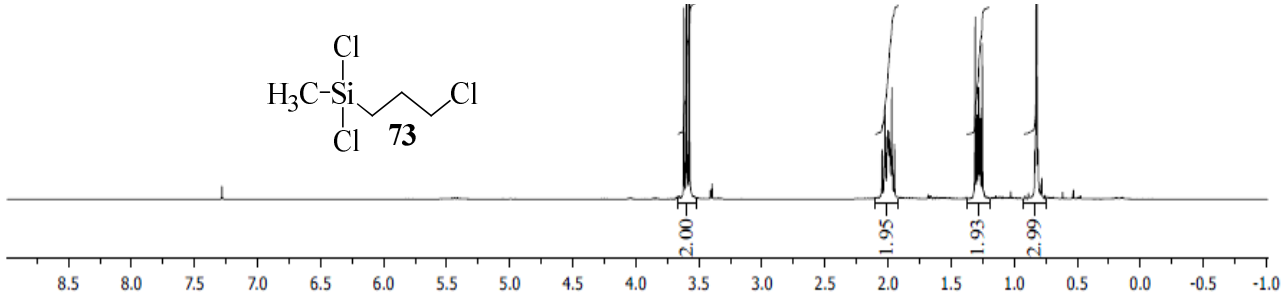

Spectrum 4. 8. (3-Chloropropyl)methyldichlorosilane, 73.

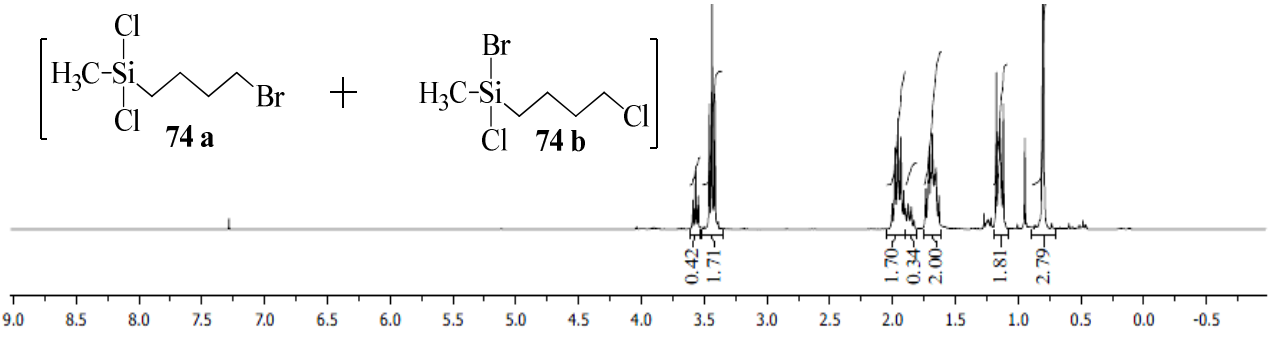

Spectrum 4. 9. (4-Bromobutyl)methyldichlorosilane, 74.

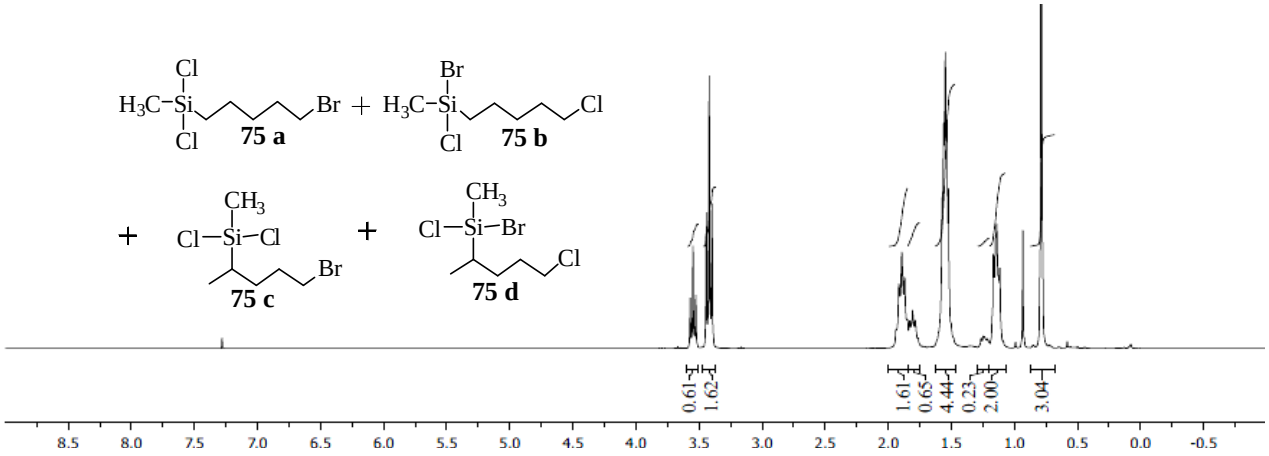

Spectrum 4. 10. (5-Bromopentyl)methyldichlorosilane, 75.

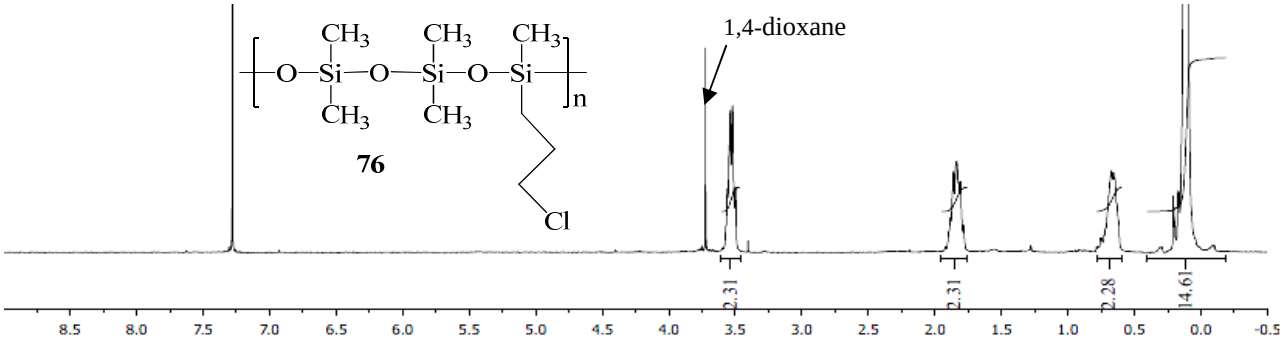

Spectrum 4. 11. Poly(3-chloropropylpentamethyltrisiloxane), 76.

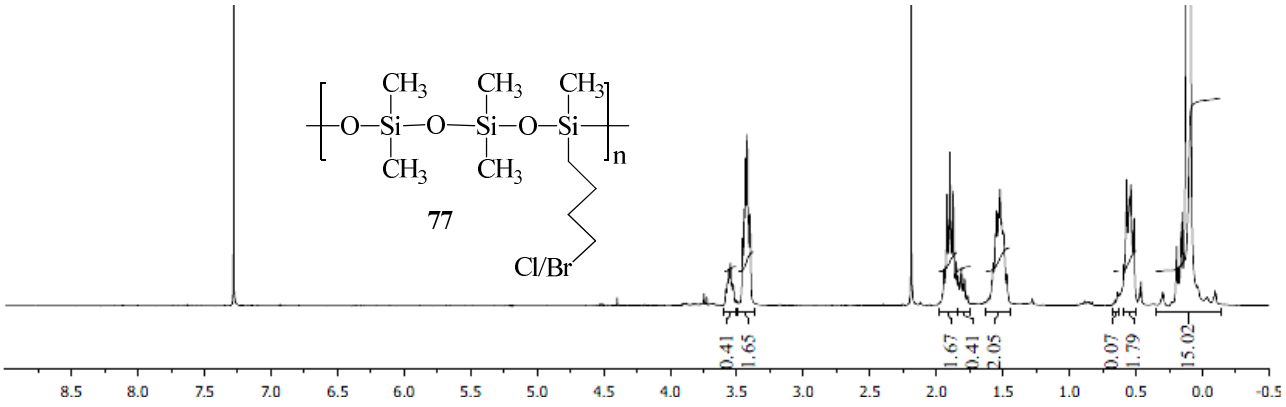

Spectrum 4. 12. Poly(4-bromobutylpentamethyltrisiloxane), 77.

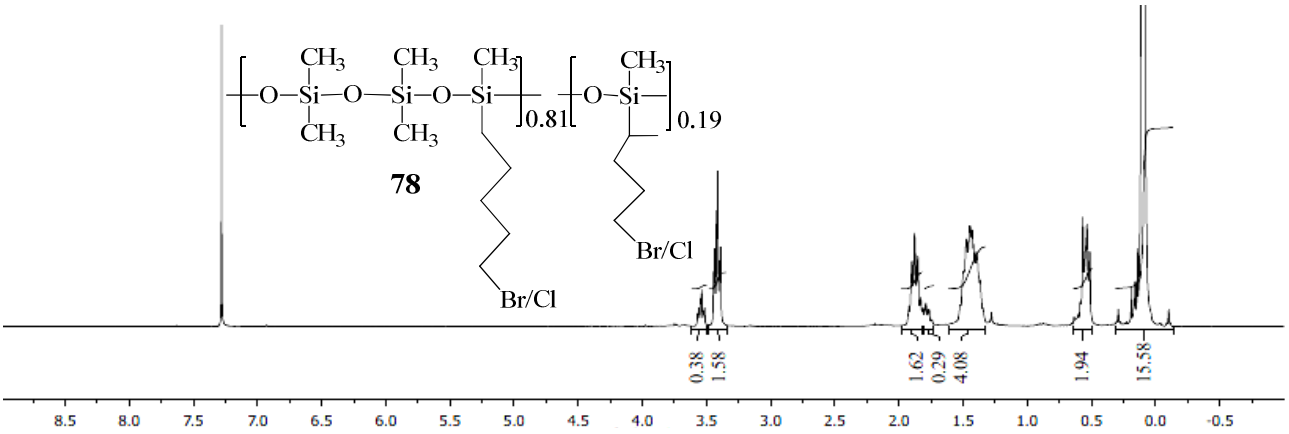

Spectrum 4. 13. Poly(5-bromopentylpentamethyltrisiloxane), 78.

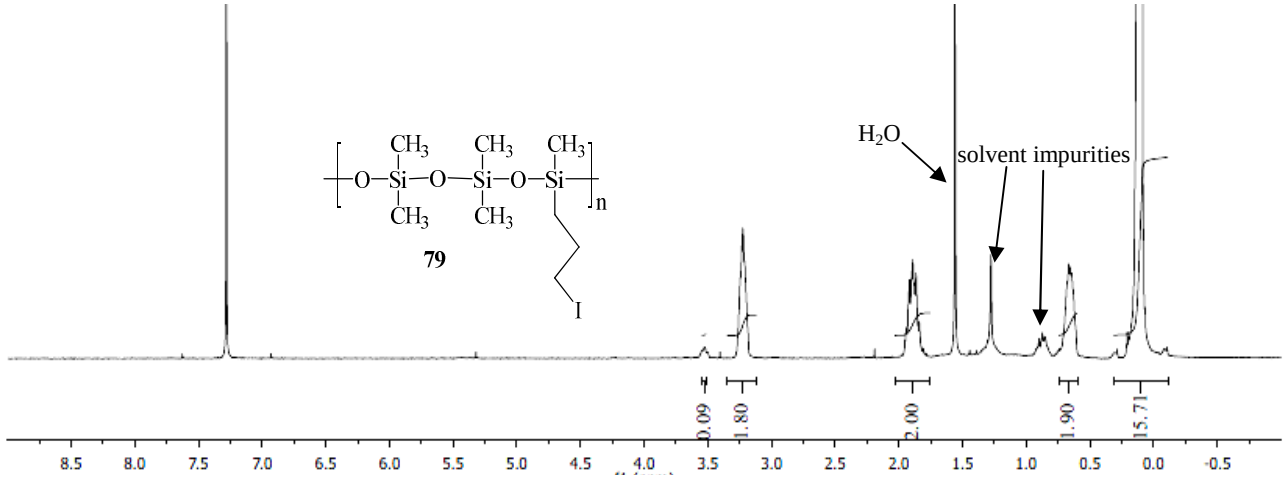

Spectrum 4. 14. Poly(3-iodopropylpentamethyltrisiloxane), 79.

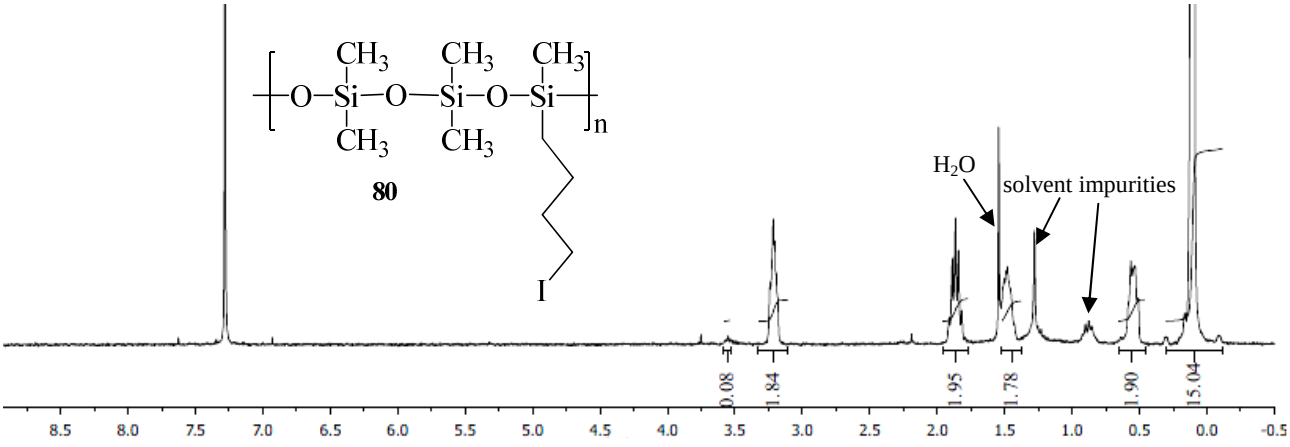

Spectrum 4. 15. Poly(4-iodobutylpentamethyltrisiloxane), 80.

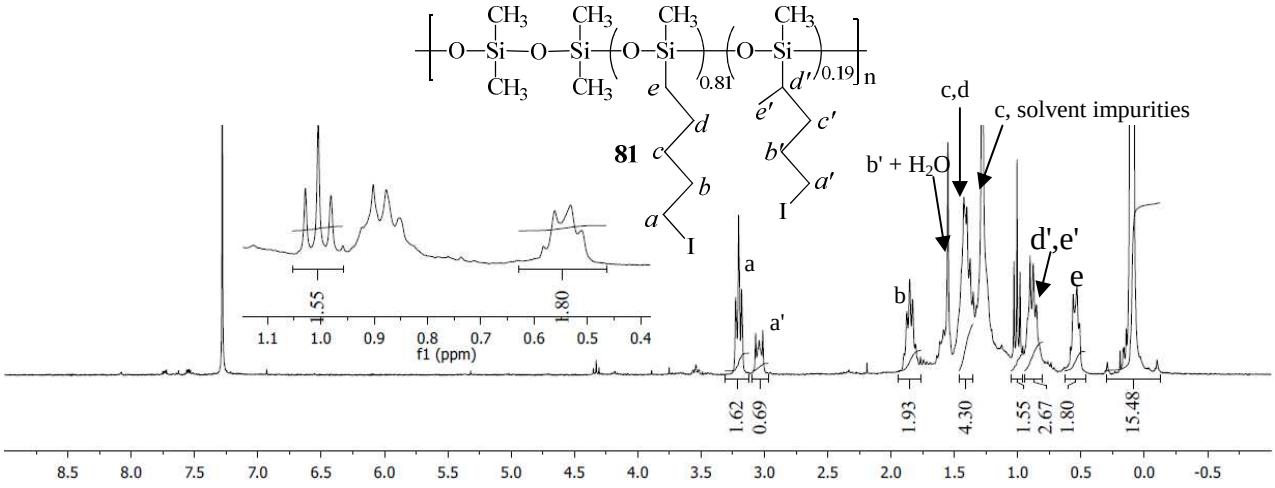

Spectrum 4. 16. Poly(5-iodopentylpentamethyltrisiloxane), 81.

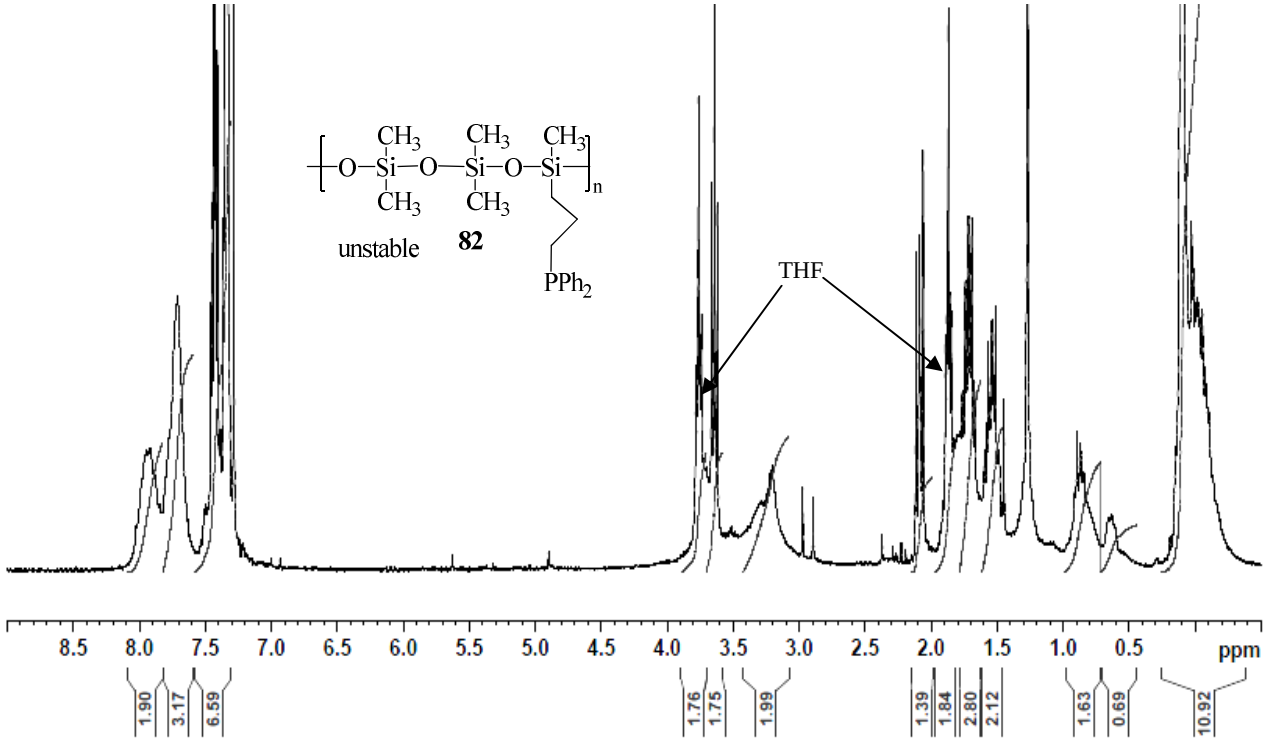

Spectrum 4. 17. Poly(3-phosphinopropylpentamethyltrisiloxane), 82.

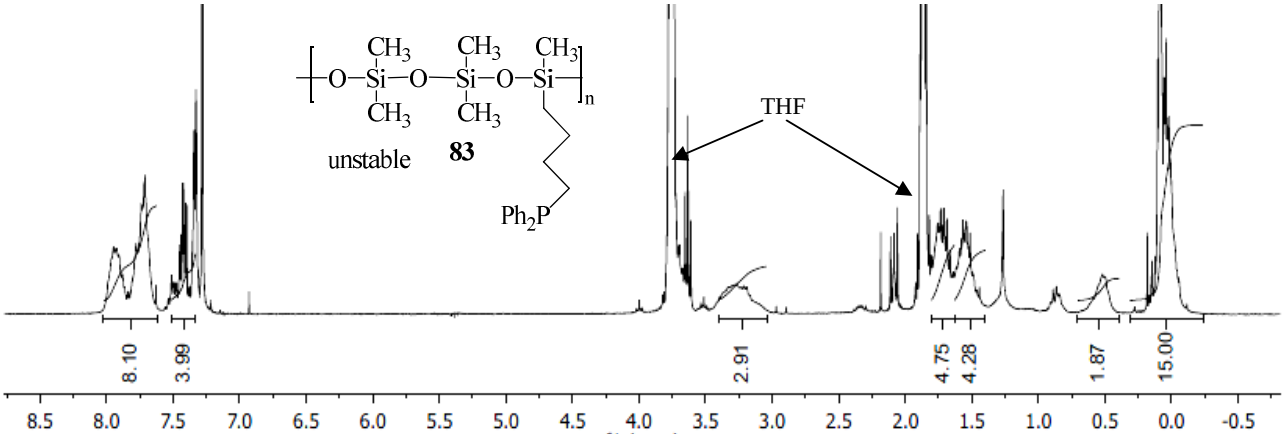

Spectrum 4. 18. Poly(4-phosphinobutylpentamethyltrisiloxane), 83.

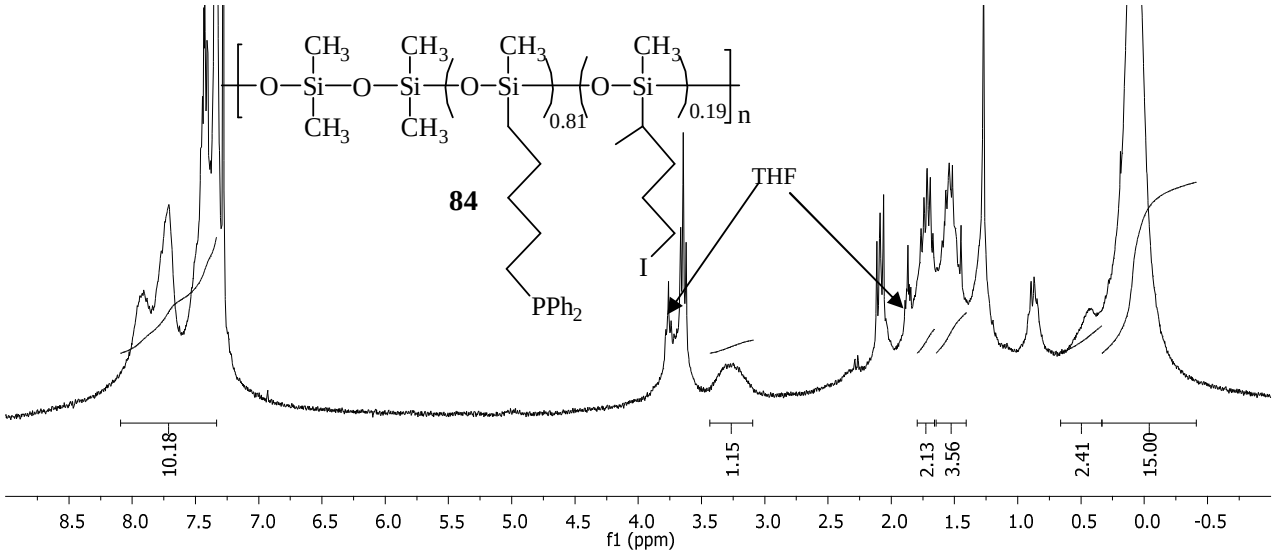

Spectrum 4. 19. Poly(5-phosphinopentylpentamethyltrisiloxane), 84.

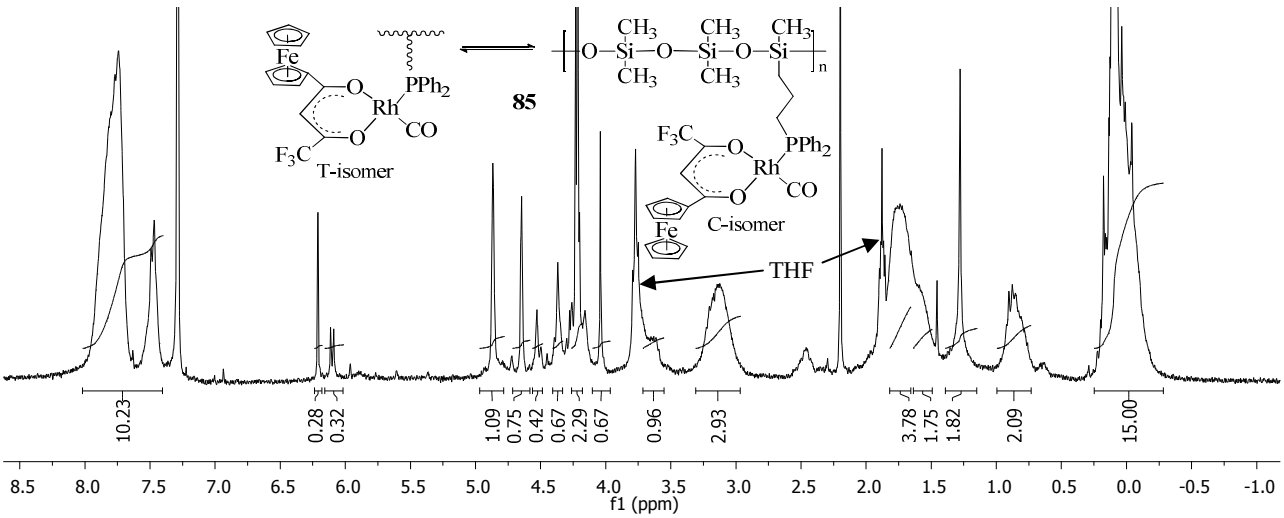

Spectrum 4. 20. Polymer 85.

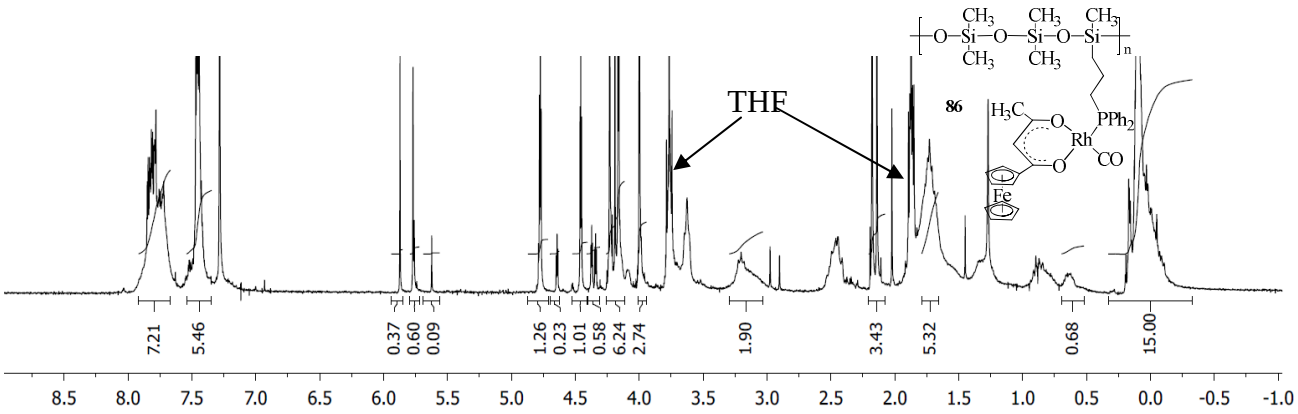

Spectrum 4. 21. Polymer 86.

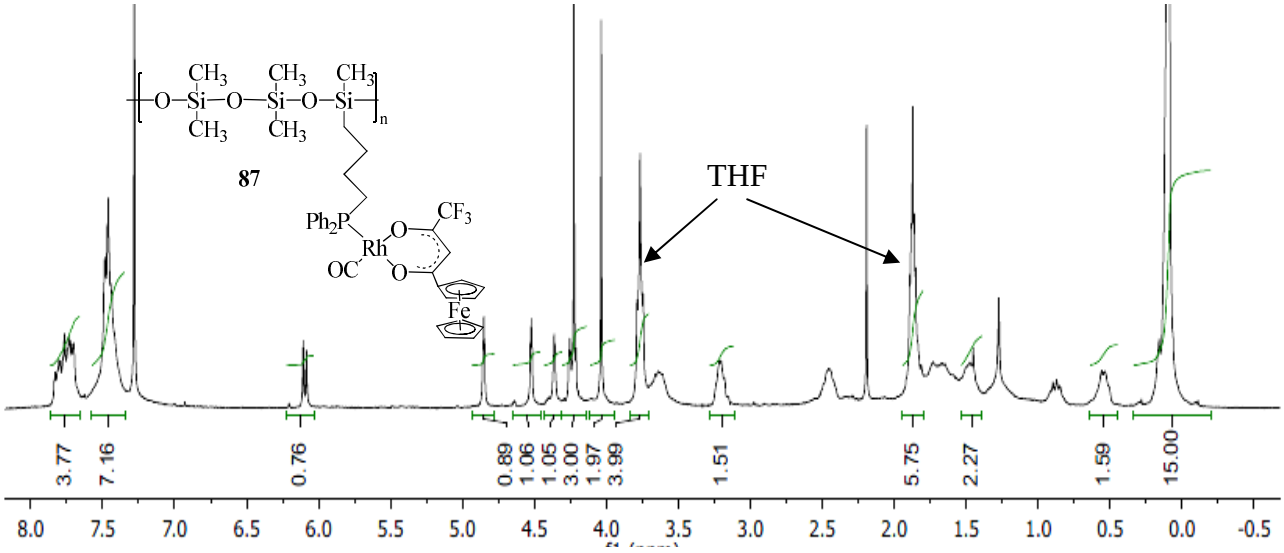

Spectrum 4. 22. Polymer 87.

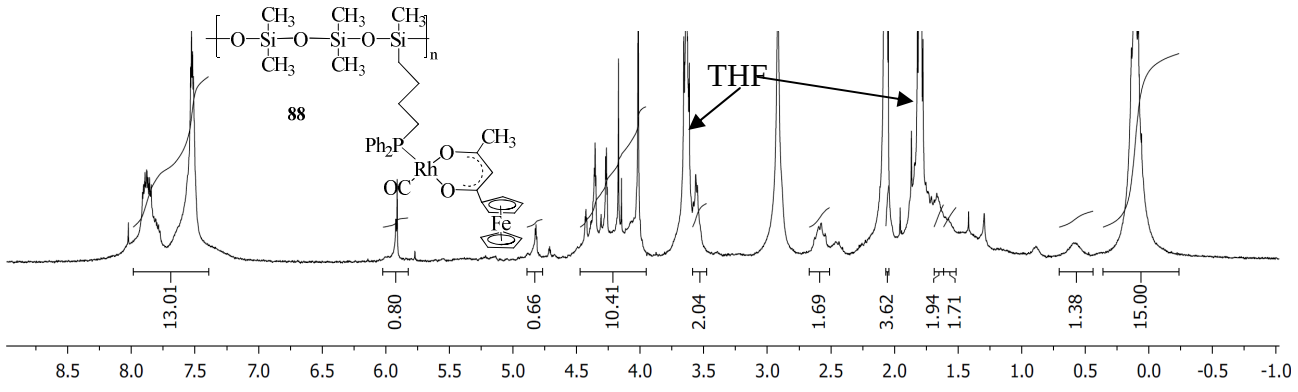

Spectrum 4. 23. Polymer 88.

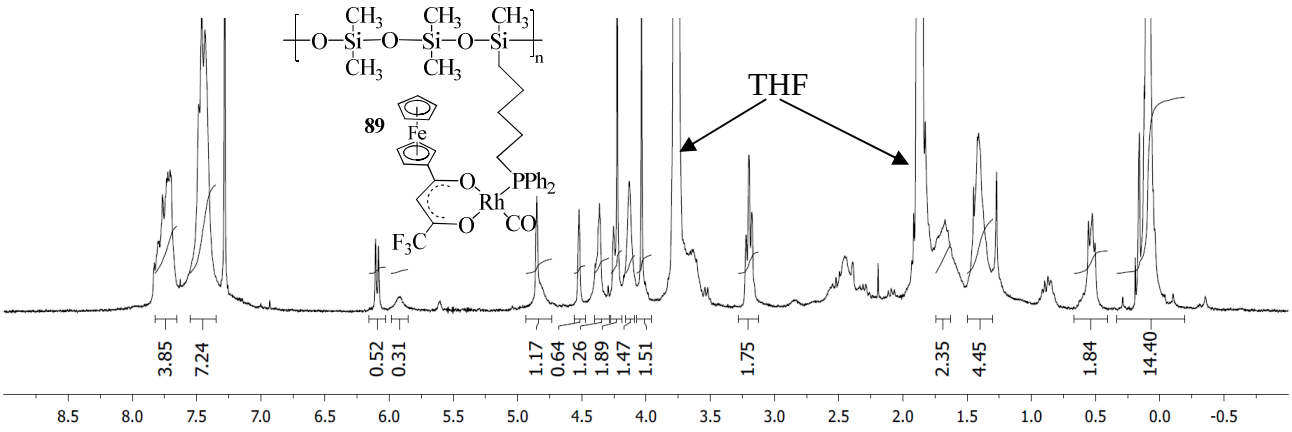

Spectrum 4. 24. Polymer 89.

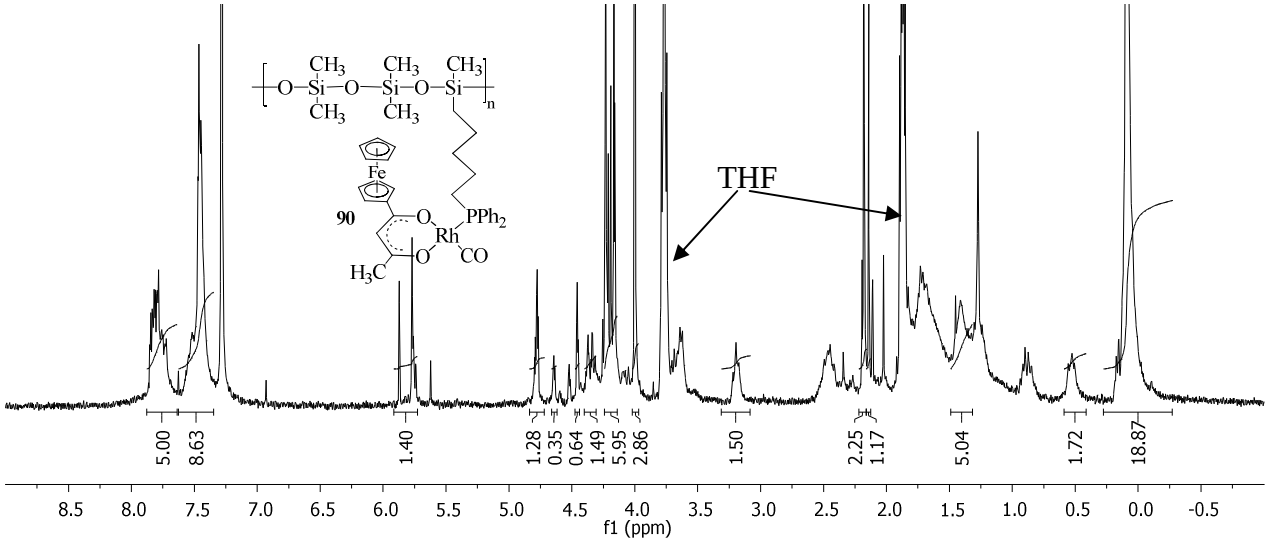

Spectrum 4. 25. Polymer 90.

^{31}P NMR Spectrums

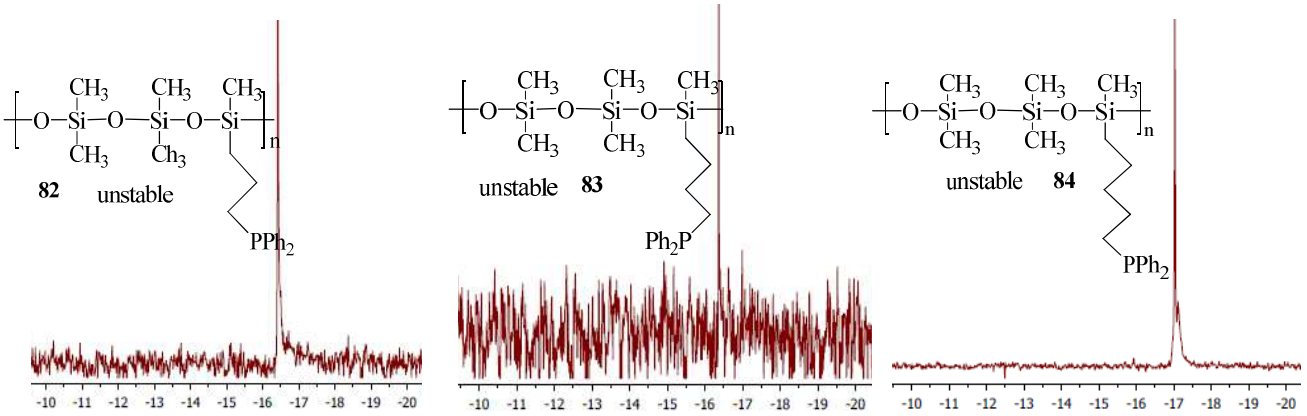

Spectrum 4. 26. ^{31}P Phosphine polymers, polymer 82, polymer 83, polymer 84.

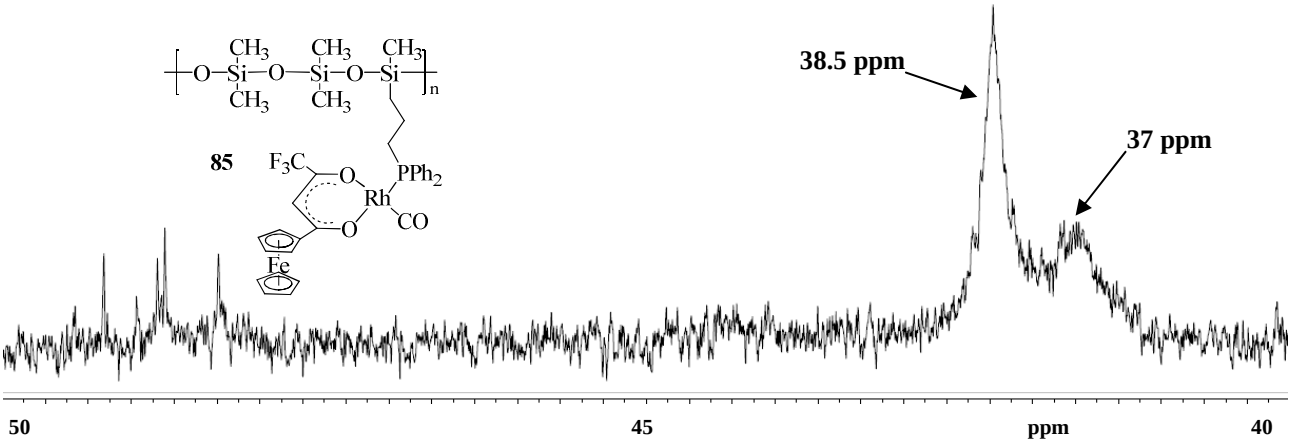

Spectrum 4. 27.^{31}P Polymer 85

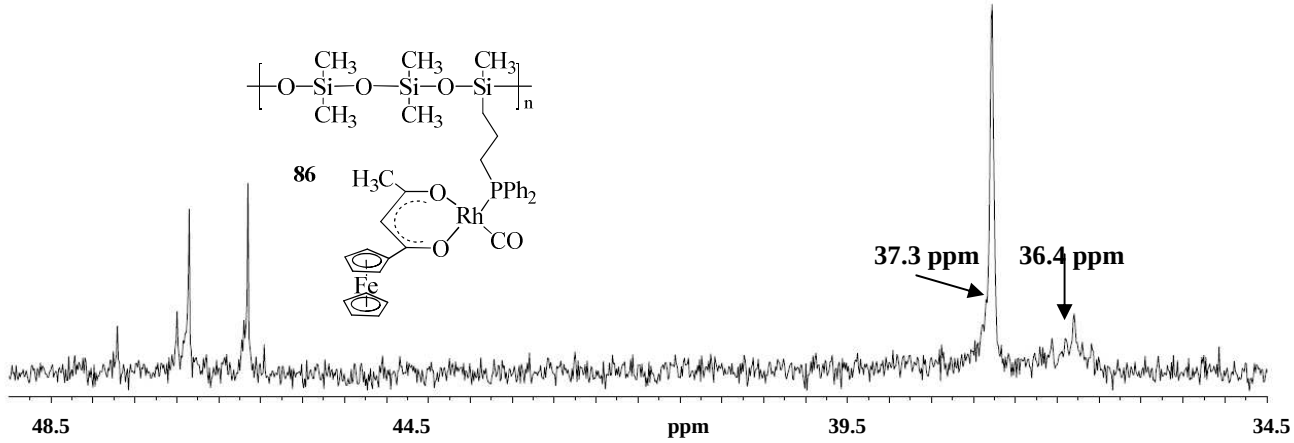

Spectrum 4. 28. ^{31}P Polymer 86.

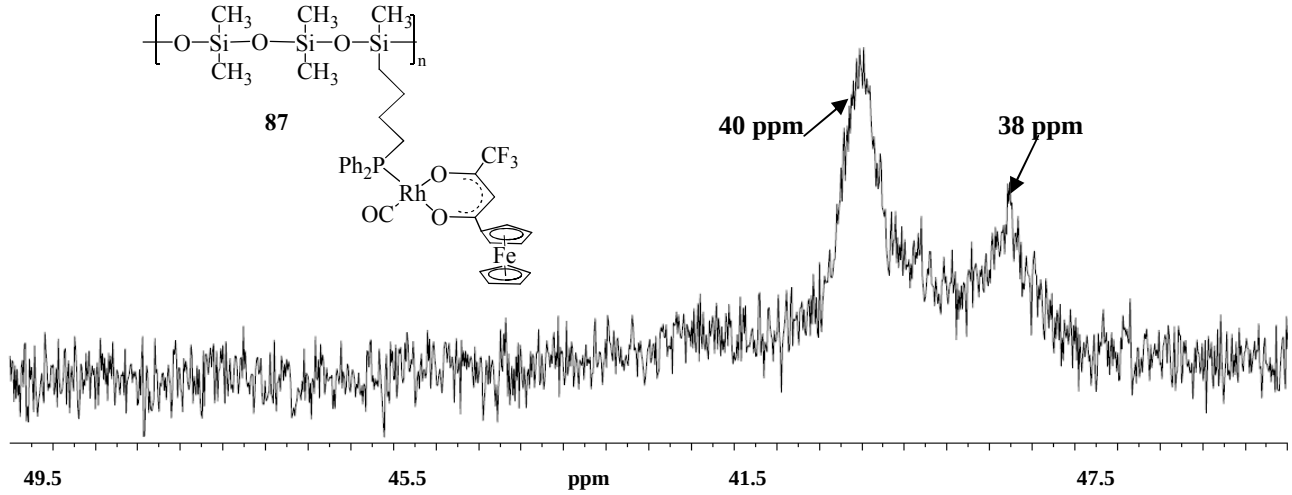

Spectrum 4. 29. ^{31}P Polymer 87.

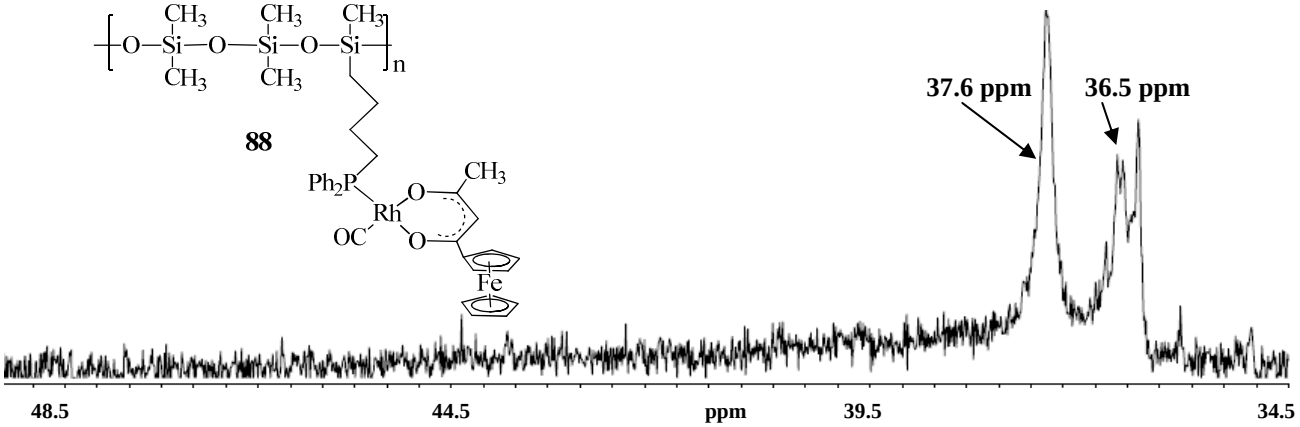

Spectrum 4. 30. ^{31}P Polymer 88.

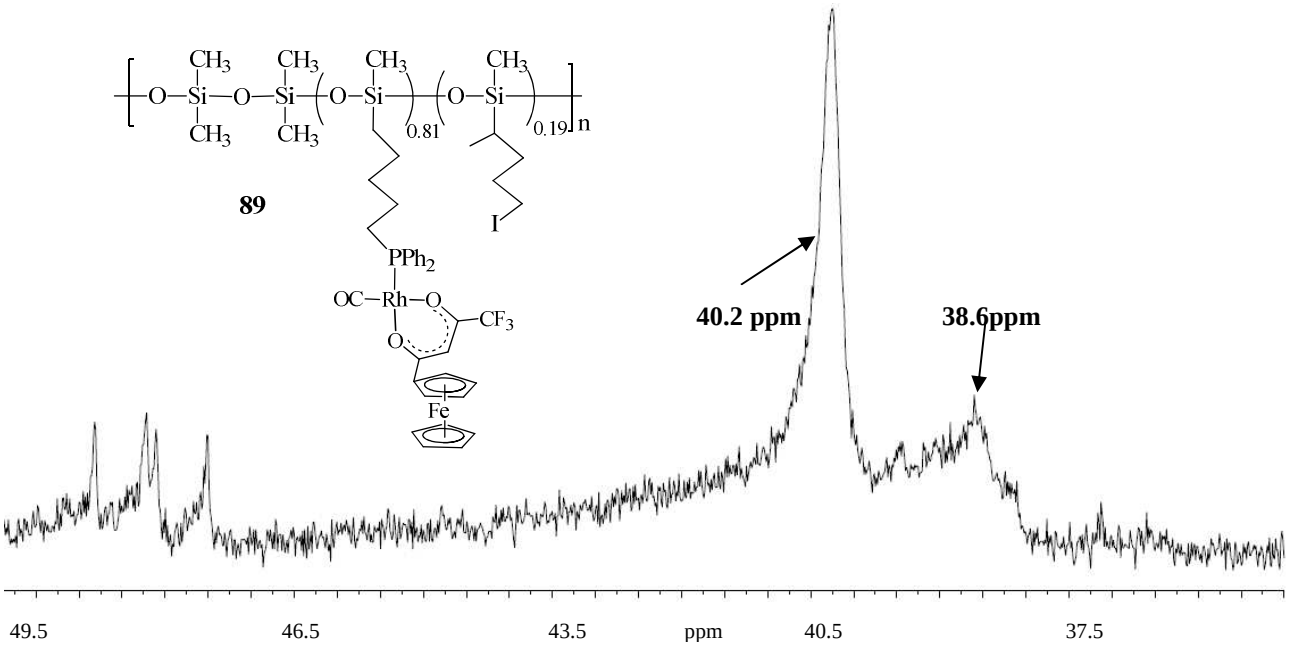

Spectrum 4. 31. ^{31}P Polymer 89.

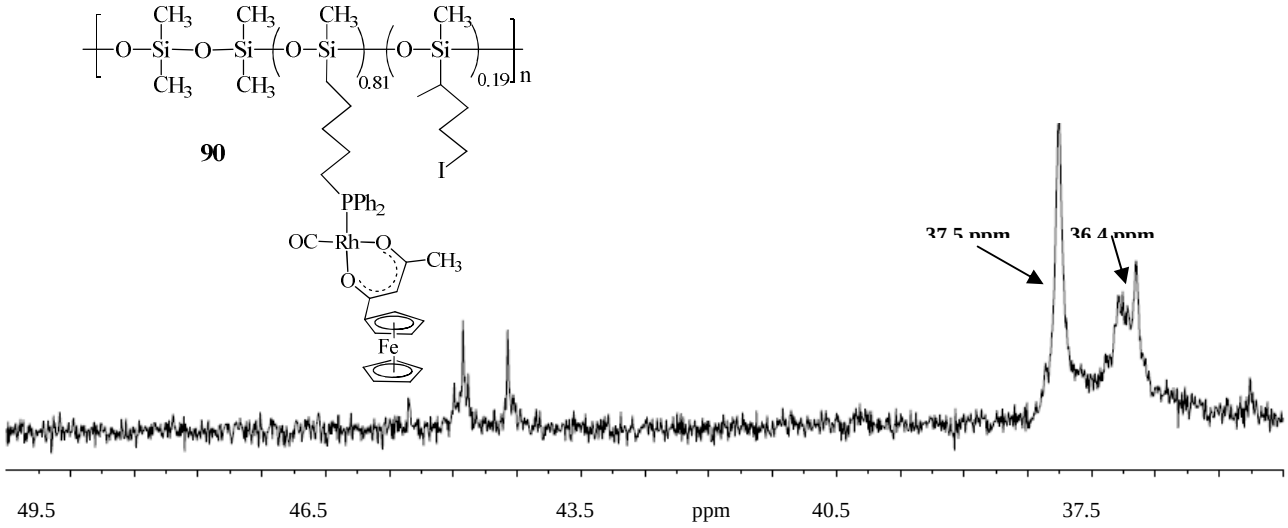

Spectrum 4. 32. ^{31}P Polymer 90.

Tables

Table A. 1. Summary of all individual k_{obs} reaction rates at different temperatures and MeI concentrations determined from the UV/vis experiment.

Temperature / °C	[MeI] / mol dm^{-3}	STAGE 1	STAGE 2
		k_{obs}	
15	0.0306	0.0036(4)	too slow to measure
25	0.0077	0.0016(4)	0.00051(4)
	0.0153	0.0028(5)	0.000443(6)
	0.0230	0.0042(5)	0.00051(5)
	0.0306	0.0057(4); 0.0055(3)[a]	0.00055(4)
35	0.0306	0.0083(5)	0.00170(6)
45	0.0306	0.0140(5)	0.00329(6)

[a] **k_{obs} determined from FTIR experiment.**

Abstract

Two ferrocene-containing β-diketonato ligands, $FcCOCH_2COR$, as well as their dicarbonyl rhodium(I) complexes, $[Rh(FcCOCHCOR)(CO)_2]$, were synthesized. Chloro/bromo functionalized polysiloxanes of the type $\{(OSiMe_2)_2OSiMe\{(CH_2)_mX\}\}_n$ with X = Cl and Br as well as iodo functionalized polysiloxanes, $\{(OSiMe_2)_2OSiMe\{(CH_2)_mI\}\}_n$, were synthesized. The latter were converted to phosphine-containing polysiloxanes, $\{(OSiMe_2)_2OSiMe\{(CH_2)_mPPh_2\}\}_n$ and used as a starting material to synthesize six new rhodium(I)-containing polysiloxane complexes of the type $\{(OSiMe_2)_2OSiMe\{(CH_2)_mPPh_2(CO)(FcCOCHCOR)Rh\}\}_n$, with Fc = ferrocenyl, R = CH_3 and CF_3, m = 3, 4, 5. Characterization techiniques included ^1H and ^{31}P NMR, electrochemistry, UV/vis and FTIR. ^1H and ^{31}P NMR data showed the existence of two isomers for each of the rhodium(I) polysiloxane complexes in solution. Elemental analysis confirmed the elemental composition of the polymers and from the XPS, the binding energies of elements were determined. The inherent viscosity for all polymers was found to be in the range of 0.011-0.28 g/dL.

The new rhodium(I) polysiloxane complexes as well as the free rhodium(I) compexes were studied by cyclic voltammetry in $CH_2Cl_2/[N^nBu_4][B(C_6F_5)_4]$. Two isomers were identified for the rhodium(I) polysiloxane complexes. In a one broad oxidation peak, Rh(1) and Rh(2) was electrochemically irreversibly oxidized first in a one-electron transfer followed by one-electron electrochemical reversible oxidations of the two ferrocenyl groups, Fc(1) and Fc(2).

A pseudo-first order kinetic study of methyl iodide oxidative addition to rhodium polymer $\{(OSiMe_2)_2OSiMe\{(CH_2)_3PPh_2(CO)(FcCOCHCOCF_3)Rh\}\}_n$ was monitored by FTIR and UV/vis techiques. A two stage mechanism was identified wherein kinetically favoured Rh(III)alkyl1 and Rh(III)acyl1 formed first at the same reaction rate in stage 1. The kinetically favoured products converted in stage 2 to the thermodynamically favoured Rh(III)alkyl2 and Rh(III)acyl2 species. Stage 1 was dependent on the CH_3I concentration and stage 2 was independent thereof. The FTIR results also showed possible existence of a rhodium(I) polysiloxane square pyramidal complex. The UV/vis-determined second-order rate constant for the first stage (k_1 = 0.1853 $M^{-1}.min^{-1}$) at 25 °C was found to be in agreement with the FTIR-determined rate constant (k_1 = 0.1499 $M^{-1}.min^{-1}$). The influence of temperature on the reaction was studied at 15, 35 and 45 °C and the activation entropy for stage 1 was found to be -97(6) $J.mol^{-1}.K^{-1}$ while for stage 2 it was 6(3) $J.mol^{-1}.K^{-1}$. Stage 1 reacted in an associative mechanism, while stage 2 involved geometrical isomerizations.

Keywords: Rhodium(I), polysiloxane, silane, phosphine, polymerization, ferrocene, β-diketone, oxidative addition.

Opsomming

Twee ferroseen-bevattende β-diketonato ligande, $FcCOCH_2COR$, tesame met hul dikarbonielrodium(I) komplekse $[Rh(FcCOCHCOR)(CO)_2]$, is gesintetiseer. Chloro/bromo gefunksionaliseerde polisiloksane van die tipe $\{(OSiMe_2)_2OSiMe\{(CH_2)_mX\}\}_n$ waar X = Cl en Br, asook jodo gefunksionaliseerde polisiloksane, $\{(OSiMe_2)_2OSiMe\{(CH_2)_mI\}\}_n$, is gesintetiseer. Laasgenoemde is omgeskakel na fosfor-bevattende polisiloksane, $\{(OSiMe_2)_2OSiMe\{(CH_2)_mPPh_2\}\}_n$ en is verder gebruik om ses nuwe rodium(I) bevattende polisiloksaankomplekse van die tipe, $\{(OSiMe_2)_2OSiMe\{(CH_2)_mPPh_2(CO)(FcCOCHCOR)Rh\}\}_n$, te sintetiseer, waar Fc = ferroseniel, R = CH_3 en CF_3, m = 3, 4, 5. Karateriseringstegnieke het ^1H en ^{31}P KMR, elektrochemie, UV/vis en FTIR ingesluit. ^1H and ^{31}P KMR data het die bestaan van twee isomere vir elk van die rodium(I)polisiloksaankomplekse in oplossing aangedui. Elementanalise het die elementsamestelling van die polimere bevestig en vanaf XPS data is die bindingsenergie van die elemente verkry. Die inherente viskositeit van al die polimere is bepaal en val in die gebied van 0.02-0.28g/dL.

Die nuwe rodium(I)polisiloksaankomplekse asook die vry rodium(I)komplekse is met sikliese voltammetrie in $CH_2Cl_2/[N^nBu_4][B(C_6F_5)_4]$ bestudeer. Twee isomere kon geïdentifiseer word vir die rodium(I)polisiloksaankomplekse. Een breë oksidasiepiek bevat die elektrochemies omkeerbare oksidasie van Rh(1) en Rh(2) as ’n enkelelektron-oordragproses, gevolg deur die enkelelektron, elektrochemiese-omkeerbare oksidasies van die twee ferroseniel groepe Fc(1) en Fc(2).

’n Pseudo-eerste orde kinetiese studie van die oksidatiewe addisie van metieljodied aan die rodiumpolimeer, $\{(OSiMe_2)_2OSiMe\{(CH_2)_3PPh_2(CO)(FcCOCHCOCF_3)Rh\}\}_n$, is volg met FTIR en UV/vis tegnieke. ’n Tweefase meganisme is geïdentifiseer waartydens die kineties verkose Rh(III) alkiel 1 en Rh(III) asiel 1 teen dieselfde reaksietempo in fase 1 gevorm het. Die kineties verkose produkte is in fase 2 omgeskakel na die termodinamies verkose produkte R(III) alkiel 2 en Rh(III) asiel 2. Fase 1 is afhanklik van die CH_3I konsentrasie, terwyl fase 2 onafhanklik is daarvan. Die FTIR resultate het getoon dat daar ook moontlik ‘n vierkantig piramidale rodium(I)polisiloksaankomplek bestaan. Die UV/Vis bepaalde tweede-orde tempokonstante vir die eerste fase ($k_1 = 0.1853 M^{-1}.min^{-1}$) by 25 °C stem ooreen met die FTIR bepaalde tempokonstante ($k_1 = 0.1499\ M^{-1}.min^{-1}$). Die invloed van temperatuur op die reaksie is bestudeer by 15, 35, en 45 °C en die aktiveringsenergie vir fase 1 is -97(6) $J.mol^{-1}.K^{-1}$, terwyl dit 6(3) $J.mol^{-1}.K^{-1}$ vir fase 2 is. Fase 1 het met ’n assosatiewe meganisme gereageer, terwyl fase 2 slegs betrokke was by geometriese isomerisasie.

I declare that the dissertation/thesis hereby handed in for the qualification Magister Scientiae in Chemistry at the University of the Free State is my own independent work and that I have not previously submitted the same work for a qualification at/in another university/faculty. I furthermore cede copyright of the thesis in favour of the University of the Free State.

Signed Date

_____ _____